Minimizing the influence of fluorescent tags on the partition of IgG in PEG-salt aqueous two-phase systems towards miniaturized rapid screening applications

Mariana Neves São Pedro

Thesis to obtain the Master of Science Degree in

Biotechnology

Supervisors: Prof. Maria Raquel Múrias dos Santos Aires-Barros

Dr. Ruben Rafael Gonçalves Soares

Examination Committee

Chairperson: Prof. Maria Ângela Cabral Garcia Taipa Meneses de Oliveira

Supervisor: Dr. Ruben Rafael Gonçalves Soares

Members of the Committee: Prof. Ana Margarida Nunes da Mata Pires de Azevedo

October 2018

"It is our choices, Harry,
that show what we truly are,
far more than our abilities."

— J.K. Rowling

Acknowledgments

Firstly, I would like to specially thank my supervisors, Professor Raquel Aires-Barros and Dr. Ruben Soares, for accepting me to work in this dissertation and the continuous guidance throughout this past year, providing support in difficult times with encouraging advice and for always pushing me to achieve my best. Second, I would like to thank Professor Ana Azevedo for the supportive input, always being present to discuss some points during this experimental work.

Also, I would like to thank everybody who work in the laboratory with me, particularly to Maria João Jacinto, Sara Rosa, Alexandra Wagner and Ana Rita Santos, who taught me and help me to perform several of the experiments presented in this work. To the people in the 7th and 8th floor who welcomed me and continuously support me. An especial acknowledgement to Rui Silva, an endless source of fluorescence knowledge, for all the helpful discussions and solutions.

A special thanks to Marta Reis, Miguel Nascimento, and the rest of family I formed during my bachelor years, for never leaving me and always encourage me to pursue my dreams and objectives. I will truly treasure your friendship for the rest of my life.

To all my friends who endure this last year with me. My writing partners and personal motivation coaches, Alexandra Balola and Susana Vagueiro, for the continuous support throughout the interminable work days, offering me a beer at the end of the day. To João Carvalho, for also being my writing partner but sadly without offering me the beer. To my lab partners in the 7th floor, Cristiana Ulpiano and Jorge João, for all the company, the advices and the friendship. To Raquel Califórnia, for always putting a smile in my face. To Rita Simões, for allowing me to be evil and being the best work partner I could ever ask for. To Pedro Monteiro, my future husband, for all the coffee, all the evil conversations and all the laughs we shared, which made this last year much more enjoyable. To Pedro Rosado, my Danny Zuko, for understanding me and continuously helping me to navigate my life.

Lastly, I would like to thank the people who shape me into the person I am today, my family: my mom and dad, for having endless amounts of patience over all my nagging and screaming, always supporting and pushing me, and keeping sure I had everything I could ever need; and my little brother, Tomás, for being my favourite person in the world, who always makes me laugh when I am feeling down, having an undying trust and believing in me, even when I do not.

Abstract

Aqueous two-phase extraction (ATPE) offer a significant potential for the selective separation of biopharmaceuticals from unclarified cell culture supernatants, as is the case of monoclonal antibodies (mAbs). However, it is often difficult to predict the behaviour of the target molecule in each condition (e.g. tie-line length (TLL), pH, neutral salt concentration), making high-throughput screening tools highly valuable to perform an empirical optimization. Microfluidic ATPE screening devices coupled to fluorescence microscopy to continuously monitor IgG partition have been recently demonstrated. These systems provide short diffusion distances and rapid molecular partition without gravity settling, resorting to minimal reagent volumes. However, the influence of fluorescent tags on IgG partition must be carefully evaluated to assess the validity of extrapolating the results to the unlabelled molecule, a critical but currently unexplored effect.

In this work, three fluorophores with different global charge and reactivity, namely BODIPY™ FL maleimide, Alexa Fluor® 430 and BODIPY™ FL NHS Ester, were selected to label IgG with different degrees of labelling. ATPE performed in microtubes or microchannels, SDS-PAGE electrophoresis and isoelectric focusing, were performed in order to characterize each labelled molecule relative to the native IgG. BODIPY™ FL maleimide, combined with tris(2-carboxyethyl)phosphine (TCEP) to generate free thiol groups without compromising the tertiary structure, was the most promising strategy. Using this fluorophore, the observed partition coefficient in a PEG 3350-phosphate system with and without the addition of NaCl, was comparable between the microtubes and microfluidic devices, and also comparable to those quantified for the unlabelled molecule using analytical protein G chromatography.

Keywords: Monoclonal antibodies, ATPE, downstream processing, microfluidic device, fluorescent tags

Resumo

A extração por duas fases aquosas oferece um vasto potencial para a separação seletiva de produtos biofarmacêuticos a partir de sobrenadantes celulares, como os anticorpos monoclonais. No entanto, o comportamento da molécula alvo em cada condição é, em muitas situações, difícil de prever (o comprimento da *tie line*, o pH, a concentração de sal, entre outros), o que torna as ferramentas de rastreio de alto rendimento extremamente valiosas para a realização desta otimização empírica. Recentemente, dispositivos microfluídicos recorrendo à microscopia de fluorescência têm sido explorados de forma a continuamente monitorizar a partição do IgG na extração por duas fases aquosas. Estes dispositivos proporcionam curtas distâncias de difusão e uma rápida partição molecular sem sedimentação por gravidade, utilizando volumes mínimos de reagentes. Contudo, a influência da marcação com fluoróforos na partição de IgG deve ser cuidadosamente estudada antes de extrapolar os resultados obtidos para a molécula não marcada, um efeito crítico, mas atualmente inexplorado.

Neste trabalho experimental, três fluoróforos com diferentes cargas e reatividade, o BODIPY™ FL maleimide, o Alexa Fluor® 430 e o BODIPY™ FL NHS Ester, foram selecionados para a marcação do IgG, obtendo vários graus de marcação para cada. De modo a caracterizar cada conjugado em relação à IgG nativa, diversas técnicas foram realizadas: extração por duas fases aquosas utilizando microtubos ou microcanais, eletroforese SDS-PAGE e focagem isoelétrica. A marcação com o BODIPY™ FL maleimide combinada com o uso do tris(2-carboxietil)fosfina (TCEP), para gerar grupos tiol livres sem comprometer a estrutura terciária, foi a estratégia mais promissora encontrada. Com este fluoróforo, o coeficiente de partição obtido num sistema PEG 3350-fosfato, com e sem a adição de NaCl, foi semelhante entre os microtubos e os microcanais, e também análogo com os valores alcançados para a molécula não marcada, quantificados por cromatografia analítica da proteína G.

Palavras-chave: anticorpos monoclonais, ATPE, *downstream processing*, dispositivos microfluídicos, fluoróforos

Table of Contents

List of Tables

List of Figures

List of Abbreviations

Abs	Antibodies
ATPE	Aqueous two-phase extraction
ATPS	Aqueous two-phase systems
BCA	Bicinchoninic acid
CDR	Complementary-determining region
DOL	Degree of labelling
DTT	Ditiotreitol
fAbs	Antibody fragments
FITC	Fluorescein isothiocyanate
IEF	Isoelectric focusing
Ig	Immunoglobulins
K_P	Partition coefficient
mAbs	Monoclonal antibodies
NaCl	Sodium chloride
PDMS	Poly(dimethylsiloxane)
PEG	Polyethylene glycol
pI	Isoelectric point
TCEP	Tris(2-carboxyethyl)phosphine
Y_{Top}	Yield in the top phase

1. Introduction

1.1. Context and motivation

Antibodies are highly specific molecules which can recognize and eliminate pathogenic and disease antigens, playing an important role in medicine as well as in analytical biotechnology.[1] In the past few years, monoclonal antibodies (mAbs) have been playing an important role in several of the main advances in the treatment of several infectious diseases, cancers and autoimmune disorders. However, unlike other therapeutic products, mAbs are required at high purity and high doses (0.1 to 1.0 g) to achieve effective treatment, being administered in a chronic regime. Therefore, with concerns about a potential shortage of the manufacturing capacity in mind, important improvements in the upstream productivity have been achieved.[2,3] Advances in the downstream processing of antibodies are thus essential since the downstream processing can undercut some of the enhancements in cell line productivity, being even considered as the bottleneck in providing these therapeutics at reliable costs and at considerable amounts, accounting for 50-80% of total manufacturing cost.[1,3,4] Hence, a simple but efficient downstream purification strategy is demanded in order to reduce costs and make these biopharmaceuticals widely available to the general population.[2]

Aqueous two-phase extraction (ATPE) presents a great potential for selective separation of a wide range of biomolecules by exploring differences in molecular solubility in each of the two immiscible phases. This technique can be a potential alternative, reducing costs by simplifying the initial clarification and primary purification steps.[2,5] Aqueous two-phase systems (ATPSs) will provide a suitable environment to maintain biological activity and protein solubility, due to the high biocompatibility, high water content and low interfacial tension, minimising product degradation. By variating certain experimental conditions, such as pH, ionic strength, and polymer molecular weight, good resolution and yields can be obtained.[1] The use of aqueous two-phase extraction for the initial purification in the downstream processing of monoclonal antibodies has been reported in a few research studies, obtaining satisfactory recovery yields and protein purity.[3,6–8]

Aiming at effectively optimizing novel purification schemes involving ATPE, high-throughput screening tools can be highly valuable to optimize the separation of complex mixtures, particularly considering that many of the factors governing partitioning of analytes in ATPE are still poorly understood. Microfluidics is characterized by shorter reaction times due to shorter distances for diffusion, as compared to macroscale devices, with the use of low volumes of reagents and analytes and by having the potential of being low cost, disposable and portable.[5] Recently, several research studies have been demonstrating the validation of microfluidic screening tools for the bioseparation of target molecules in ATPE coupled to fluorescence microscopy to continuously monitor the biomolecule partition[5,9,10], with Silva *et al*. designing a microfluidic device for the extraction of mAbs, showing that the reduction to the microscale did not greatly affect the antibody extraction yield when compared with macroscale results.[11]

In order to facilitate the optimization of ATPE-based downstream processing schemes, the initial objective of this thesis was to validate the use of a microfluidic ATPE screening device coupled to

fluorescence microscopy to rapidly quantify the IgG partition behaviour under a range of experimental conditions. However, for the use of the fluorescence microscopy, the antibody IgG must be previously labelled with a proper fluorophore, without altering the antibody proprieties, so the results can possibly be extrapolated to the unlabelled molecule. To achieve this goal, the selection of the appropriate fluorophore is crucial and will be thoroughly explored in this work for the first time, with a particular focus given to the conjugation chemistry to functionalize the IgG molecule. Numerous fluorophores are available to the IgG labelling, modifying several functional groups present in this protein, such as the primary amines present in the lysine residues, Alexa Fluor® 430 and BODIPY™ FL NHS ester, or the thiols present in the cysteine residues, BODIPY™ FL maleimide, which present an range of distinct global charge values and reactivity, being the selected fluorescent tags to be explored in this experimental work.

1.2. Monoclonal Antibodies: Relevance, Production and Purification strategies

1.2.1. Introduction to Antibodies: molecular structure and general properties

Antibodies (Abs), also known as immunoglobulins (Ig), are circulating proteins that are produced in vertebrates in response to exposure to foreign molecules, the antigens. These proteins are highly specific in their ability to recognize a wide range of antigenic structures, combined with a generally high affinity.[12]

All antibody molecules found in an individual share the same basic structural characteristics but display remarkable variability in the regions that bind antigens. This variability of the antigen binding regions, each with unique amino acid sequences, is responsible for the capacity of different antibodies to bind to a tremendous number of structurally diverse antigens.[12] This basic structure consists in a symmetric core composed of two identical light (L) chains and two identical heavy (H) chains (***Figure 1.1***), creating a large Y-shaped glycoprotein.[12] Both heavy chains and light chains consist of amine-terminal variable (V) regions that participate in antigen recognition, creating the antigen-binding sites (Fab or fragments of antigen-binding), and carboxyl-terminal constant (C) regions, with the C regions of the heavy chains interact with other effector molecules and mediate most of the biologic functions of antibodies. The heavy and light chains are covalently linked by disulfide bonds formed between cysteine residues, as well as the two heavy chains of each antibody molecule, creating a flexible region known as the hinge. The paired constant regions below the hinge create the constant fragment of the antibody, being the first region of the antibody structure to be crystallized (Fc). Because the core structural unit of each antibody contains two heavy chains and two light chains, every antibody molecule has at least two antigen-binding sites, giving the ability to bind simultaneously to two identical structures.[12]

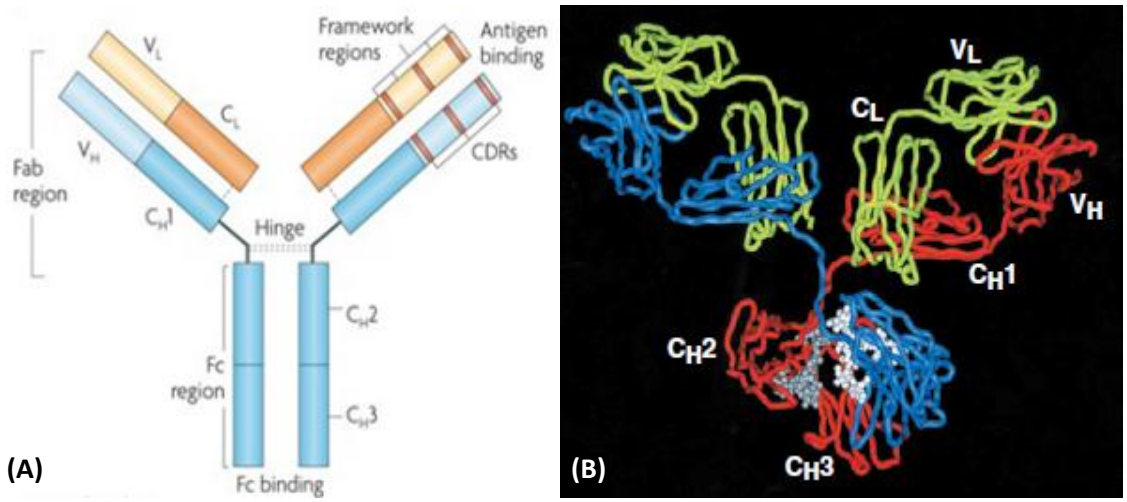

Figure 1.1 - (A) Basic structure of an Ig molecule, which contains two identical heavy and light chains, each with a constant and variable region, where the antigen binding site is located. Disulfide bonds connect the heavy and the light chains. (B) Structure of a human IgG molecule as revealed by x-ray crystallography. In this ribbon diagram of a secreted IgG molecule, the heavy chains are colored blue and red, and the light chains are colored green; carbohydrates are shown in gray. Reproduced from ref. 12.

These molecules can be divided into distinct classes, called isotypes, according to the structure of their heavy chain C regions, classified in IgA, IgD, IgE, IgG, and IgM and their heavy chains are denoted by the corresponding lower-case Greek letter (α, δ, ε, γ, and μ respectively), with the heavy chains of all antibody molecules of one isotype having essentially the same amino acid sequence. By differing in their C regions, they will diverge in what bind to and what effector functions they perform. Additionally, there are two classes (or isotypes) of light chains, called κ and λ, that are distinguished by their carboxyl-terminal constant (C) regions, which seem to be functionally indistinguishable. An antibody molecule has either two identical κ light chains or two identical λ light chains and can be associated with any class of heavy chain, not changing major proprieties of the antibody, except its specificity for an antigen.[12]

In the human serum, the most abundant immunoglobulin is IgG, accounting for about 10–20% of plasma protein. It will be further divided into four subclasses – IgG1, IgG2, IgG3 and IgG4 – according to their abundance, the most profuse being IgG1.[12,13] Although they are more than 90% identical on the amino acid sequence, each subclass has a unique profile with respect to antigen binding, complement activation, triggering of effector cells and half-life, responding to different types of antigens. Their global structures are very similar (***Figure 1.2***), but with important differences between each subclass that affect their binding to accessary molecules and receptors, affecting their functionality. This important variation is found in the hinge region, whereas fewer amino acid differences are found in the rest of the antibody.[13]

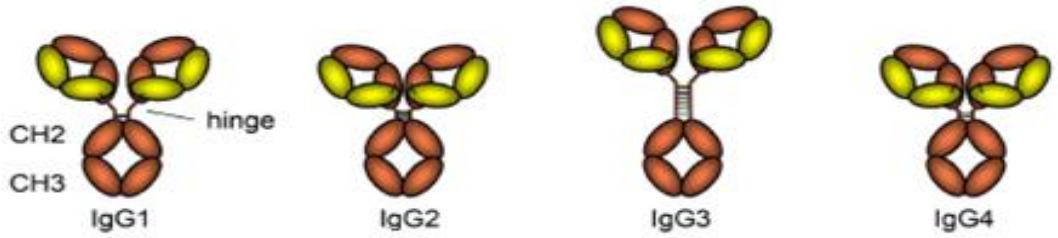

Figure 1.2 - Schematic representation of the IgG subclasses, indicating how the different heavy and light chains are linked, the length of the hinge, and the number of disulfide bridges connecting the two heavy chains. Reproduced from ref. 13.

As previously stated, the portion responsible for the antigen binding is located at the end of the variable region (***Figure 1.1***) and is called complementary-determining region (CDR). This region is composed by, in total, by six loops, three in both variable regions of the light and heavy chains, CDR1, CDR2 and CDR3. The six CDRs spread out to form a broad surface, creating a pocket that contacts with the antigens directly. The molecules which the antibodies recognize are usually much bigger than the antigen-binding region of an antibody molecule, therefore, any antibody will only bind to a portion, referred to as the epitope. This binding of the antigen to the antibody is performed by several types of noncovalent interactions, including electrostatic interactions, hydrogen bonds, van der Waals forces, and hydrophobic interactions. Since individually these interactions are relatively weak, the binding is only effective when the antigen is close enough to allow its atoms to fit into the CDR on the surface of the antibody.[12]

Because of the high complexity of most antigens, each presenting numerous epitopes that are recognized by a large number of lymphocytes. Each lymphocyte will be activated, proliferating and differentiating into plasma cells, and the resulting antibody response is polyclonal. On the other hand, when a single B lymphocyte clone produces an antibody, this will be designated a monoclonal antibody (mAb).[14]

1.2.2. Monoclonal antibodies: definition and historical context

Monoclonal antibodies are a combination of homogenous antibody molecules with affinity towards a specific antigen, being initially produced using an individual immortalized antibody-secreting cells from an animal immunized with the antigen in question.[12] This technique, despite no longer being employed, was first described by Georges Kohler and Cesar Milstein in 1975, for which they were awarded the Nobel Prize in Physiology and Medicine in 1984, and has proved to be one of the most valuable advances in all of scientific research and clinical medicine. The method relies on fusing B cells from an animal (e.g. mouse) pre-immunized with the target antigen, with a myeloma cell line and growing the cells under conditions in which the unfused normal and tumour cells cannot survive (***Figure 1.3***). The resultant fused cells that grow out are called hybridomas and each hybridoma will only make one Ig. The antibodies secreted by many hybridoma clones are screened for binding to the antigen of interest, and this single clone with the desired specificity will be selected and further expanded. The products of these individual clones are monoclonal antibodies that are each specific for a single epitope on the antigen or antigen mixture used to identify antibody secreting clones.[12]

Even though these antibodies are most easily produced by immunizing mice, patients treated with mouse monoclonal antibodies may make antibodies against the mouse Ig, called a human anti-mouse antibody (HAMA) response, eliminating the injected monoclonal antibody and also causing serum sickness.[12] For this reason, when the first therapeutic antibody, Anti-CD3 murine or OKT-3, was approved, it failed as a good treatment for transplantation rejection because OKT-3 induced the HAMA response in patients.[15] Thus, in order to reduce the immunogenicity of murine antibodies in human, genetic engineering was employed, with the construction of chimeric antibodies with human constant region and mouse variable region, and protein engineering was also applied, with the murine CDR region grafted into the human variable domain framework.[12,15] However, both chimeric and humanized

mAbs still pose a risk of eliciting an immune response because a significant portion of the antibody remains nonhuman. Recently, fully human mAbs generated from recombinant human antibody libraries or transgenic mice containing human immunoglobulin genes have emerged as alternatives with arguably improvements when compared to humanized mAbs.[16]

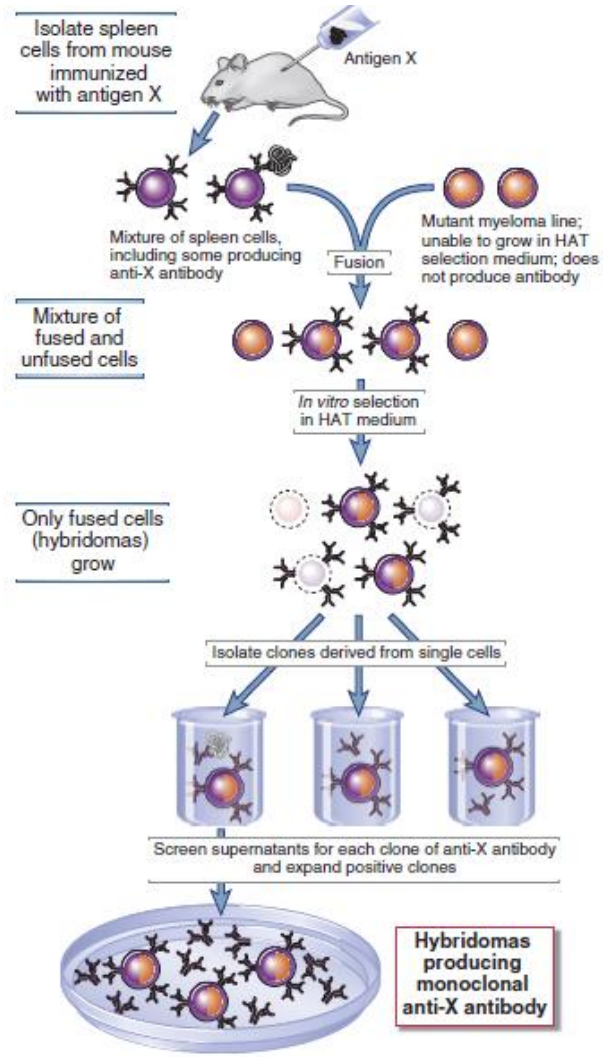

***Figure 1.3** - The generation of monoclonal antibodies. First, the immunization of mice for the production of antibodies occurs, followed by the isolation of B cells from the mice's spleen and cultivation of the myeloma cells. Next, the fusion of myeloma cells and B cells happens in order to produce the hybridoma. Finally, the selection and culture of hybridoma clones occurs and therefore the antibodies are produced. Reproduced from ref. 12.*

1.2.3. Current demand for monoclonal antibodies as biopharmaceuticals

After the discovery of the hybridoma technology in 1975 and the approval of the first monoclonal antibody product in 1986, sales growth and approval of additional products was slow until the late 1990s when the first chimeric monoclonal antibodies were approved.[17] In the following years, with the approval of humanized and then fully human monoclonal antibodies, the rate of product approvals and sales of monoclonal antibody products have increased dramatically. In 2013, global sales revenue for all monoclonal antibody products was nearly $75 billion, representing almost half of the total sales of all biopharmaceutical products.[17]

Nowadays, monoclonal antibodies, which have long been staples in both diagnostic and research fields, are also invading the therapeutic domain. The use of these molecules as therapeutic agents is attracting a great deal of attention by the pharmaceutical industry, mainly due to the safety, efficacy and quality which are now well defined for mAbs, and general acceptance by the public and medical communities.[18] In 2012, Roche™, being the largest oncology company in the world, held the largest number of approved therapeutic mAb molecules, with annual sales reaching up to US$20 billion. For example, Avastin®, approved for the treatment of brain, colon, kidney and lung cancers, generated $6.3 billion in annual sales, Rituxan®, used to treat chronic lymphocytic leukemia and non-Hodgkin's lymphoma, generated $7 billion and Herceptin, approved to treat breast and stomach cancers, generated $6 billion. Other companies have also found success in producing its mAbs: Johnson & Johnson's™ with Remicade®, used for the treatment of arthritis, generated $6.1 billion, and AbbVie™ with Humira®, also an arthritis medication, earned $9.3 billion in sales.[19]

These antibodies are set to play a significant role in the treatment of a wide number of indications, including oncology, asthma, autoimmune diseases, poisoning, viral infections and other diseases. However, the industry is mainly focused on oncology and arthritis, immune and inflammatory disorders (AIID) (***Figure 1.4***).[20,21]

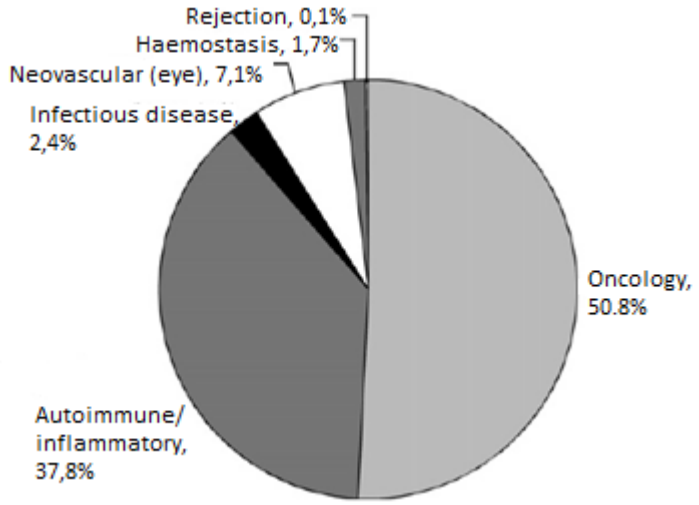

Figure 1.4 *- Monoclonal antibody sales by therapy area in 2010. Adapted from ref. 21.*

Overall, in terms of therapy areas in 2010, oncology is the leading income earner accounting for over half (50.8%) of sales, followed by inflammation and immune disorders with almost 40% of the global market revenues.[21]

It is forecasted that the number of approved monoclonal antibodies will continue to grow, along with over 300 monoclonal antibody product candidates currently in development[17], for a number of different applications. It is expected that this will result in continued growth in the sales of monoclonal antibody products in the coming years and will continue to drive the overall sales of all biopharmaceutical products. At the current approval rate of four new products per year, 70 monoclonal antibody products will be on the market by 2020, and the combined world-wide sales will be nearly $125 billion.[17]

The demand for monoclonal antibody products has resulted in a significant amount of global manufacturing capacity devoted to their production as well as to significant improvements in methods and approaches to monoclonal antibody manufacturing process design and optimization.[17]

1.2.4. Large scale production of monoclonal antibodies

As previously stated, monoclonal antibodies are a highly successful class of therapeutic products, which require extremely high levels of purity at the highest yield and with the minimum costs associated with loss of product, and, for this reason, companies have been making efforts to create processes that respond to this necessity.[4] If a therapeutic mAbs is not adequately purified, it could lose its therapeutic properties or even cause immunogenic reactions, potentially endangering the patient's health. Hence, this section gives a brief description of the existing processes used in the production of monoclonal antibodies, giving special focus on the purification steps to obtain the desired antibody.

The production of mAbs has greatly advanced since the first licensed monoclonal antibody produced in 1986, OKT-3, where production in mice was preferred due to its cost effectiveness and high concentrations of mAbs produced.[22] The growing ethical concern about mAbs production by animals and with improvements in cell line selection, media optimization or harvesting methods led to an increased emphasis on in vitro methods that are able to compete, not only in capacity, but also in cost effectiveness with the in vivo method.[23] Advances in culture media have facilitated advances in bioreactor technology over the past couple of decades, with the removal of the fetal bovine serum and replacement with chemically defined media. Aside the consideration of the cell media is the manipulation of the host cell, with an intense effort directed at producing cell lines with altered properties such as transfected Chinese hamster ovary (CHO) cell line, and/or understanding the metabolic processes involved during over-expression and posttranslational modification.[21] These improvements combined can accumulate product titers of 1–5 g/L, with some companies reporting up to 10–13 g/L for extended culture durations.[22] Additionally, the implementation of single-use bioreactor systems has emerged, offering a handful of advantages such as lower capital investment and operational costs, flexibility, improved production scheduling and higher process replication. Nevertheless, there is still a lot of work to be done in optimizing disposable bioreactor systems: in terms of aeration and mixing, the scale is limited up to 2000–2500 L, the diversity of options is restricted and there is a lack in standardization, instrumentation and some remaining performance issues. Furthermore, there is a shortage of a validation process concerning the nature, quantity and risk of leachables and extractables from the disposable plastics and the bags can also bind media components, decreasing the process performance.[23]

The escalating demands for increased protein titres, primarily for economic reasons, have shifted the bottleneck step from production to purification, with downstream processes representing between 45 and 92% of the total cost of manufacturing a recombinant protein.[24] Hence, formulating an efficient and economical purification strategy is crucial and the developed purification process must be easily scaled-up and capable of removing both process-and product-related impurities as well as clearing virus in order to ensure product safety.[24,25]

The typical commercial purification protocol for monoclonal antibodies is shown in ***Figure 1.5***, with many companies have converged on the use of very similar processes based on a very mature and robust production technology, with predictable outcomes concerning product quality, production capacity and costs.[22,26] Therefore, the downstream section will encompass three main sectors: initial recovery, purification and polishing.[25]

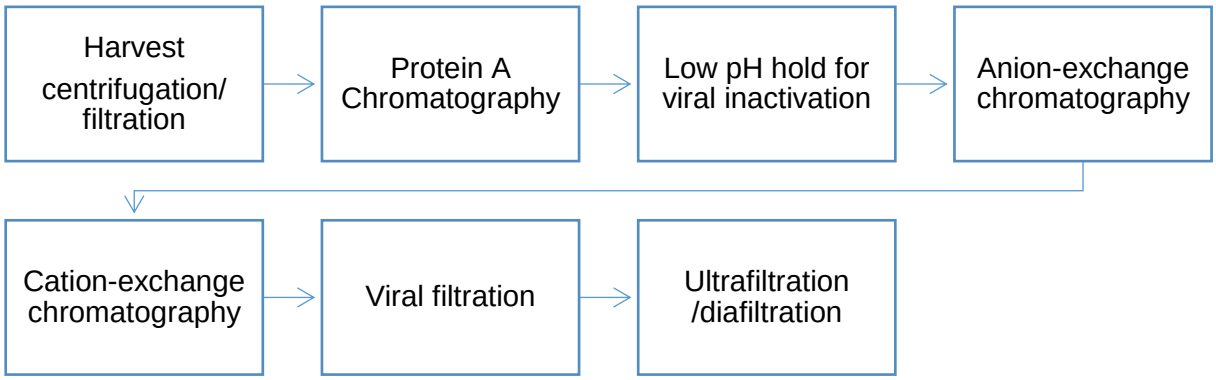

Figure 1.5 *- Consensus process flowsheet for production of recombinant therapeutic mAbs. Suspension mammalian cell cultures bioreactors operating in fed-batch mode provide high product titers in 10 to 14 days. Following harvest by centrifugation and depth filtration, Protein A chromatography captures the product, and two additional chromatographic polishing steps complete the purification. Two membrane steps are used to assure viral safety of the product, and concentrate and formulate the drug substance.*[22,25]

The harvest of the mAbs from the mammalian culture is the first unit operation in a downstream process, performed in order to remove the cells and any cell debris from the culture broth and to clarify the cell culture supernatant that contains the antibody product.[26] The current preferred process for accomplishing this initial recovery is to use a disc-stack continuous centrifugation coupled with depth filtration and can account for up to 25% of the cost of the entire downstream process.[26,27]

The next step, after cell removal, is Protein A chromatography, a critical and versatile technique used in a product that will still require the removal of a small proportion of process and product related impurities. Protein A is a naturally occurring polypeptide found in S. aureus, and after being genetically engineered, its MW is reduced to 42 kDa. The mAb will bind to the Protein A at its Fc region, with hydrophobic interactions related to specific hydrogen bonds that are established as a function of pH.[27] The procedure typically involves passing the clarified cell culture supernatant over the column at pH 6–8, under which conditions the antibodies bind and unwanted components, such as host cell proteins and cell culture media components and putative viruses, flow through the column. An optional intermediate wash step may be carried out to remove non-specifically bound impurities from the column, followed by elution of the product at pH 2.5–4, with the regeneration of the column for posterior use (***Figure 1.6***).[4,22] The low pH elution step will also serve as a viral inactivation step.[22]

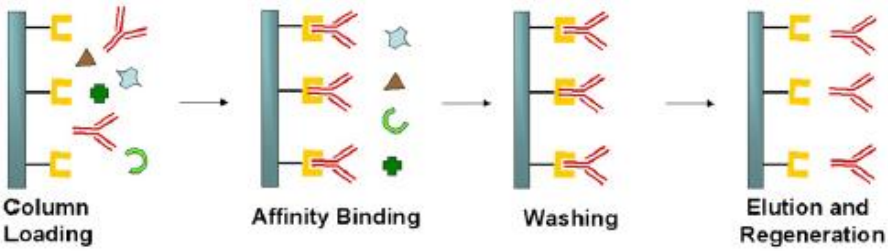

Figure 1.6 - Schematic representation of the main steps in affinity chromatography: following crude sample loading, the monoclonal antibodoes are retained by affinity binding to protein A. Next, washing is employed to remove nonspecific binding, with subsequently elution to recover purified mAbs. Reproduced from ref. 4.

After this step, the antibody product is highly pure and more stable due to the elimination of proteases and other media components that may cause degradation.[26] On the other hand, the use of this technology presents several significant drawbacks, primarily the ability of protein A to leak into the mobile phase and its high associated costs. Nevertheless, it is still widely used as a capture step in large-scale purification of monoclonal antibodies.[24]

For the polishing steps, one or two additional chromatographic polishing steps are typically required to meet the purity specifications, most commonly anion- and cation-exchange chromatography.[22] Other alternatives such as hydrophobic interaction chromatography, multimodal chromatography or size exclusion chromatography may be employed, for example.[24,26] The main objective of polishing is the final removal of trace contaminants from the solution, to achieve acceptable concentrations of these, and to obtain the final solution required according to the particular formulation to be used.[27] Separation by ion exchange chromatography is fairly selective, its resins are relatively inexpensive and it is ideal for reducing high molecular weight aggregate, charge-variants, residual DNA and host cell protein, leached Protein A and viral particles.[26]

Although chromatography has been the workhorse of downstream processes due to its simplicity and high resolving power, the chromatographic sequence can present several major limitations, being the major cost related to the column cost and relatively long cycle times, requiring buffer solutions in large volumes.[24–26] Additionally, higher-titre processes have been imposing practical limitations that will make the current technology platforms reach their limits of throughput and scalability.[25] High pressure drop across the column and the clogging of the packed bed of adsorbents with complex feeds can also occur. Thus, non-chromatographic technologies have also been developed as alternative strategies to the three chromatographic sequences, overcoming the diffusion limitations experienced by chromatographic media.[4] Membrane filtration, affinity precipitation, preparative electrophoresis or aqueous two phase extraction can be employed.[4] The latter will be further analysed in this work.

A virus retentive filtration step provides additional assurance of viral and endotoxins safety, and a final ultrafiltration step formulates and concentrates the product.[22] Overall purification yields from cell cultured fluid range from 60–80%, depending on the number of steps involved and the concentrated bulk drug substance is stored freeze-dry or as a liquid.[22,27]

1.3. Aqueous Two-phase Separation

1.3.1. The discovery of aqueous two-phase systems (ATPS)

Aqueous two-phase systems (ATPSs) are formed spontaneously upon mixing two aqueous solutions of mutually incompatible components, such as two polymers or a polymer and a salt, which above a certain critical concentration, result in the spontaneous formation of two immiscible phases.[1,28]

Beijerinck accidently found, in 1896, that when aqueous solutions of gelatin and agar were mixed, the turbid solution separated into two layers, one rich in agar and the other in gelatin, forming what will be later known as the ATPS. However, a practical biotechnological application of this technique was only later discovered by Albertsson, in 1958, when he understood that these systems could be applied as a separation technique and for downstream processing.[29,30] Since then aqueous two-phase extraction (ATPE) has been successfully applied in the downstream processing of several biological compounds, such as proteins, nucleic acids and amino acids.[28]

1.3.2. Phase diagram and partition of target molecules

ATPSs are formed when two incompatible solutes, such as two polymers(e.g. polyethylene glycol, PEG, and dextran) or a polymer and a salt (e.g. PEG and phosphate salts), are mixed at a concentration higher than a critical value, so that they separate into two phases at equilibrium.[28,31] For example, after the separation occurs and according to the density of each phase, the top phase will be rich in one polymer (PEG) and the bottom phase will be rich in the other polymer or salt (phosphate), with water as the solvent in both phases. Having water as the major constituent of both phases provides a gentle environment for biomolecules to separate and allow the polymers to stabilize their structure and biological activities. Most systems used PEGs of different molecular weights polymers due to their low toxicity, low price and low volatility.[30] Depending on the properties of the system, biomolecules such as mAbs, may partition differently between the top and bottom phases in equilibrium and many variables can be manipulated to manipulate the partition.[31] These variables will be further explored in this section.

These systems present interesting advantages both for laboratory and industry processes since they are cost-effective, easy to scale up and suitable for continuous operation. However, the use of ATPSs for protein purification has been hampered by the generally poor predictability of the partition mechanism of any given protein in a particular system. Indeed, the partitioning of biological compounds in an ATPS results not only from a complex interplay of macromolecular properties such as molecular weight, amino acid composition, hydrophobicity and electrostatic forces, but also from the system composition.[28,31]

ATPSs composed of a polymer and a salt have been widely studied and are a generally attractive cost-effective alternative to polymer–polymer systems due to the use of inexpensive phase components. Nevertheless, the high consumption of phase-forming components and, consequently, their impact on wastewater treatment is a relevant issue for the application of these systems on a large scale. Although PEG is biodegradable and non-toxic, salt disposal, like phosphate salts, can be problematic. However, the possible recycling of phase components or the use of biodegradable salts such as citrate[7] can

minimize these limitations, being a viable alternative to purify the monoclonal antibodies in a larger scale.[28]

The partitioning of soluble molecules occurs between the two bulk phases, top and bottom phases. This partition is normally characterised by the partition coefficient, K_P, calculated as the ratio of the concentration of the solute in the top phase (C_t) to that in the bottom phase (C_b):[32]

$$K_p = \frac{C_t}{C_b} \qquad \textbf{(Equation 1)}$$

Then, K_P is a function not only of the properties of the two phases and the substance, but may also be significantly influenced by other factors such as the temperature or molecule concentration.[32] For example, as the temperature increases, the PEG structure becomes more extended and as a result its preferential interaction with the protein diminutions, decreasing the partition coefficient.[33] Regarding the molecule concentration, the partition coefficient will be constant at low protein concentration, the true partitioning behaviour, and will change at a high overall protein concentration.[34]

The composition of an ATPS can be obtained from a **phase diagram** (***Figure 1.7***). These phase diagram will delineate the potential working area for a particular two-phase system and is a "fingerprint" unique to that system under set a particular set of conditions such as, for example, pH, temperature and salt concentration. These phase diagrams provide critical information to work with a given system such as (1) the concentration of phase-forming components necessary to form a system with two phases in equilibrium, (2) the subsequent concentration of phase components in the top and bottom phases, and (3) the ratio of phase volumes.[32]

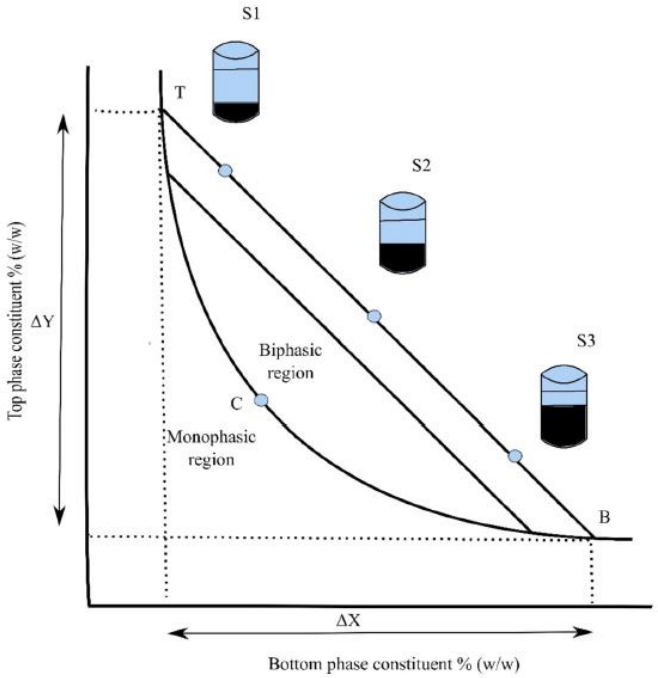

Figure 1.7 *- Schematic representation of a phase diagram. Concentrations above binodal curve (TCB) forms aqueous two-phase system. The line (TB) is a tie-line, connecting the two nodes, which lie on the binodal curve. Moving along the tie-line coordinates denote systems (S1, S2, S3) with differing total compositions and volume ratios, but with the same final concentration of phase components in the top and bottom phases. Reproduced from ref. 30.*

In the phase diagram, the **binodal curve** can be observed, which separates the regions forming a single phase (below the curve) or two immiscible phases (above the curve). Additionally, it is also possible to observe the different **tie-lines** that connect two nodes on the binodal curve and describe the final compositions of the two phases in equilibrium. Moving along the tie-line coordinates denote systems with differing total compositions of both phase forming components and volume ratios, but with the same concentration of phase components in the top and bottom phases. Also present on the binodal curve is a **critical point** (C), at which the composition and volume of both phases are equal.[32]

1.3.3. Factors influencing the partition of a target molecule

Phase separation in ATPS will be affected by different factors such as concentration and molecular weight (MW) of polymer, concentration and composition of salt and the pH.[30,35] Considering polymer-salt systems for example, although the mechanism through which salts influence ATPS is poorly understood, the type of salt and concentration of salt in the system will also influence phase formation behaviour, with a higher valency of the anion present in the salt, the lower the concentration required to form a two-phase system.[30,36] The relative effectiveness of various salts in promoting phase separation is seen to follow the Hofmeister series (a classification of ions based on their salting-out ability) and the contribution of the anion is more important than that of the cation in determining the effectiveness of a particular salt. For example, kosmotropic multivalent anions like HPO_4^{2-} and SO_4^{2-} are most effective in inducing phase separation.[32,37]

The complexity of the chemical and physical interactions that are involved in the partitioning process (for example, electrostatic and van der Waals forces, hydrogen bonding, hydrophobic interactions and steric effects) makes the behaviour of a particular biomolecule rather unique. Moreover, this also means that the partitioning of a compound can be manipulated in such a way that it should be possible to target the biomolecule to the desired phase.[28] The following properties of partitioning can be exploited individually or in conjunction to achieve an effective separation of a particular protein: hydrophobicity, where the hydrophobic properties of a phase system are used for separation according to the hydrophobicity of proteins; electrochemical, where the electrical potential between the phases is used to separate molecules or particles according to their charge; size-dependent partitioning, where molecular size of the proteins or surface area of the molecules (proteins) is the dominating factor; biospecific affinity, where the affinity between sites on the proteins and ligands attached to one of the phase polymers is exploited for separation; and, finally, conformation-dependent, where the conformation of the proteins is the determining factor.[35] Thus, the overall partition coefficient can be expressed in terms of all these individual factors:

$$K = K_0 \times K_{hfob} \times K_{el} \times K_{biosp} \times K_{size} \times K_{conf} \qquad \textbf{(Equation 2)}$$

where $hfob$, el, $biosp$, $size$, and $conf$ stand for hydrophobic, electrochemical, biospecific, size and conformational contributions to the partition coefficient and K_0 includes other factors.[35]

1.3.4. Polymer-salt ATPE in the downstream processing of mAbs: practical examples and considerations

As previously discussed, monoclonal antibodies have become very important in several areas, especially as biopharmaceuticals, and the demand of cost-effective, scalable and efficient antibodies is continuously increasing. Although, ATPS has proved to be a practical tool for the purification of a mixture of biomolecules, its use in the downstream processing of antibodies has been mostly confined to research only.[30]

For first time, in 1992, ATPS was used to purify monoclonal antibodies from hybridoma cell culture supernatant by Sulk *et al*., which proposed a process using an aqueous two-phase extraction step followed by a thiophilic adsorption chromatography. The system was composed by 5% PEG 1540 and 22% phosphate, with the monoclonal antibody preferentially associating with the PEG-rich top phase whereas other proteins such as albumin and transferrin partition into the salt-rich bottom phase. This process recovery yield in IgG1 was 71%, with 90% recovery in the ATPS step and a purification factor of 6.2.[6]

In 1996, Andrews *et al*. proposed a two-stage process for the recovery of a murine IgG1, also from a hybridoma supernatant, that involved a first extraction to the PEG-rich phase of an ATPS composed of PEG, phosphate and NaCl, followed by a second extraction with a fresh phosphate solution. In this case, a low-molecular weight PEG was also used (1450 Da), but since a lower salt concentration of 14% phosphate was chosen, it was necessary to add up to 12% NaCl to promote salting-out and to recover the majority of the antibodies in the upper phase. Therefore, the first extraction of IgG to the PEG-rich phase had a recovery yield of 90% and a purification factor of 2.7 and the second, extraction into a new phosphate-rich phase, had final purification factors ranging from 5.9 to 7.3. [7,28]

Only after ten years, in 2006, when interest in this technique has re-emerged due to the need for alternative downstream processing methods, Platis *et al*. proposed an aqueous two-phase partitioning system for the initial fractionation step of a therapeutic mAb from transgenic tobacco extracts. Using an ATPS composed of 12% PEG 1500 and 13% phosphate buffer at pH 5, a purification of 3 to 4-fold with high recovery at the bottom phase (approximately 95%) was achieved for the mAb. After a conditioning step, this bottom phase was loaded on a Protein A chromatography column. Although similar purification factors were obtained compared to a single Protein A chromatography step, the combination of aqueous two-phase extraction and Protein A chromatography not only allowed the complete removal of phenolic and alkaloid compounds from the tobacco leaves but also improved the performance of the affinity column. [28,38]

In 2007, a series of papers that reinforced the potential of using ATPE for the initial purification antibodies was published by the research group of Prof. Aires-Barros. Rosa *et al*. demonstrated the possibility of using these systems for the purification of antibodies from an artificial mixture of proteins containing human serum albumin and myoglobin. The system composed of 8% PEG 3350, 10% phosphate at pH 6 and 15% NaCl showed the best recovery yield (101%), purity (99%) and yield of native IgG (97%). A second extraction of IgG was performed to a new phosphate phase and higher

yields were obtained using 10% phosphate at pH 6. The total extraction yield was of 76% and the purity of 100%. This study also demonstrated that a shift in the partitioning of antibodies towards the phase with less impurities was possible by increasing the concentration of the neutral salt NaCl.[8,28] In another research work by the same authors, the recovery of human IgG from Chinese hamster ovary (CHO) and hybridoma cell culture supernatant was reported using PEG 6000 and phosphate. An ATPS composed of 12% PEG, 10% phosphate, 15% NaCl at pH 6 was used to purify human monoclonal antibodies from a CHO concentrated cell culture supernatant with a recovery yield of 88% in the upper PEG-rich phase and a purification factor of 4.3; and from a hybridoma cell culture supernatant with a comparable performance, providing a recovery yield of 90% and a purification factor of 4.1.[1,28]

In 2009, Rosa *et al*. explored several experimental conditions such as pH, ionic strength, volume ratio and initial antibody concentration using PEG 3350/phosphate ATPSs in order to extract human antibodies from a CHO cells supernatant in a single-stage. The conditions that favoured the extraction were low pH values, high NaCl concentration and high-volume ratios. A multi-stage equilibrium aqueous two-phase extraction was also studied and mAb recovery yields of 89% and protein purities of 75% could be achieved using a PEG/phosphate ATPS with NaCl. This represents significant improvements when compared to a single-stage trial performed at the same experimental conditions, where a 61% recovery yield and 55% protein purity were obtained.[3]

In conclusion, the previously discussed literature has shown the great potential of ATPE for the purification of antibodies from a cell culture supernatant, providing high recovery yields and purities.

1.4. Miniaturization of an Aqueous Two-phase System

Despite the diverse possible applications of polymer–salt based extraction systems for the downstream processing of monoclonal antibodies, the use of these systems has so far been limited due to the poor predictability and the large number of parameters influencing the partitioning result. Also, performing an empirical screening of several conditions can be time-consuming, labour-intensive and require large volumes of reagents. For these reasons, robotic high throughput screening platforms are a promising breakthrough to effectively optimize ATPE[39]: the necessity of being ‘first on the market’ combined with the need to cut production costs highlights the demand for strategies and techniques allowing fast process development while at the same time covering a large number of potential process parameters in order to reach an optimal process performance.[40] Recently, microfluidic high throughput screening devices have been used for diverse applications, ranging from the analyses of the presence of toxins in a sample[41] or the detection of disease specific antigene[42]. The main advantages of working in a microfluidic environment are related to the small sample size required, often falling into the µL or nL-scale, shorter reaction times, portability, low cost, the great control over the fluid and surface conditions, versatility in design, and potential for parallel operation and for integration with other miniaturized devices.[43] Hence, a miniaturized ATPS can be a powerful solution to speed up the bioprocess design, reducing costs, since it is an automated screening approach allowing parameter evaluation of a multi-parameter space within a short period of time.[39]

1.4.1. Fabrication of microfluidic devices

Typically, microfluidic devices can be fabricated from silicon, glass and polymers, or combinations of these materials. Silicon can be a promising substrate, already existing technologies originated from the semiconductor industry, but it presents two major drawbacks: high cost and its optical opacity, limiting its applications in real-time optical detection. In this context, glass is a far more promising alternative with well-defined surface chemistries and superior optical transparency. Nevertheless, when considering cost, time and labor, polymers are becoming more attractive and some of the various materials typically used are poly(styrene), polyvinyl chloride (PVC), poly(carbonate) and poly(dimethylsiloxane) (PDMS). Among these, PDMS is by far the dominant material considering its numerous advantages such as its elastomeric properties, biocompatibility, optical transparency and easiness of molding. However, this material presents a disadvantage, its high native hydrophobicity, which generally difficult the flow of liquids into the microchannels and promotes non-specific protein adsorption. Nevertheless, these issues can be easily overcome by surface modifications.[44]

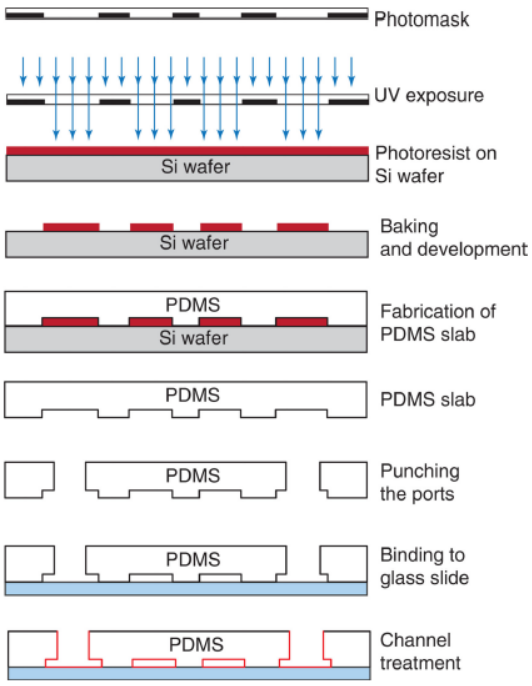

Figure 1.8 - Representation of the steps involved in the micro-fabrication process. Reproduced from ref. 47.

The typical method employed for the fabrication of PDMS structures is soft lithography (***Figure 1.8***).[45] First, a photomask is fabricated by patterning an opaque material (e.g. aluminium or chromium), which will be used to expose the photoresist (e.g. SU-8 photoresist) with UV light in order to imprint the desired design in the silicon wafer. After the baking and the development of the exposed photoresist will occur, followed with the coating of the structure with PDMS, forming a mold which will be used to fabricate several structures by lift-off.[46] It may be required to seal the PDMS structure, reversibly or irreversibly, against a variety of materials including PDMS and glass. With PDMS, surface oxidation to increase the bond strength by activating layers of cross-linked PDMS in oxygen plasma can be performed, generating silanol groups (OH) at the surface of the PDMS layers that when brought together form covalent siloxane bonds (Si–O–Si).[47]

1.4.2. Considerations about ATPE performed at the micro-scale

At the micro-scale, there are some physical phenomena that gain a larger magnitude whereas others became negligible. For example, in a microfluidic ATPS, turbulence and convective mixing are typically absent and a laminar flow becomes predominant. The type of flow present in a stream of liquid is indicated by the value of the Reynolds number, Re, defined by:

$$Re = \frac{\rho v D_H}{\mu} \qquad \textbf{(Equation 3)}$$

where ρ is the fluid density, v is the fluid velocity, D_H is the hydraulic diameter and μ is the fluid dynamic viscosity. When Re is a high value, turbulent flow is present, whereas, in microfluidic devices, the value of the Re typically displayed is minor or in the magnitude of 1, indicating the laminar flow.[48]

Therefore, without turbulence molecular transport occurs perpendicularly to the flow direction (assuming residence times >> diffusion coefficient) by diffusion only, according to Fick's first law:

$$N = D\left(\frac{\Delta c}{x}\right) \qquad \textbf{(Equation 4)}$$

where N is the solute flux, D is the diffusion coefficient, x is the distance of diffusion, Δc is the molar concentration difference between two points in space at x distance from each other. Therefore, in a microfluidic ATPS, the partition occurs exclusively by diffusion at the interface between phase 1 and 2 according with:

$$N = D\left(\frac{c_1 - c_2 K}{x}\right) \qquad \textbf{(Equation 5)}$$

where c_1 is the molar concentration in the top phase, c_2 is the molar concentration in the bottom phase and K is the partition coefficient of the solute in a ATPS.[49]

When adapting this type of extraction to a micro-scale, it becomes an intrinsically continuous process, meaning that each phase is continuously pumped parallel to each other through the channel, with the liquid flow velocities becoming the critical variables to consider. Also, the laminar flow characteristics of microfluidics allows multiphase formation and stabilization with more than two inlets (n), which can potentially be useful for numerous applications (***Figure 1.9***).

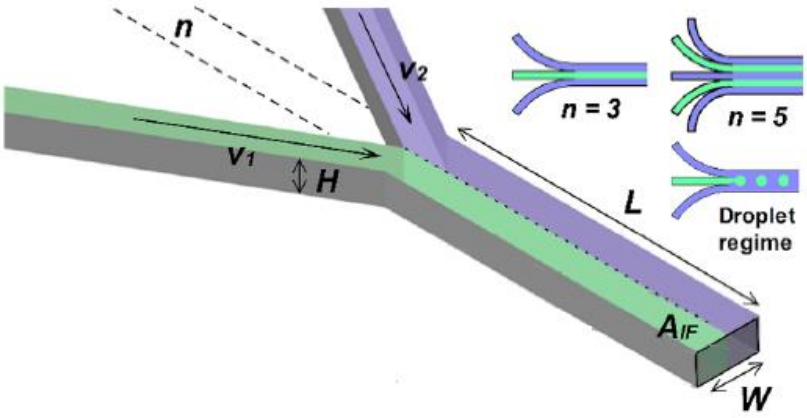

Figure 1.9 *- Representation of an aqueous two-phase extraction performed in a microfluidic channel. L corresponds to the length of the microchannel, W to the width of the microchannel, H to the height of the microchannel, n to the number of inlets converging into the main separation channel, v1 and v2-to the liquid velocities of each of the immiscible phases 1 and 2, and AIF to the total interfacial area between the phases, identified as a dotted line. Reproduced from ref. 49.*

In addition, the interfacial effects will be more significant at the microscale, such as a lower Bond (Bo) number:

$$Bo = \frac{\Delta \rho g L^2}{\sigma} \qquad \textbf{(Equation 6)}$$

where $\Delta\rho$ is the difference in densities, g the acceleration of gravity, L the characteristic length scale and σ the surface tension, implying that gravity related effects are negligible; and adjustable Weber (We) and Capillary (Ca) numbers:

$$We = \frac{\rho v^2 L}{\sigma} \quad \textbf{(Equation 7)}$$

$$Ca = \frac{\mu v}{\sigma} \quad \textbf{(Equation 8)}$$

where v is the linear velocity of the liquid and μ the dynamic viscosity, making e inertial and viscous forces either significant or negligible. The manipulation of these two numbers allows droplet formation or the preferential wetting of the microchannel surface by one of the phases, in conditions where the inertial forces are not sufficiently high to maintain a planar interface. Concluding, the flow velocities and channel dimensions have to be optimized for each system so that a stable flow-regime is formed.[49]

Because of this type of behaviour, microfluidics is particularly attractive to perform ATPE due to the possibility of creating a parallel laminar flow of the phases with the interface running along the microchannel as a result of the laminar flow, the very large surface area-to-volume ratio and the easy separation of the phases, leading to the possibility of continuous processing and to a possible increase in separation efficiency.[50]

1.4.3. Applications of miniaturized ATPE

In 2005, Nam et al., separated live and dead CHO-K1 (Chinese Hamster Ovary) cells by continuous-flow extraction in a microfluidic device using aqueous two-phase extraction. PEG 8000 and dextran T500 (5%) were selected as model polymer solutions and the separation efficiency of live and dead CHOK-1 cells from the culture broth was compared in the macroscale and microfluidic device. At the microscale, most live cells were distributed to PEG-rich phase, while dead cells were found at the interface, with a recovery and fractionation efficiency of live cells being 100% and 97.0%, respectively.[51]

Tsukamoto *et al*., in 2009, used a microfluidic ATPE to isolate leukocyte and erythrocyte cells from whole blood cells: erythrocytes moved to the dextran-rich phase while leukocytes remained in the PEG-rich phase.[52]

Huh *et al*., in 2010, developed a microfluidic ATPE to purify bacteriorhodopsin from the membrane of *Halobacterium salinarium*, followed by a three-flow desalting system, used to remove the salts. Similar purity and yield were achieved relative to conventional bacteriorhodopsin separation techniques.[53]

In 2011, Hu *et al*. established a microfluidic aqueous PEG/detergent two-phase system for the purification of membrane proteins from crude cell extract, replacing the conventional discontinuous agitation method with continuous extraction, resulting in significantly increased extraction speed and efficiency. Approximately 90% of the purified proteins were membrane proteins (the highest extraction efficiency reported up to date), including membrane-associated proteins and integral membrane proteins with multiple transmembrane domains.[54]

In 2012, Silva *et al*. designed an ATPE in a microfluidic device for the extraction of mAbs since microscale process techniques are an effective tool to accelerate bioprocess design and optimization.

Fluorescence microscopy was used for the measurement of the phenomena of diffusion and partition of IgG from phosphate-rich phase to PEG-rich phase with NaCl. The reduction to the microscale did not greatly affect the antibody extraction yield when compared with macroscale results, while simultaneously reducing the operation time, demonstrating the potential of this approach for process optimization.[11] The same authors, in 2014, determined the characteristic ATPS binodal curves resorting to a microfluidic device, rapidly testing a wide range of concentrations inside the microchannel with a few µL of each solution.[50] In 2017, the same authors developed a microfluidic platform to determine the partition coefficients of biomolecules in different ATPSs using fluorescence microscopy to track the fluorophore labelled molecules, allowing for a significantly faster screening.[5]

Jacinto *et al*., in 2015, optimized the purification of Human Immunodeficiency Virus (HIV) virus-like particles (VLP) in multiple polymer-polymer and polymer-salt systems. Using PEG–ammonium sulphate as the optimum system to maximize the partition coefficient, values of 4.4 and 3.9 were obtained in microtubes and microchannels, respectively, highlighting a good correlation between batch and continuous modes and the macro and microscale.[9]

In 2017, Bras *et al*. presented a methodology for the rapid screening of affinity-based ATPE conditions to extract antibodies, using a microfluidic device toolbox composed of two microfluidic structures. The first structure allowed the screening of the partition coefficients under 8 extraction conditions simultaneously whereas the second structure allowed the testing of multi-step extraction protocols using the optimized conditions from the first structure. The volumes used in this microfluidic device were less than 20 µL of each phase-forming solution per experiment, being a cost-efficient approach to study the partition in a ATPS. The results showed a good correlation between the partition coefficients obtained for microscale and macroscale approaches was demonstrated, thus validating the microfluidic device in question.[10]

Concluding, the combination of ATPS and high throughput screening techniques resorting to a miniaturized approach is highly promising, potentially facilitating future explorations in research labs and paving the way towards industrial applications.[39]

1.5. Fluorescence and Fluorescent Probes

1.5.1. Fundamentals of fluorescence

Fluorescence is the property of some atoms and molecules to absorb light of a particular wavelength and, after a brief interval of time, typically ranging from ns to µs (designated fluorescence lifetime), emit light at longer wavelengths.[55] In the absence of an excitation source, a molecule sits on the lowest energy level of the ground state, S_0. By exciting the molecule with light of an appropriate wavelength (sufficient to overcome the energy barrier between S_0 and S_1), the incident photons promote excitation to upper vibrational levels of the first singlet excited state, S_1. The electrons then decay non-radiatively to the lowest level of the excited state and subsequently to any of the vibrational levels of the ground state, thus emitting fluorescence (***Figure 1.10***).

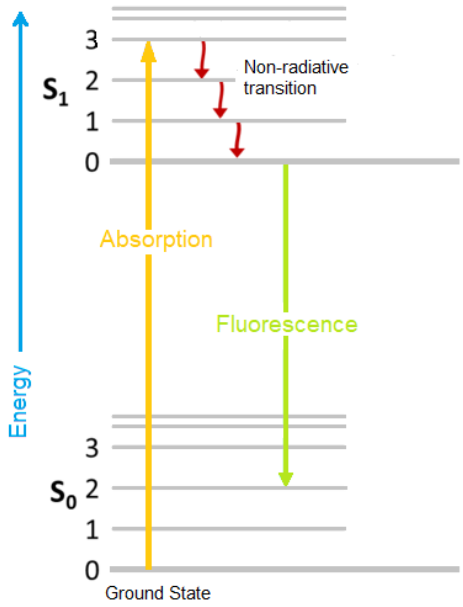

Figure 1.10 - Jablonski diagram of the fluorescence phenomenon.

Once a molecule is excited by the absorption of a photon, it can return to the ground state with emission of fluorescence, but other pathways for de-excitation are also possible and may compete with this emission: internal conversion (direct return to the ground state without emission of fluorescence), intersystem crossing (possibly followed by emission of phosphorescence), intramolecular charge transfer and conformational change.[56]

This phenomenon presents several characteristics, for example, the energy of emission is less than that of excitation, i.e., it has a longer wavelength than the exciting light, an effect known as the Stoke's shift.[57] Another general property is that the same fluorescence emission spectra are usually independent of the excitation wavelength, designated as Kasha's rule, due to, upon excitation into higher vibrational levels, the excess energy is quickly dissipated.[58]

The Fluorescence intensity is proportional to the amount of light absorbed multiplied by the quantum yield, Q, which is a measurement of the efficiency of photon emission, defined by the ratio of the number of emitted photons (over the whole duration of the decay) to the number of absorbed photons.[55,56] Beer's law asserts that for low optical densities, the amount of fluorescence, F, is proportional to the product of the light absorbed by the fluorophore concentration and the quantum yield:

$$F = I_0 \varepsilon [C] X Q \qquad \textbf{(Equation 9)}$$

where I_0 is the intensity of the light beam, ε is the molar extinction coefficient of the fluorophore, $[C]$ is the concentration of the fluorophore and X is the pathlength through the solution.[55]

A fluorophore, *i.e.* a fluorescent chemical compound, can be divided into two general classes, intrinsic and extrinsic. Intrinsic fluorophores are those that occur naturally and include the aromatic amino acids, NADH, flavins, derivatives of pyridoxyl, and chlorophyll. Frequently the molecules of interest are non-fluorescent or the intrinsic fluorescence is not adequate, thus extrinsic fluorophores are added to the sample to provide fluorescence or to change the spectral properties of the sample. A few

examples of this substances are dansyl, fluorescein and rhodamine. A good fluorescent probe should display a high intensity, be stable during continued illumination (low photobleaching effects), and does not significantly disturb the biomolecule or process being studied.[58]

In the case of proteins, it is frequently desirable that these are labelled with fluorophores with longer excitation and emission wavelengths relative to the intrinsic fluorescent aromatic amino acids. In that sense there are numerous fluorophores available for covalent and noncovalent protein labelling.[58] For this labelling, the proper choice of a fluorescent probe is critical to obtain unambiguous interpretation of the obtained results[56]. Thus, several points must be taken into consideration:

- The entire fluorescence process is cyclical and, unless the fluorophore is irreversibly destroyed in the excited state (photobleaching), the same fluorophore can be repeatedly excited and detected, generating many thousands of detectable photons per unit time.[59] However, almost all fluorophores are gradually photobleached upon continuous illumination, especially in fluorescence microscopy where the light intensities are high.[58]
- Fluorescence quenching is defined as a bimolecular process that reduces the fluorescence quantum yield. Self-quenching occurs when one fluorophore is quenched by another and tends to occur when high loading concentrations or labelling densities are used.[59]
- Environmental factors can influence the fluorescence properties, such as the solvent polarity and the pH of the aqueous medium.[59]

1.5.2. Examples of labelling mechanisms: amine and thiol modifications

Amine modification

The primary targets for amine modification of proteins are the lysine residues and the free amine at the N-terminus, present in virtually all proteins. The most significant factors affecting an amine's reactivity are the class (aliphatic or aromatic) and the basicity. Aliphatic amines, like the lysine's ε-amino group, are moderately basic and reactive with most acylating reagents but the concentration of the free base form of aliphatic amines below pH 8 is reduced. Therefore, the kinetics of amine acylation is strongly pH dependent and a pH from 8.5 to 9.5 is usually optimal for modifying these lysine residues. In contrast, the α-amino group at a protein's N-terminus usually has a pKa of 7, thus it can be selectively modified by reaction at near neutral pH.[59,60]

For example, a typical IgG antibody molecule has around 90 lysine residues, of which, about 30 will be modified under conditions of high acylating reagent concentration and prolonged incubation. However, to preserve the antigen binding affinity for example, this typically requires a degree of labelling of less than 10 dyes per IgG, which is considered a low fractional modification of available targets, creating polydisperse mixtures containing a range of dye:protein stoichiometries.[59] To maximize the modification of amines a high concentration of protein in the reaction medium is essential and by adjusting the molar ratio of dye to target molecule, the level of modification can be controlled to create an optimal product.[60]

Succinimidyl esters are reliable reagents for amine modification because the amide bonds they form are as stable as peptide bonds (***Figure 1.11***). These reagents show good reactivity with aliphatic amines and very low reactivity with other functional groups, such as aromatic amines, alcohols, phenols (including tyrosine) and histidine.[59]

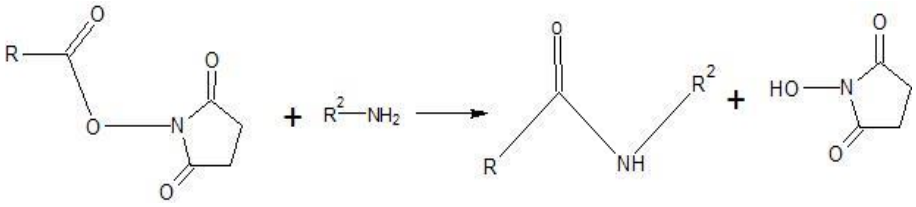

Figure 1.11 - Standard succinimidyl ester modification reaction, forming an amide bond. Adapted from ref. 59.

Thiol modification

In this case, the primary targets of thiol-reactive probes are cysteine residues, which are significantly less common in proteins than lysine residues. Therefore, the relatively low abundance of cysteine residues allows modification with less risk of protein precipitation and fluorescence self-quenching interactions which can hinder the amine-reactive modification. However, in proteins with multiple cysteine residues, the reactivity of an individual cysteine can be highly dependent on both its local environment and the hydrophobicity of the reactive dye.[59]

The maleimide group can be used to label the cysteine residues. The double bond of maleimides undergo an alkylation reaction with sulfhydryl groups to form stable thioether bonds. Maleimide reactions are specific for thiols in the pH range of 6.5–7.5. One of the carbons adjacent to the maleimide double bond undergoes nucleophilic attack by the thiolate anion to generate the addition product (***Figure 1.12***).[60]

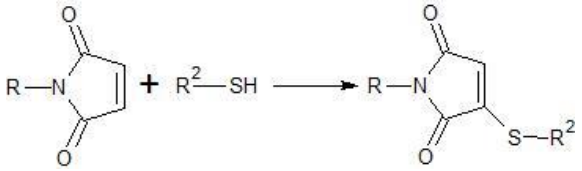

Figure 1.12 - Standard reaction of a thiol with a maleimide, forming a thioether. Adapted from ref. 59.

Occasionally, even proteins containing structurally critical disulphides can be partially reduced to yield a useful thiolate derivative. IgG molecules contain four disulphide groups: holding together the two heavy chains and holding the light chain–heavy chain pairs together. Selective reduction of some or all of the disulphide groups can result in an antibody molecule that still maintains its antigen binding capability, which can be acceptable for biosensing applications, for example. However, for ATPE, the selective separation in both phases will be highly dependent on the surface properties of the proteins[34], so reduction of all of the disulphide groups could heavily affect the characteristics of the antibody, and thus the molecular partition behaviour. Reductants, such as tris(2-carboxyethyl)phosphine (TCEP) (***Figure 1.13***), in a non-denaturing environment, can be used at low concentrations to perform this type of partial cleavage. The advantages of this molecule in disulphide reduction is: excellent stability in aqueous solution, lack of reactivity with other common functionalities in biomolecules and lack of odour.[60]

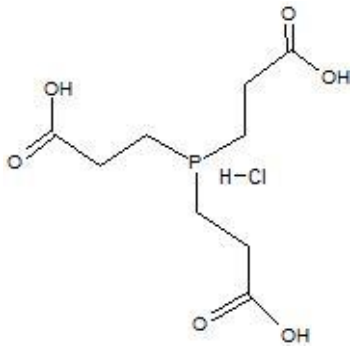

Figure 1.13 - Chemical structure of the or tris(2-carboxyethyl)phosphine (TCEP) molecule. Adapted from ref. 60.

The reaction of TCEP with biological disulphides proceeds with initial cleavage of the S - S bond followed by oxidation of the phosphine (***Figure 1.14***). The stability of the phosphine oxide bond formed is sufficient to prevent reversal of the reaction. Since this reaction is performed without any added -SH compounds, subsequent conjugation with the generated sulfhydryl groups can be done without removal of excess TCEP or reaction by-products.[59,60]

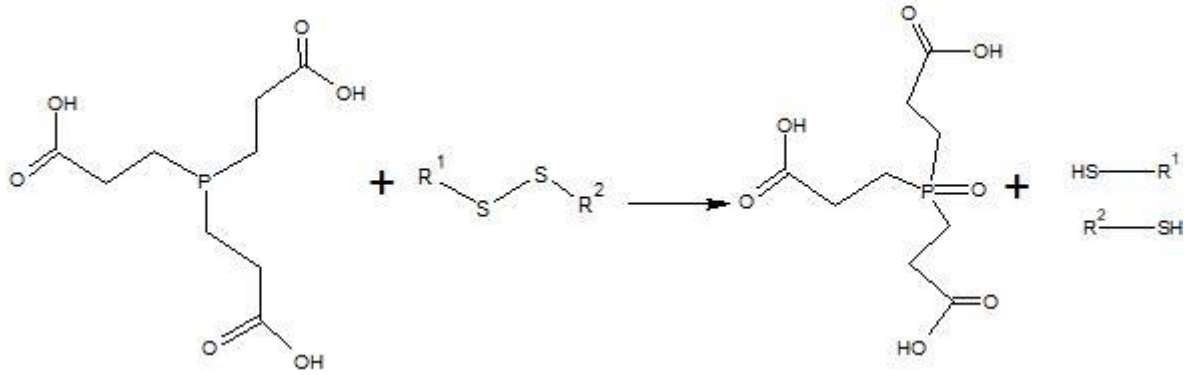

Figure 1.14 - Chemical reaction of TCEP with disulphides, beginning with the initial cleavage of the S-S bond followed by oxidation of the phosphine. Adapted from ref. 59.

Sun *et al*., in 2005, reported that the use of a 2.75 molar excess of TCEP over the concentration of a monoclonal IgG resulted in the reduction of only two disulphide bonds in the hinge region of the antibody, leaving all other disulphides intact.[60,61]

Following conjugation with any dye, it is crucial to remove as much unconjugated labelling reagent as possible, usually by gel filtration, dialysis or bioconjugate precipitation. The presence of free dye, particularly if it remains chemically reactive, can greatly complicate subsequent experiments with the bioconjugate.[59]

1.5.3. Fluorophores employed in miniaturized ATPE: practical examples and considerations

In 2012, Silva *et al.* designed an ATPE in a microfluidic device for the extraction of mAbs resorting to fluorescence microscopy to follow the partition from the salt-rich phase to the PEG-rich phase. The IgG was tagged with fluorescein isothiocyanate (FITC), with an excitation and emission spectrum peak wavelengths of approximately 495 and 519 nm, respectively.[11] Later studies, in 2017, by the same authors and also using fluorescence microscopy, several biomolecules of interest (IgG, bovine serum

albumin, protein A and insulin) were also tagged with FITC to determine the partition coefficients in different ATPS.[5]

In 2015, Jacinto *et al*., constructed a continuous microfluidic ATPE device to purify a Human Immunodeficiency Virus (HIV) virus-like particles (VLP) with a PEG–ammonium sulphate system. The extraction was monitor through fluorescence microscopy and the VLP from HIV was produced in Chinese Hamster Ovary (CHO) cell cultures with a covalent bond to a Green Fluorescent Protein (GFP) tag. This study showed a good correlation between the macro and microscale, both in terms of K_P and protein purity.[9]

Bras *et al*., in 2017, presented a methodology for the fast screening of the necessary conditions to extract biopharmaceuticals, such as monoclonal antibodies, using a microfluidic channel-based toolbox composed of two microfluidic structures. This toolbox used fluorescence to follow the biomolecule's extraction, with LYTAG fused to GFP and IgG being labelled with FITC.[10]

Concluding, the aforementioned work showed, in great detail, the use of microfluidic aqueous two-phase extraction platforms employing fluorescence microscopy can be operated for the purification of a diversity of biomolecules. However, the fluorophores chosen were the FITC, which mainly labels the primary amines of proteins[60], and the GFP, a protein with a vast size (27 kDa) which has been reported to cause functional perturbations.[59] Although both fluorescent tags have valuable applications in studying protein dynamics in living cells and bioimaging[62,63], in ATPE, the molecular partition into the two immiscible phases is highly dependent on the surface properties of the proteins[34] and the labelling can interfere with these proprieties. In these experimental works, no previous complementary studies on the surface proprieties of the molecule, to access any possible modification, were revealed. The molecular weight and overall charge of the labelled molecules should have been evaluated, especially when the fluorophores could cause significantly changes in these characteristics. Therefore, the obtained results cannot be undoubtedly extrapolated to the unlabelled molecule.

2. Materials and Methods

2.1. Materials

2.1.1. Chemicals

PEG polymers with molecular weights of 1500 (Acros Organic), 6000 (Fluka Analytical), 3350 and 8000 Da (Sigma-Aldrich) were each dissolved in Milli-Q water in order to obtain stock solutions with a concentration of 50% (w/w). The salts, sodium phosphate monobasic anhydrous and potassium phosphate dibasic, were both acquired from AppliChem PanReac and stock solutions of 40% (w/w) in Milli-Q water were prepared, where the acid form (NaH_2PO_4) is 0.43-fold the amount of the basic form (K_2HPO_4) of the salt in order to obtain a pH value of 7. Sodium chloride (NaCl) was purchased from AppliChem PanReac and dissolved in Milli-Q water to prepare a stock solution of 20% (w/w). Phosphate buffered saline (PBS) was acquired from Sigma-Aldrich. Alexa Fluor® 430 NHS ester (with an excitation wavelength of 430 nm and an emission wavelength of 545 nm) was obtained from Life Technologies, whereas BODIPY™ FL maleimide and BODIPY™ FL NHS ester (with an excitation wavelength of 503 nm and an emission wavelength of 509 nm) were both purchased from Lumiprobe.

The reagents used for SDS-PAGE gels were ammonium persulphate (APS), N,N,N,N-tetramethylethylenediamine (TEMED), 30% acrylamide/bisacrylamide-solution, purchased from Sigma-Aldrich, and SDS micropellets (sodiumdodecyl sulphate) acquired from BIO-RAD. Coomassie brilliant blue R-250 was acquired from GE Healthcare, ethanol from Manuel Vieira & Companhia (Irmão) Sucessores Lda, acetic acid from Fisher Chemical, silver nitrate solution and formaldehyde solution from AppliChem PanReac, sodium thiosulfate and sodium carbonate from Sigma-Aldrich. For the isoelectric focusing (IEF), the kit and the marker used were obtained from GE Healthcare and trichloroacetic acid solution and glutaraldehyde were purchased from Merck and Sigma-Aldrich, respectively.

2.1.2. Labelling of IgG with fluorescent tags

Human normal immunoglobulin, with the commercial name Gammanorm®, was obtained from Octapharma (Lachen, Switzerland), with a concentration of 165 $mg.mL^{-1}$ and 95% IgG (59% IgG1; 36% IgG2; 4.9% IgG3; 0.5% IgG4 and a maximum of 82.5 $\mu g.mL^{-1}$ of IgA).

To prepare the IgG conjugated with Alexa Fluor® 430 NHS ester, a protocol from Pinto *et al.* was followed.[64] The commercial antibody mixture was first diluted in 0.1 M sodium bicarbonate buffer to a concentration of 20 $mg.mL^{-1}$. Then, the diluted IgG solution was conjugated to the amine-reactive dye by mixing a 100:1, 50:1 and 25:1 molar ratio of reactive dye solution to antibody to obtain different degrees of labelling. The reaction was incubated in the dark with mild agitation for 1 hour at room temperature. In order to remove the non-conjugated dye, the final solution was washed with PBS in a series of 8 diafiltration steps using Amicon Ultra-0.5 centrifugal filter units (MWCO of 10 kDa), centrifuged at 14,000 × g for 10 minutes.[64]

To obtain the antibody conjugate with BODIPY™ FL NHS Ester, the Gammanorm® was diluted to a final concentration of 5 mg.mL^{-1} in 0.1 M sodium bicarbonate at a pH of 9.0. Next, the dye was mixed with the diluted solution of IgG in a vortex for 3 seconds, in a proportion of 100:1 molar ratio of antibody to reactive dye solution. To achieve a higher degree of labelling with this fluorescent tag, 10% of PEG 3350 was added (to the total volume), solubilizing the dye and preventing the formation of aggregates. Then, the reaction was incubated in the dark with mild agitation for at least 4 hours at room temperature. To eliminate any non-conjugated dye, the final solution was washed with PBS in a series of 8 diafiltration according to the same protocol described above.

Finally, for the labelling with BODIPY™ FL maleimide, the Gammanorm® was first diluted to a final concentration of 8.5 mg.mL^{-1} in PBS. Next, the dye was mixed with the diluted solution of IgG, in a proportion of 20 mol dye to 1 mol IgG, in a vortex for 3 seconds. The resulting solution was incubated in the dark for 2 hours with mild agitation. Finally, to remove any free dye the solution was washed with PBS in a series of 10 diafiltration steps using the same protocol described above, modified with a shorter centrifugation time of 5 min. To generate free thiol groups without compromising the tertiary structure, an additional step was performed before the antibody-dye conjugation comprising the addition of the reducing agent tris(2-carboxyethyl)phosphine (TCEP) dissolved in PBS in a molar proportion of 0.5 to 1 mol of IgG[60], mixing in a vortex for 3 seconds.

2.2. Aqueous two-phase extraction studies

2.2.1. mL-scale experiments

Aqueous two-phase systems were prepared by weighting the corresponding stock solutions of PEG polymers and salts to achieve the desired final composition of each system. The ATPS prepared had a total volume of 1.5 mL and were spiked with the biomolecule of interest in Eppendorf tubes, vortexed for 30 seconds and then centrifuged for 5 minutes at 1400 $\times\, g$, to separate the two phases. The top phase was then retrieved using a micropipette and the bottom phase with a syringe, each being placed in a new 1.5 mL Eppendorf, taking extra care not to disturb the interface. The samples were recovered for the subsequent determination of IgG concentration.

The partition coefficient, K_P, was previously characterized in the ***Equation 1*** and the extraction yield of the top phase of the antibody IgG, Y_{Top}, was defined:

$$Y_{Top} = \frac{m_{top}}{m_{total}} \qquad \textbf{(Equation 10)}$$

where m_{top} is the mass of IgG in the upper phase and m_{total} is the mass of IgG added to the system.

2.2.2. nL-scale experiments

As described above, the ATPSs were prepared by weighting the corresponding stock solutions of PEG polymers along with the appropriate salts, with a total volume of 1.5 mL. The tube was then vortexed for 30 seconds and centrifuged for 5 minutes at 1400 $\times\, g$, the top phase was retrieved using a micropipette and the bottom phase with a syringe, each being placed in a new 1.5 mL Eppendorf tube. The bottom phase was then spiked with the labelled biomolecule of interest and both samples were

taken for the determination of labelled IgG concentration. In these experiments, the partition coefficient, K_P, was defined as the ratio of the IgG concentration in the PEG phase to that in the salt phase.

2.3. Microfluidic device fabrication

The fabrication of the two designs of microfluidic devices used in this experimental work started by designing the microchannels in a CAD software, subsequently transferred to a 1.5 µm thick layer of positive photoresist layer, spin-coated on top of an opaque 200 nm thick film of aluminium, previously deposited in a Nordiko 7000 magnetron sputtering system. The exposure of the photoresist was performed at 405 nm using direct write lithography (Heidelberg DWL II). After developing the photoresist, the unprotected aluminium was fully etched by wet etching using an aluminium etchant standard mix. In order to fabricate the molds, an SU-8 layer was spin-coated on top of a clean silicon substrate. The SU-8 photoresist was purchased from Microchem and the spin-coater was a Laurel WS-650-23. The mask was then placed over the SU-8, with the aluminium surface facing down, after 4 minutes of pre-exposure bake at 95°C on a hotplate. The mask-silicon substrate stack was exposed to a UV light source, inducing the polymerization and hardening of the polymer, during a post-exposure bake for 5 minutes, at 95°C. Afterwards, the development of the non-exposed resist was performed by submerging the substrate on a propylene glycol monomethyl ether acetate (PGMEA) 99% solution, purchased from Sigma-Aldrich. Then, the substrate was subjected to a final 150°C baking step for 15 minutes. The microfluidic device was fabricated by pouring PDMS pre-polymer (SYLGARD 184 silicon elastomer kit), previously mixed with 1:10 parts reticulating agent and degassed in a desiccator, over the SU-8 mould. The PDMS was left to reticulate in an oven at 70°C for 90 minutes and then peeled off from the mold and access holes were punched with a blunt needle through the inlets and outlets of the structure. The PDMS structures were sealed against glass slides after performing an oxygen plasma treatment on both sides (Harrick Plasma PDC-002-CE, 800 mTorr, 1 minute exposure) and joining the two parts. Additionally, an epoxy mold was fabricated from a PDMS structure. The epoxy glue was spread evenly on top of the PDMS structure to a height of approximately 1 mm. The epoxy glue was then degassed for 48 hours, followed by a curing step at 120°C for 30 minutes in a convection oven.

2.4. Analytical methods

2.4.1. Quantification of non-labelled IgG

For the protein quantification in the top and bottom phases after ATPE, three different methodologies were tested: UV absorption at 280 nm, bicinchoninic acid (BCA) method and protein G affinity chromatography. The first technique evaluated was UV absorption at 280 nm, based on the intrinsic absorption of the tyrosine, tryptophan and phenylamine amino acid residues in the IgG molecules. The spectrometer used was a SpectraMax Plus 384 Microplate Reader from Molecular Devices (Silicon Valley, CA, USA). The samples from the top and bottom phases were diluted 10 times in Milli-Q water and placed in a 96-well microtiter plates. To avoid interference from PEG and phosphate, all samples were analysed against blanks containing the same phase composition, but without IgG. To validate the IgG concentration, a calibration curve was constructed using Gammanorm® stock solutions,

with a concentration ranging from 10 to 500 μg.mL^{-1} (***Figure A1*** – Supplementary Material). The bicinchoninic acid (BCA) method was performed resorting to the same spectrometer and using a protein assay kit supplied by Thermo Fisher Scientific. In this case the absorbance was measured at 562 nm. Similarly to the previous method, all samples were measured against blanks containing the same phase composition without IgG. Samples were also diluted 10 times in Milli-Q water. A calibration curve was measured to determine the IgG concentration, using Gammanorm® IgG as a standard, with a concentration ranging from of 25 to 2000 μg.mL^{-1} (***Figure A2*** – Supplementary Material). The concentration of IgG was also determined by affinity chromatography in an Äkta™ Purifier 10 system from GE Healthcare (Uppsala, Sweden) equipped with an analytical POROS Protein G affinity column (2.1 x 30 mm) from Applied Biosystems (Foster City, CA, USA). The adsorption buffer was composed by 50 mM sodium phosphate buffer and 150 mM NaCl, at pH 7.4, whereas elution was carried out by decreasing the pH value to 2, with a buffer composed of 12 mM HCl and 150 mM NaCl. The samples containing the antibody were first diluted 15 times in the adsorption buffer, before injection in the column. The absorbance was monitored at 215 nm and IgG concentration was determined from a calibration curve obtained using Gammanorm® IgG as a standard, with a concentration range of 0.2 to 20 μg.mL^{-1} (***Figure A3*** – Supplementary Material).

2.4.2. Quantification of labelled IgG

2.4.2.1. mL-scale experiments

To determine the IgG concentration in the top and bottom phases, each phase was flowed in a 100 μm tall, 200 μm wide and 5 mm long straight microchannel, using a syringe pump (New Era Pump Systems, Inc., NE-1000 model) at a flow rate of 1 μL.min^{-1}. The fluorescence was measured using a Leica (Solms, Germany) DMLP fluorescence microscope coupled to a CCD color camera XC30, Olympus (Shinjuku, Tokyo, JP). A band pass filter for excitation between 450 and 490 nm and long pass emission above 515 nm was used to monitor the labelled IgG in the microtube. Polyethylene tubing was acquired from Instech Solomon and 1 mL syringes were purchased from CODAN (Lensahn, Germany). The images were obtained with several exposure times, ranging from 250 ms to 1 s. The fluorescence intensity values were measured using ImageJ software from the National Institutes of Health (Bethesda, MD, USA) as the average grey scale intensity inside the channel after subtracting the background signal. This background corresponds to the signal intensity outside the microchannel.

2.4.2.2. nL-scale experiments

Both the PEG and salt-rich phases containing the labelled IgG antibody were loaded in each of the two inlets of the microfluidic structure at a flow rate of 0.2 μL.min^{-1} and 1 μL.min^{-1}, respectively, using two independent syringe pumps (New Era Pump Systems, Inc., NE-1000 model and Kd Scientific, Legato® 100 model). This microfluidic structure comprises two inlet 50 μm wide channels, converging to a 100 μm wide and 15 cm long main channel, which splits into three outlet channels. The height of the microchannel is 20 μm throughout the entire structure. The location of the interphases and the IgG partitioning phenomena were monitored using the aforementioned microscope and fluorescence filter. Several fluorescence images were obtained through the microfluidic channel, with several different

exposure times, ranging from 250 ms to 1 s, taking into consideration that each dye and conjugates provide different intensities of fluorescence emission. The analysis of the images was also performed with ImageJ software after subtracting the background value, measuring the fluorescence intensity in each side of the interphase at the end of the microchannel (L = 15 cm) in order to estimate the K_P.

2.4.3. Determination of the degree of labelling of the labelled IgG

The degree of labelling (DOL) of the conjugated antibody solution was performed considering the absorbance of the labelled protein - at 280 nm and at the wavelength corresponding to the absorption maximum of the dye - and the extinction coefficients of the protein and the dye, at the same wavelengths, according to the next equation[64]:

$$DOL = \frac{A_{exc} \times MW}{1.4 \times (A_{280} - A_{exc} \times CF) \times \varepsilon_{dye}} \quad \textbf{(Equation 11)}$$

where A_{exc} corresponds to the absorbance value of the protein labelled with the dye at its excitation wavelength; A_{280} to the absorbance value at 280 nm; MW to the molecular weight of IgG (150 000 g.mol^{-1}); CF to the correlation factor for the contribution of the dye in the absorbance of the labelled protein at 280 nm; ε_{dye} to the extinction coefficient of the dye at the excitation wavelength; and 1.4 to the constant used to correlate the absorbance values with the protein concentration in mg.mL^{-1} (valid only for IgG antibodies). For the dye Alexa Fluor® 430 NHS ester, the used values were 430 nm for the absorption maximum, a CF of 0.28 and an ε_{dye} of 16 000 L.mol^{-1}.cm^{-1}.[64,65] In the case of BODIPY™ FL, the absorption maximum was 505 nm, the CF was 0.027 and the ε_{dye} was 80 000 L.mol^{-1}.cm^{-1} (information provided by the supplier).[66,67]

2.4.4. Determination of the molecular weight of non-labelled and labelled IgG

The molecular weight of the different samples was tested by SDS-PAGE, namely non-labelled IgG, IgG labelled with Alexa Fluor® 430 NHS ester, IgG labelled with BODIPY™ FL NHS ester and IgG labelled with BODIPY™ FL maleimide, all at a concentration of 1 mg.mL^{-1}. Samples were applied in a 12% acrylamide gel, prepared from a 40% acrylamide/bisacrylamide stock solution (29:1). The samples were prepared for a final volume of 50 µL, by adding 20 µL of each sample, 5 µL of Milli-Q water and 25 µL of sample loading buffer (62.5 mM Tris-HCl, pH 6.2, 2% SDS, 0.01% bromophenol blue and 10% glycerol), followed by boiling for 10 minutes at 100°C, and then 20 µL of this solution were loaded into the gel. The molecular weight marker used was Precision Plus Protein™ Dual Color Standards (BIO-RAD), with 3 µL of solution loaded into the gel. The gel ran for 120 minutes at 110 mV using a running buffer that contained 192 mM glycine, 25 mM Tris, and 0.1% SDS, pH 8.3. To detect the protein bands, two different protocols were used: first a standard Coomassie protocol, and subsequently a silver stain protocol, since the majority of the bands in the gel were not shown using only the first method. The Coomassie protocol consists in the staining with an aqueous solution containing 0.1% Coomassie Brilliant Blue R-250 in 30% ethanol and 10% acetic acid for 1 hour, followed by the destaining, achieved by successively washing the gels with 30% (v/v) ethanol and 10% (v/v) acetic acid, until the background colour disappeared. The silver staining protocol starts with a washing step in 30% ethanol, for at least

10 minutes, followed by two washing steps with Milli-Q water, for 10 minutes each. Next, sensitization was performed, for 10 minutes, with 0.02% of sodium thiosulfate, followed by three washing steps with Milli-Q water, each for 30 seconds. Afterwards, staining was achieved by immersion in a 0.15% silver nitrate solution for 30 minutes, proceeded by another washing step with Milli-Q water, for one minute. Finally, the development was performed using a solution containing 3% sodium carbonate and 0.05% formaldehyde, followed by 5% acetic acid to stop the reaction.

2.4.5. Determination of the isoelectric point of non-labelled and labelled IgG

The isoelectric point of the non-labelled and labelled IgG molecules was evaluated by isoelectric focusing (IEF).

To perform the IEF of the protein samples, PhastGel® IEF 3-9 with 50x46x0,45 mm was used. PhastGel® IEF media are precast homogeneous polyacrylamide gels (5% T and 3% C) containing 2%-6% Pharmalyte® as carrier ampholytes. IEF was performed using a Pharmacia PhastSystem Separation (Amersham Biosciences). Each run was performed at 500 Vh for approximately 30 min. The prefocusing step takes 10 minutes.

The IEF markers used were a Broad IEP Kit, pH 3-10 from GE Healthcare, with the different components, namely, amylglucosidase (pI 3.50); methyl red (pI 3.75); trypsin inhibitor (pI 4.55); β-lactoglobulin A (pI 5.20); bovine carbonic anhydrase B (pI 5.85); human carbonic anhydrase B (pI 6.55); myoglobin, acidic band (pI 6.85); myoglobin, basic band (pI 7.35); lentil lectin, acidic (pI 8.15); lentil lectin, midDOLe (pI 8.45); lentil lectin, basic (pI = 8.65) and trypsinogen (pI 9.30).

The IEF gels were subsequently silver stained, following a sequence of steps: (i) the fixation of the gel with a 20% (w/v) trichloroacetic acid solution, for 5 minutes at 20°C; (ii) one washing step with a 50% (v/v) ethanol, 10% (v/v) acetic acid solution, for 2 minutes at 50°C; (iii) another washing step with a 10% (v/v) ethanol, 5% (v/v) acetic acid solution, for 6 minutes at 50°C; (iv) incubation step in a sensitizer solution composed of 8.3% glutaraldehyde, for 6 minutes at 50°C; (v) one washing step with a 10% (v/v) ethanol, 5% (v/v) acetic acid solution, for 8 minutes at 50°C; (vi) another washing with Milli-Q water, for 4 minutes at 50°C; (vii) another incubation step in a 0.5% (w/v) silver nitrate solution, for 10 minutes at 40°C; (viii) one washing step with Milli-Q water, for 1 minute at 30°C; (ix) development step using 0.015% formaldehyde in 2.5% sodium carbonate solution, at 30°C, until the satisfying bands intensity was reached; (x) and, lastly, to stop this reaction, a solution composed of 5% (v/v) acetic acid is used, for 5 minutes at 50°C.

3. Results and Discussion

3.1. Quantification of non-labelled IgG

Firstly, to select an appropriate methodology to quantify the amount of IgG partition to both phases, top and bottom, three different techniques where explored: UV absorption, bicinchoninic acid (BCA) assay and affinity chromatography in Äkta™ Purifier 10 system equipped with an analytical POROS Protein G affinity column.

A system previously explored and optimized by Azevedo *et al*. composed by 7.04% PEG 6000, 14.37% phosphate, 15% NaCl and at a pH 7[1] was selected and reproduced with each of the quantification methods. The results obtained by the authors of the paper, measured by quantified by protein A affinity chromatography and also using Gammanorm® IgG, were a partition coefficient, $\log K_p$, of 1.88 and yield in the top phase of the system, Y_{top}, of 91.5% and the values obtained for each of the techniques are shown in ***Table 3.1***.

Table 3.1 *- Values obtained for the two parameters explored, the partition coefficient ($\log K_p$) and yield in the top phase of the system (Y_{top}) for each of the studied methodologies, UV absorption at 280 nm, BCA assay and affinity chromatography with a POROS Protein G affinity column. All the K_P values achieved are the average of two experiments and the error represents ±SD, except for the protein G affinity chromatography, with only experiment being performed.*

Parameters evaluated	UV absorption	BCA	Affinity chromatography
$\log K_p$	0.03 ± 0.01	0.14 ± 0.01	1.72
Y_{top} (%)	34.4 ± 6.42	23.2 ± 4.4	91.3

The first method evaluated, UV absorption at 280 nm, did not show satisfactory results. This might have occurred due to this method not being sensitive enough to the detect the concentration since the detection limit of the calibration curve used was 500 µg.mL^{-1}. The bicinchoninic acid (BCA) assay was carried out next, and, for this method to be accurate, the concentration of NaCl must be below 1 M[68] and the overall system used before had a concentration of 2.57 M, interfering with the complex formed and might affect the results.[69] Another possible explanation was an enhanced protocol might be required, with an higher temperature and higher incubation time, to allow the total reduction of the Cu^{2+} ions by the peptides bonds. Finally, affinity chromatography with a Protein G affinity column was performed, as it is more sensitive and any interfering components will be present in the flow-through, not interfering with the specific signal. This will result in the quantification of the molecule of IgG alone, since it will be the only component to bind specifically to the column, eluting lastly. Therefore, the partition coefficient and the yield achieved with this method were comparable to those obtained by Azevedo *et al*.[1], being selected for further studies.

Next, the appropriate system to perform further mL and nL-scale studies had to be optimized, accessing the behaviour of the non-labelled IgG when it partitions in different ATPE conditions. A system where the antibody partitions to the PEG-rich phase and the concentration of salt in the bottom phase would not compromise the IgG solubility was firstly pursued. ATPSs with three types of PEG with different molecular weights (1500, 3350 and 8000) and a phosphate salt (composed of NaH_2PO_4 and KH_2PO_4) were selected as the model systems, varying the concentrations of each component

simultaneously in order to ensure an increase in TLL without a simultaneous change in volume ratio, according to ***Table 3.2***. The range of selected concentrations was in accordance with the phase diagrams compiled by Zaslavskyz[70], knowing that these concentrations would generate two immiscible phases.

Table 3.2 - Composition of the systems used to study the behaviour of the non-labelled IgG.

Molecular weight of the polymer	Composition (PEG/phosphate salt)
PEG 1500	15/15; 17/17; 19/19
PEG 3350	12/12; 13.5/13.5; 15/15
PEG 8000	12/12; 13.5/13.5; 15/15

Resorting to affinity chromatography in Äkta™ Purifier 10 system equipped with an analytical POROS Protein G affinity column, the non-labelled IgG was measured, and the results obtained regarding partition coefficients and yields are shown in ***Figure 3.1*** and ***Table A1*** (Supplementary Material). With this method, it should be taken into consideration that the concentration of IgG used in the systems had to be optimized as 30 µg.mL^{-1}, in order to provide a UV absorbance peak significantly above the baseline.

By observing ***Figure 3.1***, the partition of the antibody, at lower concentrations of polymer and phosphate, is favoured to the salt-rich bottom phase (K_P<1) by the electrostatic interaction between the positively charged IgG and the negatively charged phosphate ions.[1] However, with the increase of the concentration of PEG/salt, meaning an increase in the TLL, the partition of IgG will shift from the salt-rich bottom phase to the PEG-rich top phase (K_P>1). According to the literature, the successful purification of antibodies using ATPE has been achieved by partitioning the antibodies to the top phase.[7] Therefore, a system composed of 19% PEG 1500 and 19% of phosphate (K_P of 8.25±0.39 and Y_{top} of 89.17±0.45%) would be the ideal system for further studies since the partitioning of IgG to the PEG-rich phase is favoured by using a low molecular-weight PEG (low volume exclusion effects), at pH values higher than the isoelectric point and at high ionic strengths in the salt-rich phase.[7] However, to perform the subsequent nL-scale experiments, the labelled IgG is typically dissolved in the phosphate-rich phase and, for this system, the concentration of salt in the bottom phase is very high (27.71 %w/w[70]), as can be observed in ***Table 3.3***, which would impair the solubility molecule and induce precipitation. Taking this into account, a new system was chosen to facilitate the miniaturized system, in which the antibody can be selectively partitioned to the top phase by adding the neutral salt NaCl.[1] The system composed of 12% PEG 3350 and 12% of phosphate (K_P of 0.73±0.01 and Y_{top} of 38.38±0.19%) was selected, presenting a significantly lower salt concentration (17.92 %w/w[70]) in the bottom phase. The effect of adding a neutral salt on IgG partition was subsequently evaluated and the results are shown in ***Figure 3.2*** and ***Table A2*** (Supplementary Material).

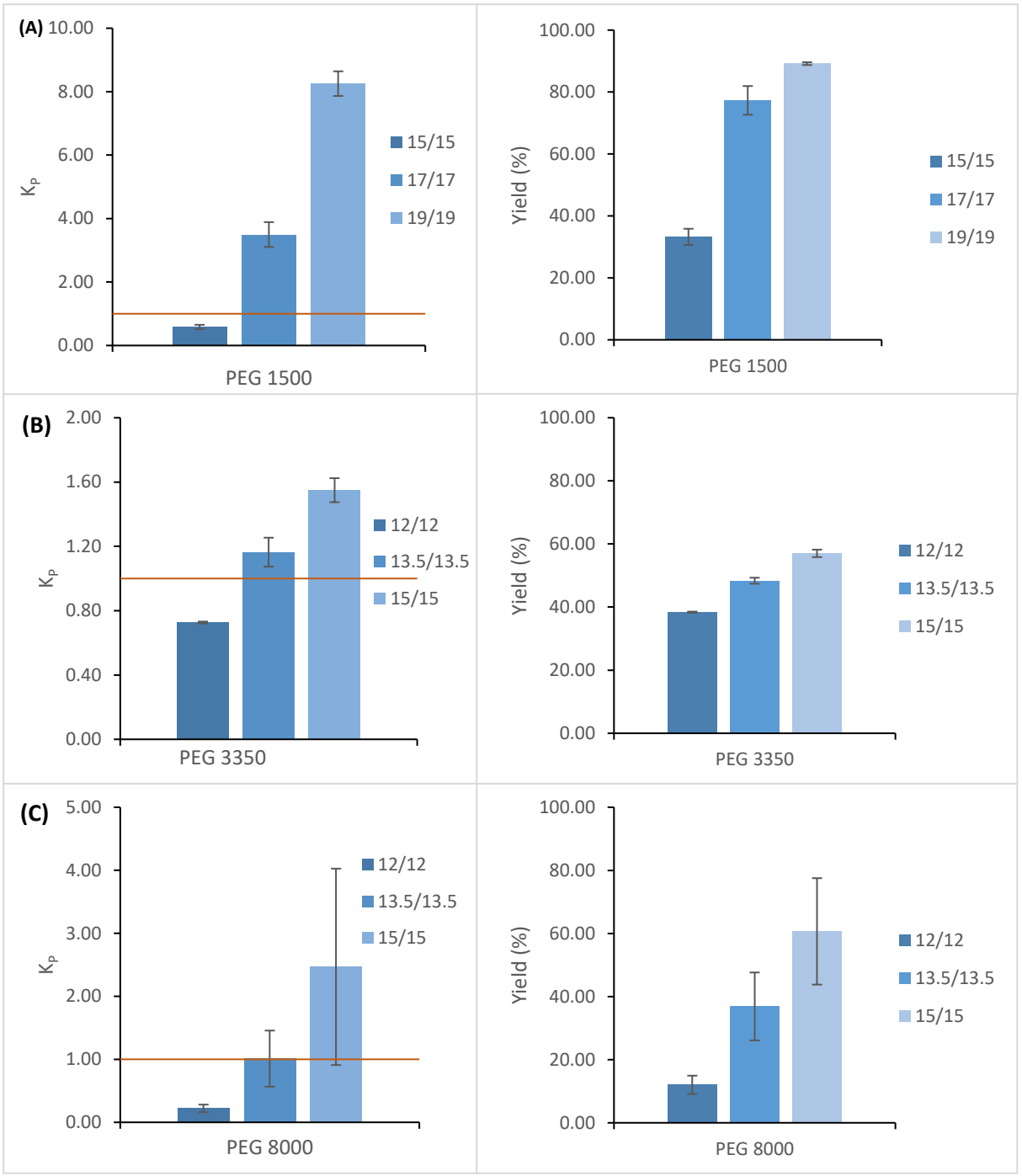

***Figure 3.1** - Graphic representation of the partition coefficient, K_P, and the yield in the top phase of the system, Y_{top}, for the non-labelled IgG (concentration in the system of 30 µg.mL^{-1}), quantified by protein G chromatography in Äkta™ Purifier 10 system: (A) PEG 1500, with concentrations of polymer/salt of 15/15, 17/17 and 19/19; (B) PEG 3350, with concentrations of polymer/salt of 12/12, 13,5/13,5 and 15/15; and (C) PEG 8000, with concentrations of polymer/salt of 12/12, 13,5/13,5 and 15/15. The line, K_P=1, delimitates the IgG partition behaviour: when K_P<1, the partition is favoured to the salt-rich phase and when K_P>1, the partition is favoured to the PEG-rich phase. All the K_P values achieved are the average of two experiments and the error bars represent ±SD.*

***Table 3.3** – Phase composition of the systems 19/19 PEG 1500/salt and 12/12 PEG 3350/salt after the formation of the two-phase systems. Adapted from ref. 62.*

	19% PEG 1500 / 19% Salt		**12% PEG 3350 / 12% Salt**	
	PEG (%w/w)	Salt (%w/w)	PEG (%w/w)	Salt (%w/w)
Top phase	35.13	3.46	24.58	4.88
Bottom phase	0.98	27.71	1.01	17.92

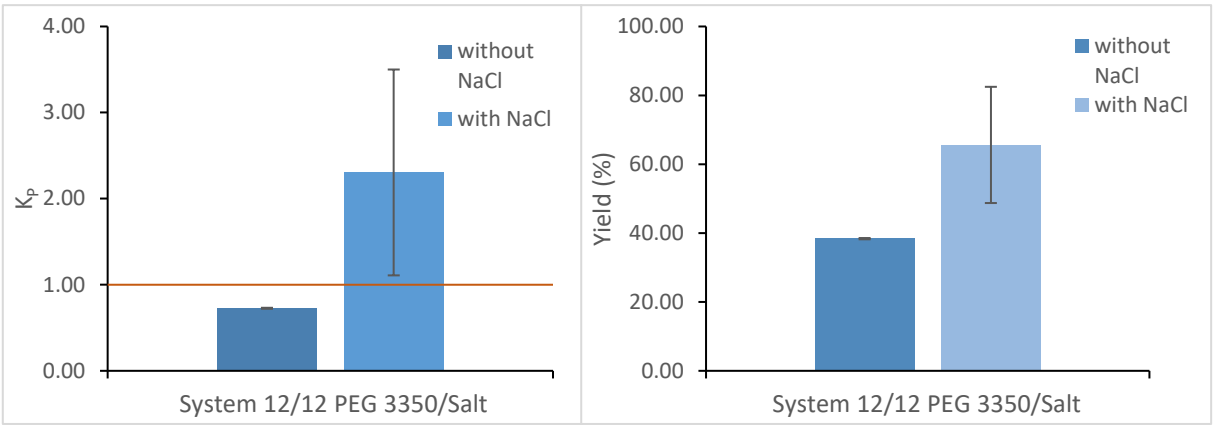

Figure 3.2 - Graphic representation of the partition coefficient, K_P, and the yield in the top phase of the system, Y_{top}, for the non-labelled IgG (concentration in the system of 30 µg.mL^{-1}), quantified by protein G chromatography in Äkta™ Purifier 10 system: PEG 3350, with concentrations of polymer/salt of 12/12, without and with the addition of 7.5% of NaCl. All the K_P values achieved are the average of two experiments and the error bars represent ±SD.

In PEG/salt systems, the ionic strength of the salt-rich phase is relatively high and the addition of a neutral salt, such as NaCl, will lead to an even higher ionic strength. This increase will induce the removal of bound water and, consequently, the exposure of hydrophobic zones of the protein surface, and ultimately precipitation may occur by salting-out. This means that the partitioning of IgG to the phosphate-rich phase may no longer be thermodynamically favoured and the partition to the PEG-rich phase will be more favourable.[1] This effect can be observed in the ***Figure 3.2*** when adding 7.5% of NaCl to the previously system, the partition coefficient and the yield in the top phase significantly increase to 2.30±1.20 and 65.60±16.87%, respectively.

Thus, to evaluate the effect of specific fluorescent tags on the IgG partition, the systems 12% PEG 3350 and 12% of phosphate salt, without and with the addition of 7.5% of NaCl, were selected where in the first, the IgG molecule partitions preferentially to the salt-rich phase, and in the second, it partitions to the PEG-rich phase. Knowing the expected partition behaviour of the non-labelled IgG, it is possible to test the results obtained using each of the systems above when labelling the IgG molecules with different fluorophores and conjugation chemistries, aiming at achieving labelling conditions which allow an extrapolation of the results to the unlabelled molecule.

3.2. Fluorophores employed, the labelling protocol and determination of the degree of labelling

For this experimental work, two different fluorophores and two different conjugation chemistries were selected to label the IgG molecule, Alexa Fluor® 430 NHS ester, BODIPY FL™ NHS ester and BODIPY FL™ maleimide, each providing different characteristics namely the (1) labelling mechanisms, (2) global bioconjugate charge, (3) water solubility and (4) quantum yields.

Alexa Fluor® 430 NHS Ester (***Figure 3.3***) is a bright, green-fluorescent dye, with a molecular weight of 701.8 g.mol^{-1}, an extinction coefficient of 16 000 L.cm^{-1}M^{-1}. It is pH-insensitive from pH 4 to pH 10 and has high quantum yields and long fluorescence lifetimes. This fluorophore labels the primary amines of proteins, amine-modified oligonucleotides, and other amine-containing molecules, forming an amide bond (***Figure 1.11***).[65] The excitation is near its absorption maximum, at 431 nm, and is

accompanied by an extremely large Stokes shift and a strong yellow-green fluorescence, with an emission maximum at approximately 541 nm.[59]

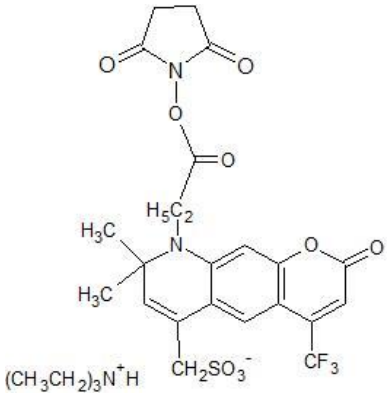

Figure 3.3 - Chemical structure of the fluorophore Alexa Fluor® 430 NHS Ester.

Regarding the labelling, this dye presents good water solubility and a global mononegative charge[59], which makes the bioconjugation step simpler and the resulting conjugates will have a lower tendency to precipitate or aggregate.[59] Since the typical IgG molecule has approximately 30 lysine residues that can be modified by the succinimidyl ester group, the degree of modification must be controlled. Therefore, to obtain conjugates with a range of different degrees of labelling (DOL), that is, the number of conjugated dye molecules per molecule of protein, the molar ratio of dye to IgG had to be adjusted. The molar ratios used were 100:1, 50:1 and 25:1 of reactive dye solution to IgG, achieving DOL values of 7.6, 4.1 and 2.4, respectively.

The BODIPY™ dyes are based on an unusual boron-containing fluorophore. This type of fluorophores displays several characteristics, such as:

- High extinction coefficient (80 000 $L.cm^{-1}M^{-1}$) and high fluorescence quantum yield:
- Lack of ionic charge and spectra that are relatively insensitive to solvent polarity and pH (the structure lacks an ionizable group);
- Narrow emission bandwidth, resulting in a higher peak intensity;
- Relatively long excited-state lifetime;
- Relatively nonpolar and the chromophore is electrically neutral, minimizing dye-induced perturbation of conjugate functional properties.[60]
- A major disadvantage of this fluorophore is a very small Stokes shift, resulting in the dyes transfer to each other with a Förster distance near 57 Å.[58]

The amine-reactive BODIPY™ FL NHS ester (***Figure 3.4***) can be used to create green-fluorescent bioconjugates. This reactive moiety is sulfonated to increase water solubility and the molecular weight of this dye is 389.16 $g.mol^{-1}$. The excitation maximum is at 503 nm and an emission maximum at approximately 509 nm. This dye also labels the primary amines of proteins (***Figure 1.11***).[67]

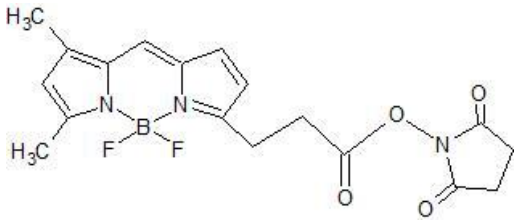

Figure 3.4 - Chemical structure of the fluorophore BODIPY™ FL NHS ester.

For the BODIPY FL™ NHS ester, although the conjugation principle is the same as for the Alexa Fluor® 430 dye, the bioconjugation step was not so straightforward due to the high hydrophobicity and neutral charge of the BODIPY molecules. The highest achieved DOL value was 1.4, even with the fluorescent dye being in excess to the IgG molecule (molar ratio of 100:1). Since this dye has a very poor solubility in water, the free dye will rapidly form aggregates and precipitate, not being available for conjugation with the IgG.[71] To minimize this problem, a low-molecular weight PEG (3350 Da) was added in solution to help solubilize the dye and prevent the formation of intermolecular interactions and aggregates, since the PEG molecules will bound to the water molecules, becoming heavily hydrated and improving water solubility of hydrophobic molecules.[72] Furthermore, being an inert polymer, it will not interact with the protein.[72,73] By adding 10% PEG to the bioconjugation step, the DOL was improved to a value of 2.6.

Finally, the thiol-reactive BODIPY™ FL maleimide (***Figure 3.5***) also presents a small size, with a molecular weight of 414.2 g mol^{-1}. The excitation maximum and emission maximum are identical to the BODIPY™ FL NHS ester, 503 and 509 nm, respectively. For this labelling to happen, the thiol groups present in the protein will be added across the double bond of the maleimide group, forming a thioether (***Figure 1.12***).[66]

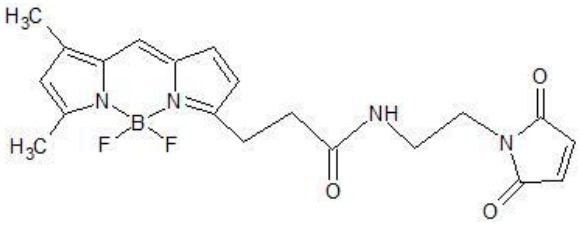

Figure 3.5 - Chemical structure of the fluorophore BODIPY™ FL maleimide.

The labelling with this fluorophore was more challenging. Although the IgG molecule has cysteines disulphide bonds connecting the heavy and the light chains, these are well protected within the structure and are typically not available for conjugation. The addition of TCEP can selective reduce some or all of the disulphide groups in a protein and make them more available for the labelling.[60] The tested molar ratio was relatively low of 0.5 mol of TCEP per 1 mol of IgG, previously optimized in our laboratory (***data not shown***), since the objective was to reduce only a single disulphide bond, leaving all other disulphide bonds intact.[61] The DOLs achieved for this dye were 0.5 and 0.6, with and without using TCEP, respectively. A higher DOL was expected when using TCEP due to the free sulfhydryl groups are more available for labelling. However, this measurement only provides the average proportion of the fluorescent dye to protein in solution, not giving the information if the dye is effectively bonded to the antibody. Therefore, further studies are required to characterize these two conjugates must be executed since these values might not be reliable.

In conclusion, *Table 3.4* shows the different degree of labelling obtained for each of the three fluorophores used in this experimental work.

Table 3.4 – Summary of the several fluorophores used for the labelling of the IgG molecule and the respective degree of labelling obtained.

	Degree of Labelling (DOL)
IgG labelled with BODIPY FL™ maleimide without using TCEP	0.6
IgG labelled with BODIPY FL™ maleimide using TCEP	0.5
IgG labelled with Alexa Fluor 430 NHS ester	7.6
	4.1
	2.4
IgG labelled with BODIPY FL™ NHS Ester	2.6
	1.4

3.3. Determination of the molecular weight of the labelled IgG

The next step was to evaluate if the binding of the different fluorophores would not change the conformation and structure of the IgG molecule. Thus, an SDS-PAGE electrophoresis was performed, as it will separate the charged molecules by their molecular masses in an electric field.[74] Since the denaturation of the tagged IgG was not intended, a native SDS-PAGE was first performed, without any denaturing conditions, that is, without an heating step or the addition of ditiotreitol (DTT). into the samples to be tested. The denaturation by heat would affect the weak interactions in a protein, primarily hydrogen bonds[74], and the reducing reagent DTT would cleave the disulphide bridges by reduction[75], breaking the IgG molecule into heavy (H) and light (L) chains, which was not desirable since the intent was to study the native structure. The obtained results can be observed in *Figure 3.6*.

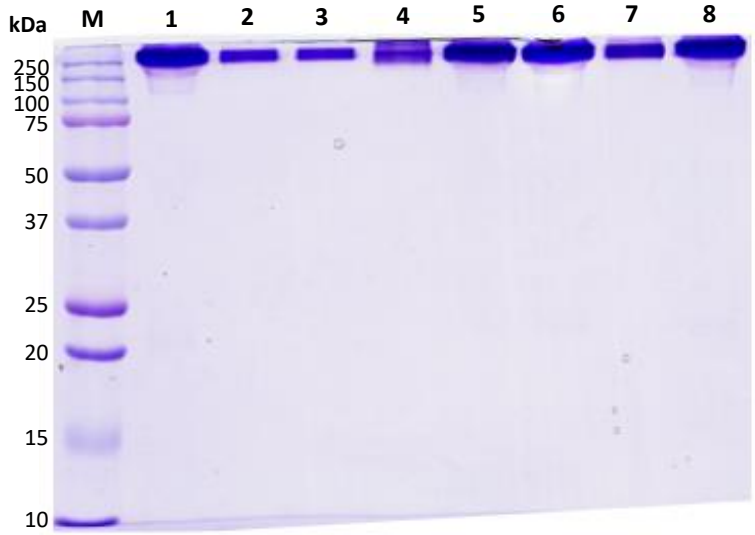

Figure 3.6 - Determination of the molecular weight of the different IgG labelled with the three fluorophores and with different degrees of labelling, through native SDS-PAGE electrophoresis, with staining with Coomassie protocol. M: Protein molecular weight marker; 1: IgG non-labelled; 2: IgG-BODIPY ™ FL maleimide using TCEP, DOL 0.5; 3: IgG-BODIPY ™ FL maleimide without using TCEP, DOL 0.6; 4: IgG-Alexa Fluor® 430, DOL 7.6; 5: IgG-Alexa Fluor® 430, DOL 4.1; 6: IgG-Alexa Fluor® 430, DOL 2.4; 7: IgG-BODIPY ™ FL NHS Ester, DOL 2.6; and 8: IgG-BODIPY ™ FL NHS Ester, DOL 1.4.

Due to the larger size of the native structure of the IgG molecule when compared to the fluorophores, the conjugates will remain retained in the beginning of the gel, and no significant differences in molecular weight were able to be detected (*Figure 3.6*). However, it allows to confirm that the use of the TCEP in the labelling with BODIPY FL™ maleimide did not reduce the disulphide groups more than intended since no additional bands were observed in this gel. Therefore, denaturation by heating (100°C for 10 minutes) is required in the samples to break the hydrogen bonds[74] and disrupt secondary and tertiary structure. Even though this technique is not ideal to study the molecular weight of a protein, it served as a preliminary assay and it allowed to take a few conclusions. The respective gel is shown in *Figure 3.7*. A silver staining protocol was required since the majority of the bands in the gel were not visible with the Coomassie method.

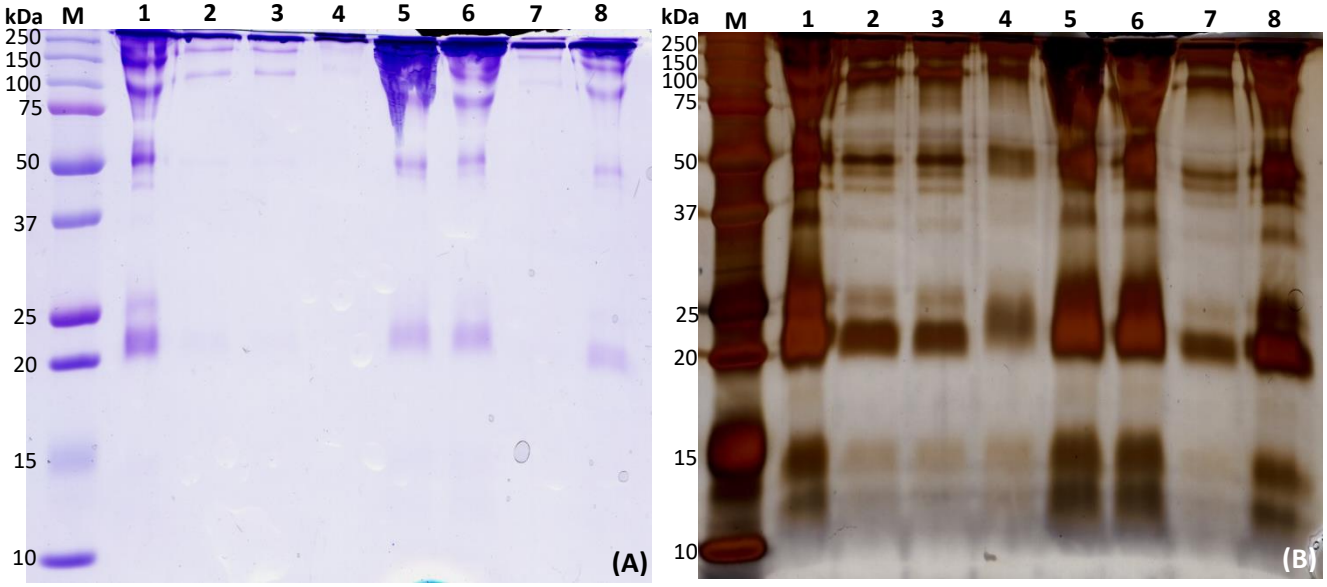

Figure 3.7 - Determination of the molecular weight of the different IgG labelled with the three fluorophores and with different degrees of labelling, through SDS-PAGE electrophoresis without denaturating conditions, with (A) staining with Coomassie protocol and (B) staining with silver stain protocol. M: Protein molecular weight marker; 1: IgG non-labelled; 2: IgG-BODIPY ™ FL maleimide using TCEP, DOL 0.5; 3: IgG-BODIPY ™ FL maleimide without using TCEP, DOL 0.6; 4: IgG-Alexa Fluor® 430, DOL 7.6; 5: IgG-Alexa Fluor® 430, DOL 4.1; 6: IgG-Alexa Fluor® 430, DOL 2.4; 7: IgG-BODIPY ™ FL NHS Ester, DOL 2.6; and 8: IgG-BODIPY ™ FL NHS Ester, DOL 1.4.

Regarding the BODIPY™ FL maleimide, considering that this dye has a low molecular weight of 414.2 $g.mol^{-1}$ [66], combined with a low degree of labelling, no differences can be observed in the bands obtained for the non-labelled or labelled IgG, as can be observed in *Figure 3.7*.

Focusing on the Alexa Fluor® 430 NHS ester dye, the higher degrees of labelling obtained are expected to influence the overall molecular weight of the conjugates significantly. Since this tag has a molecular weight of 701.8 $g\ mol^{-1}$ [65], the total molecular weight of the antibody can increase as much as ~ 5 kDa. For the higher degree of labelling of 7.6, this shift in the - the light (~25 kDa) and heavy chains (~50 kDa), can be easily observed in *Figure 3.7*, when compared to the non-labelled IgG. The bands also appear more faded when compared to the remaining samples. As previously mentioned, a typical IgG antibody molecule has around 30 lysine residues which can be modified[59] and the DOL will only calculate an average value. Therefore, a diversity of conjugates can be formed during the labelling, variating from 0 to 30 dye molecules per protein, causing a different interaction between the conjugates

and the gel's mesh. Also, a change in the IgG structure might be another possible explanation, supporting the previous conclusion that this dye will modify the molecular weight and native structure of the conjugate dye-IgG. On the other hand, for the other two degrees of labelling, 4.1 and 2.4, the bands present in the gel are similar to those of the non-labelled IgG, highlighting the lower influence of the labels on the molecular weight.

Finally, regarding the BODIPY ™ FL NHS Ester, considering the relatively low degrees of labelling obtained (2.6 and 1.4) and the relatively small molecular size of the dye (389.16 $g.mol^{-1}$ [67]), no significant differences in molecular weight were also observed.

Concluding, no major differences in molecular weight could be observed between the several dye-IgG conjugates and the native non-labeled molecule, except for the Alexa Fluor® 430 NHS ester, with a degree of labelling (DOL) of 7.6, where a ~ 5 kDa shift could easily be detected.

3.4. Determination of the isoelectric point of the labelled IgG

Isoelectric focusing was the following technique used to characterize the labelled IgG since it allows the separation of different molecules according to their isoelectric point (pI).[74] The resulting gels for the three different fluorescent tags, with a diversity of degrees of labelling, are shown in ***Figure 3.8***.

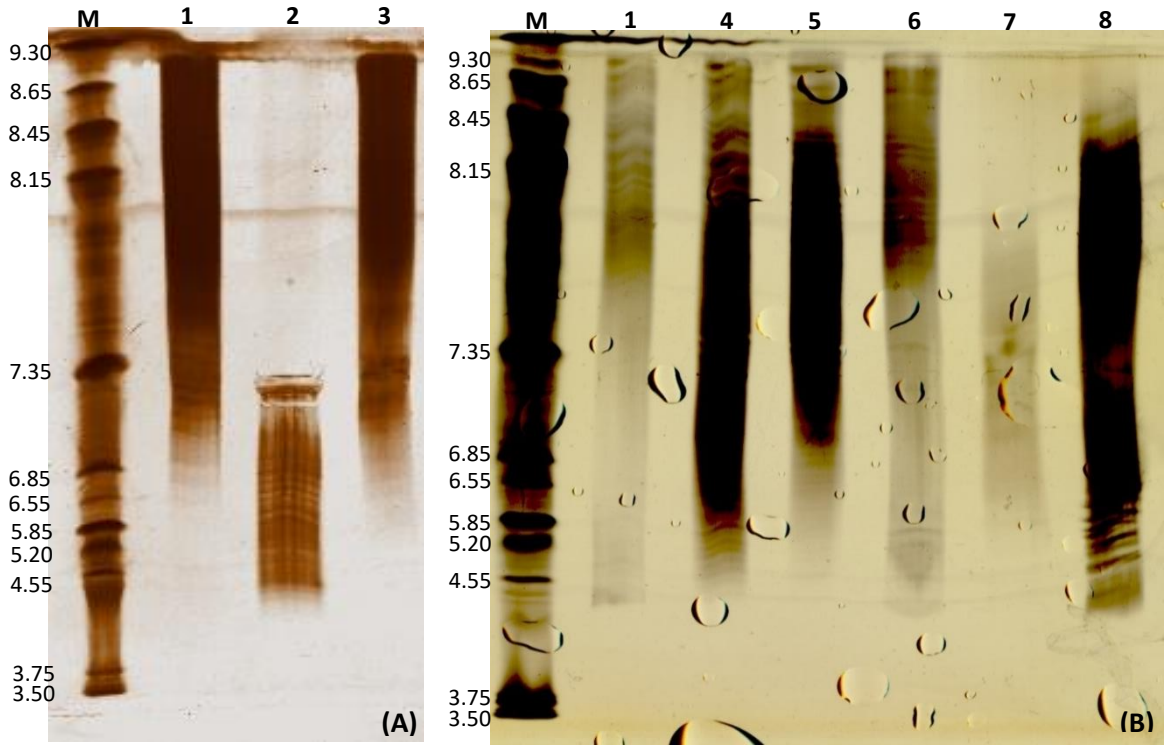

Figure 3.8 *- Determination of the pI of the different IgG molecules labelled with the three fluorophores and with different degrees of labelling, via isoelectric focusing (IEF). M: Protein molecular weight marker; 1: non-labelled IgG; 2: IgG-Alexa Fluor® 430, DOL 7.6; 3: IgG-BODIPY ™ FL maleimide without using TCEP, DOL 0.6; 4: IgG-Alexa Fluor® 430 NHS ester, DOL 4.1; 5: IgG-Alexa Fluor® 430 NHS ester, DOL 2.4; 6: IgG-BODIPY ™ FL maleimide using TCEP, DOL 0.5; 7: IgG-BODIPY ™ FL NHS Ester, DOL 2.6; and 8: IgG-BODIPY ™ FL NHS Ester, DOL 1.4. The concentration of IgG used in (A) was 1 $mg.mL^{-1}$ and in (B) 0.5 $mg.mL^{-1}$.*

The antibody used, Gammanorm IgG, is a mixture of different subclasses of IgG (59% IgG1; 36% IgG2; 4.9% IgG3; 0.5% IgG4), and, even though these are more than 90% identical on the amino acid

sequence level[64], each subclass has a unique profile with different molecular weights and pIs. For this reason, in ***Figure 3.8***, it is not possible to determine a well-defined value for the non-labelled antibodies, but instead a band ranging from pH values of 6.5 up to 9. Therefore, at physiologic pH values (the pH used in the further ATPE studies), IgG will have mostly a positive overall charge.

Regarding the dye BODIPY™ FL maleimide, based on the results shown in ***Figure 3.8***, the pI of the two samples studied, with and without the use of TCEP, are not altered by the labelling procedure relative to the non-labelled molecule. This result was expected since the fluorophore lacks ionic charge[60] and the labelling is performed by the addition of the fluorophore to free sulfhydryl groups, which are formed from the disulphide bonds present in the IgG structure, creating an electrically neutral dye-protein conjugate.

For the fluorophore BODIPY™ FL NHS ester, although this dye is still not charged, it will label the primary amine groups present in the lysine residues, neutralizing the positively charged groups in the protein. Therefore, the labelling procedure will turn the dye-protein conjugate more negative (*i.e.* decrease in the pI), generating a pI ranging 4.55 to 8.45 for the degree of labelling of 1.4 and 5.85 to 8.15 for the degree of labelling of 2.6.

Lastly, a dramatic shift in the pI was observed using Alexa Fluor® 430 NHS ester, especially at a higher degree of labelling of 7.6, resulting in a range of pIs from 4.55 to 7.35. As previously stated, this significant alteration in the pI value is not only due to the neutralization of positively charged amine side-chains of the lysine residues present in the protein, but also due to the intrinsic negative charge[59], of the fluorophore. For the lower degrees of labelling, namely 4.1 and 2.4, the pI values ranged between 5.20 to 8.45 and 6.55 to 8.65, respectively. Thus, as expected, the degree of labelling of the conjugate will also influence the pI value, with a higher number of dye molecules labelling the primary amines producing a more negatively charged protein at a physiologic pH values.

In conclusion, with the isoelectric focusing assay, a significant change in the pI was observed only when using fluorophores which will label the primary amines, suggesting that BODIPY™ FL maleimide is a more promising fluorophore since the antibody properties, the molecular weight and the pI are not modified by the labelling procedure. Additionally, the degree of labelling of the conjugate was also proven to be crucial to the antibody proprieties, with the pI and molecular weight dramatically changing with the increasing number of dye molecules attached to the IgG structure, especially for the fluorophore Alexa Fluor® 430.

3.5. Aqueous two-phase extraction using microtubes (mL-scale)

Afterwards, the first experiments of ATPE were performed, with the labelled IgG concentration from each phase collected from a ATPS and later being quantified using a straight microchannel, with 100 µm high, 200 µm wide and 5 mm of length (***Figure 3.9***), resorting to a fluorescence microscope.

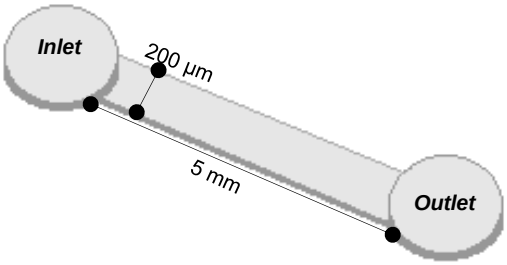

Figure 3.9 - Schematics of the microchannel used for fluorescence signal quantification in the mL-scale experiments, with 100 µm high, 200 µm wide and 5 mm length.

Each phase was continuously flowed into the microstructure and a fluorescence micrograph was taken in the middle of the channel, followed by quantification of the corresponding fluorescence intensity values. An example of these fluorescence micrographs, for the IgG labelled with the fluorophore BODIPY™ FL maleimide using TCEP, is shown in *Figure 3.10*.

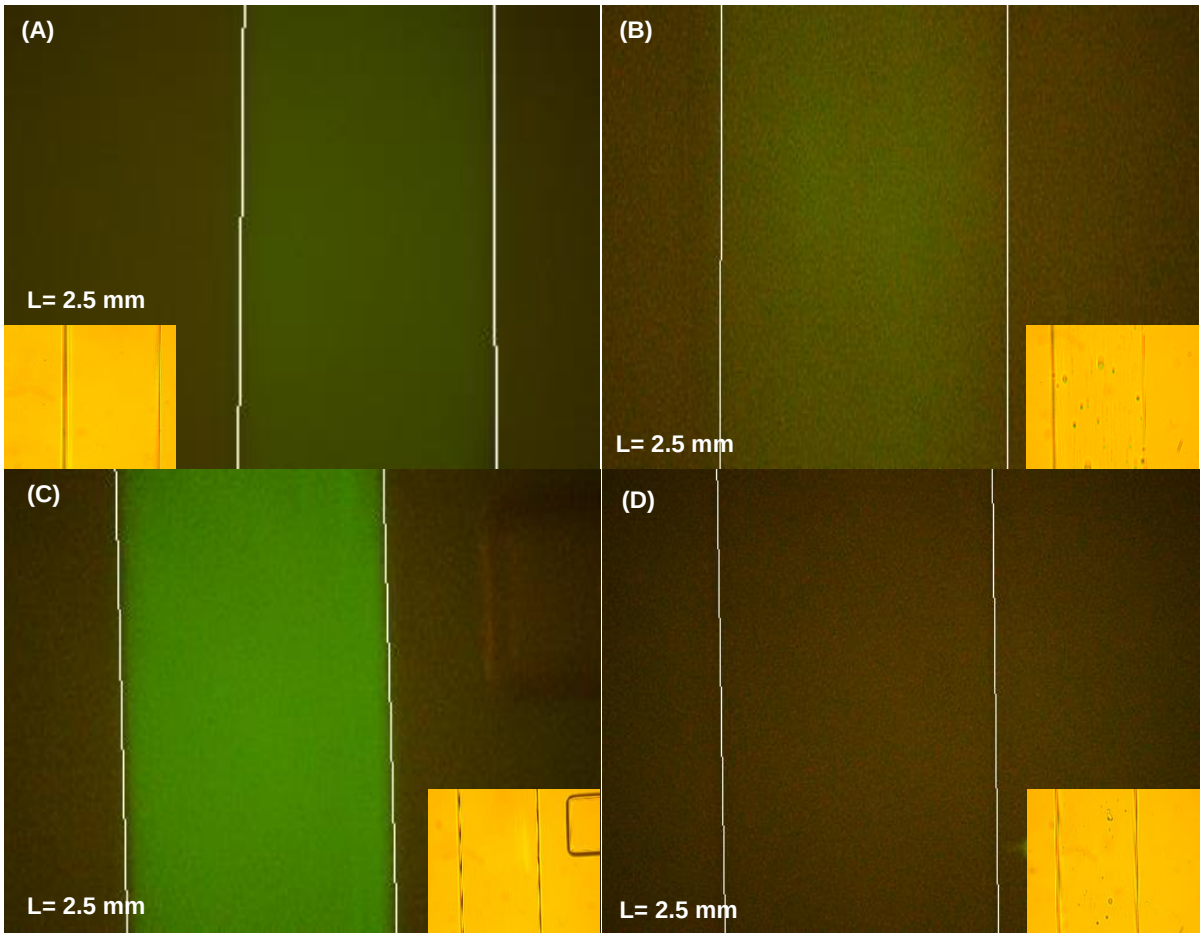

Figure 3.10 - Fluorescence micrographs captured in the middle of the straight microchannel, for the PEG-rich phase (A) and the salt-rich phase (B) of the system 12/12 PEG 3350/salt without the addition of NaCl and the PEG-rich phase (C) and the salt-rich phase (D) of the system 12/12 PEG 3350/salt with the addition of NaCl; with IgG labelled with BODIPY™ FL maleimide using TCEP, DOL 0.5, at a concentration of 20 µg.mL^{-1}, with an exposure time of 1000 ms and gain of 0 dB. The corresponding bright field images are also presented as an inset.

The exposure times and gain used to capture these micrographs are described in *Table 3.5*, being optimized for each fluorescent dye and used in the following experiments involving fluorescence microscopy.

Table 3.5 - Exposure times (ms) and gain (dB) used for the fluorescence micrographs collected through the microfluidic channel, for each fluorophore in the ATPS experiments performed.

	Exposure Time (ms)	Gain (dB)
BODIPY™ FL maleimide	1000	0
Alexa Fluor® 430 NHS ester	500	0
BODIPY™ FL NHS ester	250	0

To optimize the concentrations of the dye-protein conjugates for this quantification method, the concentration 20 μg.mL^{-1} was firstly selected in order to minimize the use of reagents and precipitation effects, while assuring a measurable fluorescence signal. Although this concentration was optimal for both BODIPY™ FL fluorophores, for the IgG labelled with Alexa Fluor® 430, a significant aggregation and precipitation effect could be observed, according with ***Figure 3.11***.

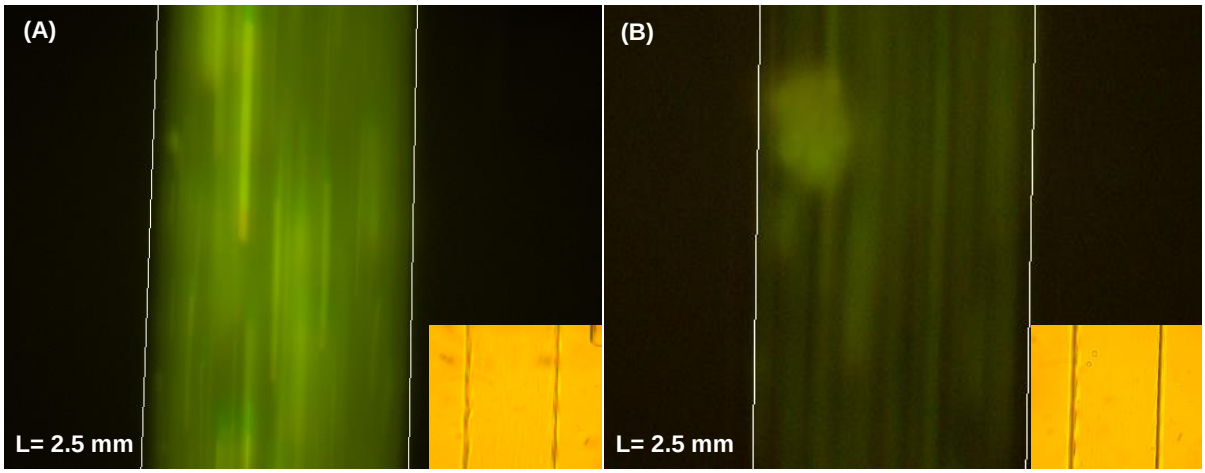

Figure 3.11 - Fluorescence micrographs captured in the middle of the straight microchannel, for the PEG-rich phase (A) and the salt-rich phase (B) of the system 12/12 PEG 3350/salt without the addition of NaCl with IgG labelled with IgG-Alexa Fluor® 430 NHS ester, DOL 4.1, at a concentration of 20 μg.mL^{-1}, with an exposure time of 500 ms and gain of 0 dB. The corresponding bright field images are also presented as an inset.

In accordance with the results from the isoelectric focusing, the labelling of the primary amines of the IgG molecule by the Alexa Fluor® 430 will generate a significantly more negatively charged dye-protein conjugate relative to the remaining fluorophores under study. This shift in pI makes the protein more neutral under the pH conditions (physiological conditions) used in the tested ATPE. When this happens, the proteins will possess both positively and negatively charged groups and the anisotropic charge distribution on the protein surface gives rise to dipoles, making protein–protein interactions, such as aggregation, highly energetically favourable.[76] Therefore, the concentration of the tagged IgG had to be further reduced down to 15 μg.mL^{-1} to avoid this aggregation effect, as shown in ***Figure 3.12***.

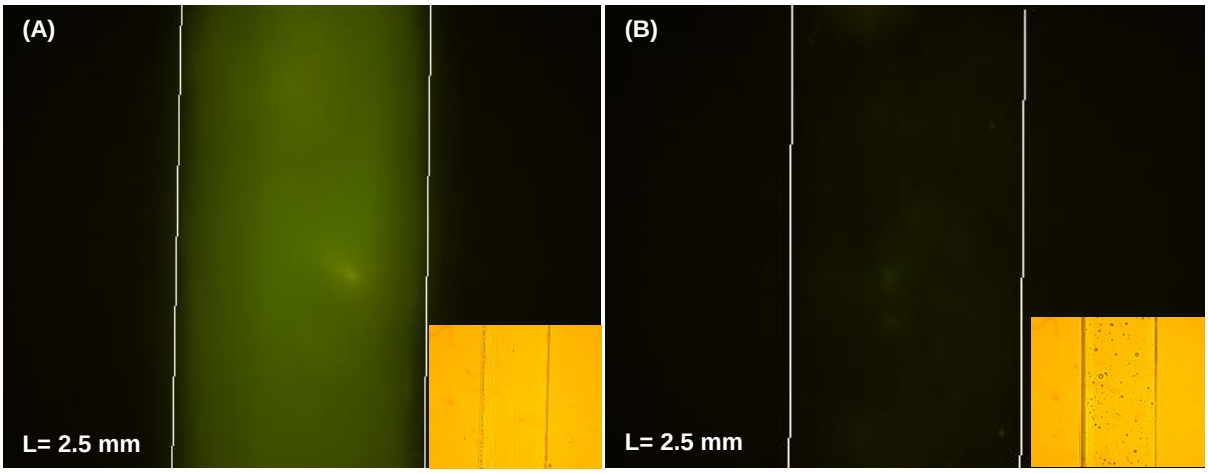

Figure 3.12 - Fluorescence micrographs captured in the middle of the straight microchannel, for the PEG-rich phase (A) and the salt-rich phase (B) of the system 12/12 PEG 3350/salt without the addition of NaCl with IgG labelled with IgG-Alexa Fluor® 430 NHS ester, DOL 4.1, at a concentration of 15 µg.mL^{-1}, with an exposure time of 500 ms and gain of 0 dB. The corresponding bright field images are also presented as an inset.

For each fluorophore, the partition coefficient, K_P, was calculated using the fluorescence value obtained for each phase, with the straight microchannel, and the results are represented in ***Figure 3.13*** and ***Table A3*** (Supplementary Material).

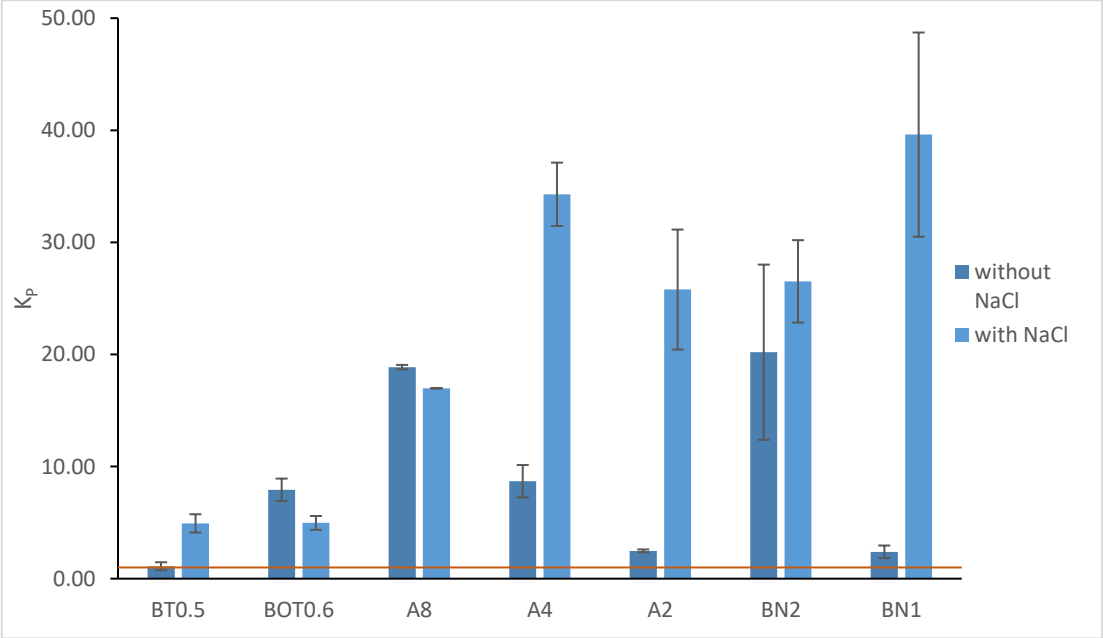

Figure 3.13 - Graphic representation of the partition coefficient, K_P, of the several labelled IgG molecules in the 12/12 PEG 3350/salt system, with and without the addition of NaCl, with both phases being quantified separately by fluorescence microscopy in a straight microchannel. BT0.5: IgG-BODIPY™ FL maleimide using TCEP, DOL 0.5; BT0.6: IgG-BODIPY™ FL maleimide without using TCEP, DOL 0.6; A8: IgG-Alexa Fluor® 430 NHS ester, DOL 7.6; A4: IgG-Alexa Fluor® 430 NHS ester, DOL 4.1; A2: IgG-Alexa Fluor® 430 NHS ester, DOL 2.4; BN2: IgG-BODIPY™ FL NHS Ester, DOL 2.6; and BN1: IgG-BODIPY™ FL NHS Ester, DOL 1.4. The concentrations of the dye-protein conjugate were 20 µg.mL^{-1} and 15 µg.mL^{-1} for the BODIPY™ FL and the Alexa Fluor® 430, respectively. The line, K_P=1, delimitates the IgG partition behaviour: when K_P<1, the partition is favoured to the salt-rich phase and when K_P>1, the partition is favoured to the PEG-rich phase. All the K_P values achieved are the average of two experiments and the error bars represent ±SD.

By observing the results obtained for most of the dye-protein conjugates, in ***Figure 3.13***, the effect of adding 7.5% of NaCl to the systems can be quantified, with the partition coefficient increasing significantly. As previously stated, the partitioning of IgG to the PEG-rich phase is thermodynamically favoured due to a higher ionic strength which leads to the removal of bound water and exposure of the

hydrophobic zones on the protein surface and ultimately may occur precipitation by salting-out.[1] However, for the BODIPY™ FL maleimide without using TCEP and the Alexa Fluor® 430 with the degree of labelling of 7.6, this effect is not visible, even with a slight decrease in the K_P being detected. In the first case, the K_P values obtained were 7.93±1.00 and 4.97±0.62, without and with the addition of the neutral salt, respectively. A possible explanation can be the presence of free fluorophore, since without using TCEP, a lower number of free sulfhydryl groups are available for dye conjugation.[59,60] Therefore, the molecule of dye does not easily react with the antibody and, due to its poor solubility in water, the elimination of this unconjugated fluorophore by diafiltration might not be totally achieved, forming microscopic aggregates which will not be filtered through the Amicon membrane. These aggregates will later interfere with the determination of DOL, creating a dubious value since this method does not take into account if the dye is actually bonded to the antibody, only the proportion of the molecules of dye per protein. To investigate the partition of this free fluorophore, a system of the 15/15 PEG 1500/salt and 15/15 PEG 8000/salt without NaCl were performed with only the addition of the unconjugated dye and it was observed for both systems that this molecule solely partitions to the PEG-rich phase, probably due to this phase being more hydrophobic, favouring the partition of hydrophobic molecules towards this phase.[34] Additionally, for a lower molecular weight molecule, the excluded volume effect will not be present.[33] For the system containing the neutral salt, the same type of behaviour was expected, however a substantial decrease in the K_P value was observed. The addition of salt will lead to the global decrease in the solubility of the free fluorophore and ultimately precipitation in the interphase may occur (less water in the system since the NaCl molecules form stronger hydrophilic interactions with water[77]). Therefore, this free fluorophore can be interfering with the quantification of the labelled IgG and further investigation will be required to confirm its presence. For the other dye, Alexa Fluor® 430 with the degree of labelling of 7.6, the coefficient partitions, 18.67 and 16.98, are similar. As previously mentioned, this conjugate has a pI value close to the pH of the system, generating a neutral charged molecule which will partition to the more hydrophobic PEG-rich phase.[34] Also, a slight decrease in the K_P value was observed with the addition of NaCl: the salt molecules will interact with water and weaken the interactions between water and the protein. This will result in protein–protein interactions and subsequently lead to protein precipitation in the interphase[77], reducing the fluorescence measured in the PEG-rich phase. Concluding, the fluorophore BODIPY ™ FL maleimide, when using TCEP for the labelling (1.11±0.36 and 4.93±0.81, without and with the addition of NaCl, respectively), showing the most comparable results to the non-labelled IgG (0.73±0.01 and 2.30±1.20, without and with the addition of NaCl, respectively).

3.6. Aqueous two-phase extraction using a microfluidic device (nL-scale)

Finally, the aqueous two-phase extraction was performed at the nL-scale, using a serpentine microfluidic structure with two inlets and three outlet channels, resorting to a fluorescence microscope to continuously monitor the labelled IgG concentration in the PEG and salt-rich phases (***Figure 3.14***). The small cross-section dimensions of the 15 cm long separation microchannel will provide fast diffusion times across the channel width, creating a continuous partition under laminar flow conditions and

allowing for both phases to flow parallel to each other along the serpentine channel, designed to increase the microchannel length while keeping a small footprint.[11]

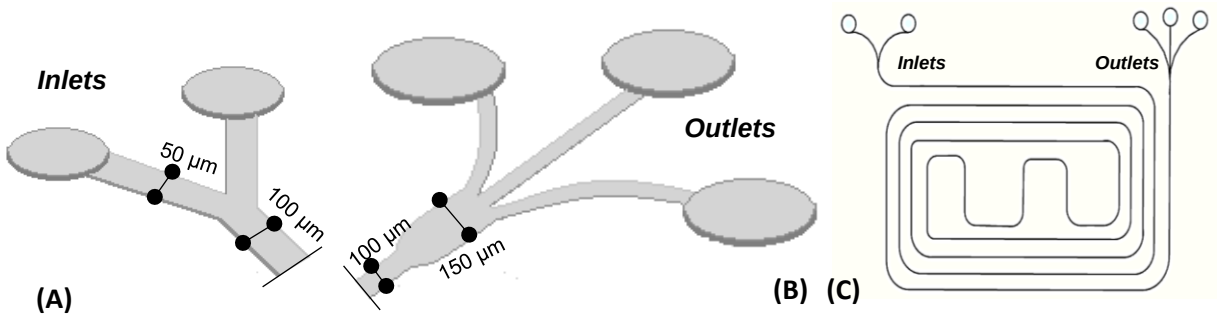

Figure 3.14 - (A) Schematics of the two inlets of the microfluidic structure which converge to a main 15 cm long separation channel. (B) Schematics of the three outlets of the microfluidic structure. (C) Top view of the microfluidic structure design used for the molecular partition experiments in the miniaturized ATPE. The height of the microchannel is 20 µm high throughout the entire structure.

The salt-rich phase was spiked with the labelled IgG antibody and both phases were loaded to the two inlets of the microfluidic structure. The flow rates for each phase were carefully selected to create a stable interface between both immiscible phases throughout the entire length of the microfluidic channel: 0.2 µL.min^{-1} for the PEG-rich phase and 1 µL.min^{-1} for the salt rich phase.[11] In order to enable the tracking of the labelled IgG partition from one phase to the other, several fluorescence micrographs were acquired throughout the length of microfluidic channel. An example of these micrographs, for the conjugate IgG-BODIPY™ FL maleimide labelled without using TCEP, is presented in ***Figure 3.15***. Visible images were also captured, with an exposure time of 100 ms, to monitor the interphase stability. The exposure times and gain used to capture these images match those used in the experiments at the mL-scale, for each dye (***Table 3.5***).

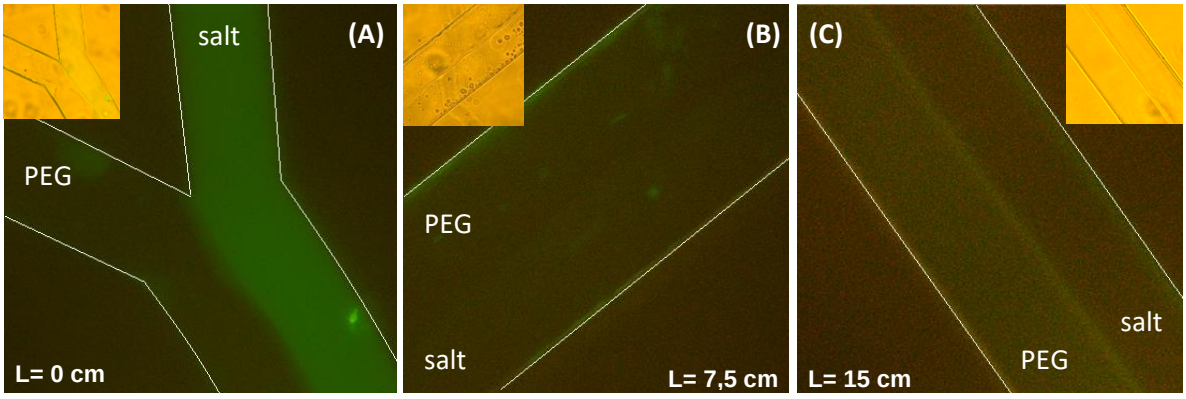

Figure 3.15 - Examples of the fluorescence micrographs obtained throughout the microfluidic channel, with the system 12/12 PEG 3350/salt without the addition of NaCl, with the salt-rich phase spiked with IgG labelled with BODIPY™ FL maleimide without using TCEP, DOL 0.6, at a concentration of 50 µg.mL^{-1} (the exposure time of 1 s and gain of 0 dB): (A) at the beginning of the channel, length 0 cm; (B) in the middle of the channel, length of 7,5 cm; and (C) at the end of the channel, length 15 cm. The corresponding bright field images are also presented as an inset.

By observing the example in ***Figure 3.15***, in the beginning of the separation channel (***A***), the labelled IgG will be fully in the salt-rich phase, and throughout the length of the separation channel (***B***), the fluorescent molecule will gradually partition to the polymer-rich phase until the end part of the channel (***C***), where the dye-protein conjugate is mostly in the PEG-rich phase. A decrease in fluorescence can be observed through the microfluidic channel, especially in systems where the labelled

antibody partitions to the salt-rich phase, due to the difference in flow rates employed (~ 5-fold faster salt-rich phase compared to the PEG-rich phase).

To calculate the partition coefficient, the image captured at the end of the microchannel was used (***Figure 3.15C***), measuring the fluorescence value in each phase and subtracting to the background value. The results obtained for all the conjugates studied will be subsequently discussed, divided into three sections for each fluorophore and compared with the K_P values achieved by the other quantification methods, namely (1) the fluorescence microscopy in a straight microchannel, at mL-scale, and (2) the protein G chromatography, for the non-labelled IgG.

3.6.1. BODIPY™ FL maleimide

For the fluorophore BODIPY™ FL maleimide, the optimal concentration of 50 μg.mL^{-1} of the conjugate spiked in the salt-rich phase was selected in order to generate a sufficiently high signal to allow quantification in both phases, avoid precipitation and still be comparable to the non-labelled IgG quantified by protein G chromatography (30 μg.mL^{-1}) and to the labelled IgG quantified by the straight microchannel at the mL-scale (20 μg.mL^{-1}). To confirm the presence of free fluorophore in the dye-protein conjugate labelled without using TCEP, protein G chromatography was performed for both labelled IgG, with and without the use of TCEP, as it is more sensitive and reproductive technique, where all the interfering components that might exist will be present in the flow-through, not binding to the column, and the IgG molecule will be the only component binding specifically to the column, selectively eluted later. Therefore, this quantification method allows the quantification of only the IgG molecule, since the free fluorophore, if it exists, will be eluted first, not binding to the column. The K_P values were calculated using the fluorescence value obtained for each phase and the results obtained by all three quantification methods are shown in ***Figure 3.16*** and ***Table A4*** (Supplementary Material).

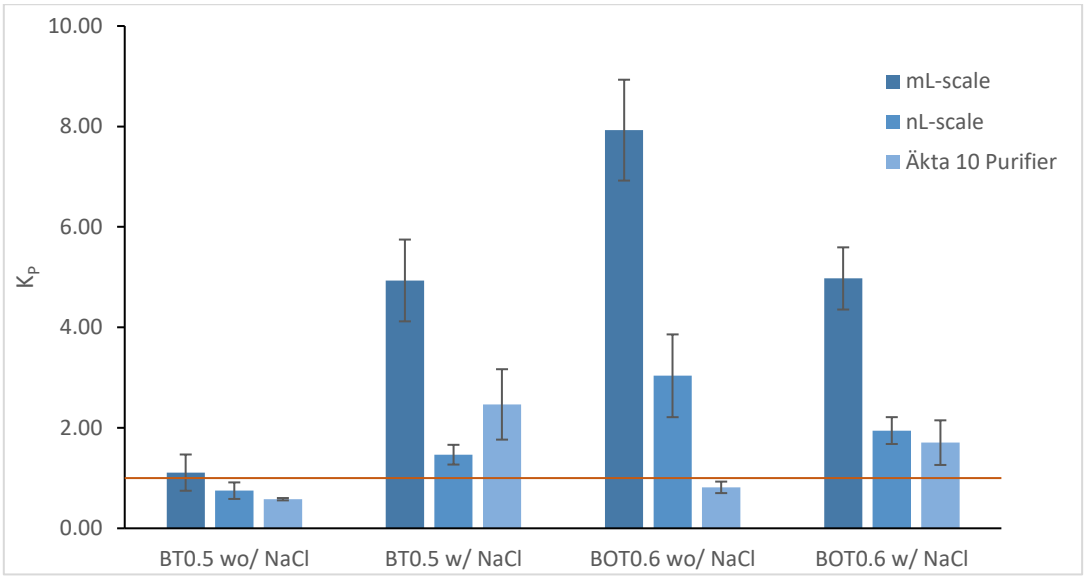

Figure 3.16 *- Graphic representation of the partition coefficient, K_P, of the IgG-BODIPY ™ FL maleimide using TCEP, DOL 0.5 (BT0.5) and the IgG-BODIPY ™ FL maleimide without using TCEP, DOL 0.6 (BT0.6), in the 12/12 PEG 3350/salt system, with and without the addition of NaCl, using different quantification methods, namely (1) mL-scale ATPE followed by fluorescence microscopy in a straight microchannel (20 μg.mL^{-1}), (2) ATPE in a microfluidic device (50 μg.mL^{-1}) and (3) protein G chromatography in Äkta™ Purifier 10 system (30 μg.mL^{-1}). The line, K_P=1, delimitates the IgG partition behaviour: when K_P<1, the partition is favoured to the salt-rich phase and when K_P>1, the partition is favoured to the PEG-rich phase. All the K_P values achieved are the average of two experiments and the error bars represent ±SD.*

By analysing ***Figure 3.16***, the first conclusion that can be drawn is that the K_P values obtained for the mL-scale, although showing the same overall trend, are significantly higher in magnitude when compared to the nL-scale. For example, for the system 12/12 PEG 3350/salt with the addition of NaCl, the BODIPY™ FL maleimide using TCEP in the labelling presents a coefficient partition of 4.93±0.81 in the mL-scale and 1.47±0.20 in the nL-scale. The difference in these values can be explained by the cross-contamination of fluorescence between both co-flowing phases at the nL-scale, *i.e.*, when estimating the fluorescence value for each the PEG-rich and salt-rich phase in the serpentine microchannel, light contamination from one phase can affect the measurement of the other phase.[10] Additionally, the concentrations used in each quantification method are also slightly different, which can have an important effect on the solubility of the protein in each phase and, therefore, the partitioning observed at low protein concentrations may be different to that observed at high concentrations.[34]

When performing the nL-scale studies, the presence of free fluorophore was once more a possible source of interference in the analysis of BODIPY™ FL maleimide without using TCEP. Although the conjugates having identical degrees of labelling, the achieved K_P values are significantly different, especially in the system without the addition of NaCl: 0.75±0.16 for the BODIPY™ FL maleimide using TCEP and 3.04±0.82 for the BODIPY™ FL maleimide without using TCEP. As previously observed, the free fluorophore, a low molecular weight molecule, will exclusively partition to the PEG-rich phase (K_P>1), due to the ionic strength present in the salt-rich prevailing over the excluded volume effect, which can explain the distinct values. Additionally, the PEG-rich phase is more hydrophobic than the salt-rich phase, which will favour the partition of hydrophobic molecules towards this phase.[34] Therefore, to investigate the presence of this free fluorophore, protein G chromatography was carried out as this method would allow to specifically identify the conjugate without interference from the free dye. As previously hypothesized, the results obtained for this quantification method confirm the presence of free fluorophore in solution since the partition coefficients obtained, for the BODIPY™ FL maleimide with and without the addition of TCEP, are comparable for each condition: without NaCl, 0.58±0.02 and 0.82±0.11, and with the addition of NaCl, 2.47±0.70 and 1.71±0.44, respectively. Hence, as the values for the protein G chromatography are comparable, it was possible to conclude that the presence of free fluorophore will affect the fluorescence measurements, and severely biasing the obtained K_P values. Thus, a reducing agent, like TCEP, is required to the thiol groups become more available, without disrupting the ternary structure, and making the labelling process more effective for this fluorophore.

Concluding, when comparing the partition coefficients acquired for the non-labelled IgG and the fluorophore BODIPY™ FL maleimide labelled with the use of TCEP by protein G chromatography, the values are comparable, as this dye appears to be the ideal fluorophore to label the IgG and obtain meaningful information that can be extrapolated to the native non-labelled molecule.

3.6.2. Alexa Fluor® 430 NHS ester

Regarding the Alexa Fluor® 430 dye, the optimal concentration used to spiked the salt-rich phase was of 25 μg.mL^{-1} in order to minimize precipitation and formation of aggregates. Nevertheless, the concentration of the protein-dye conjugate still had to generate an adequate signal and be comparable

to the non-labelled IgG quantified by protein G chromatography (30 µg.mL^{-1}) and to the labelled IgG, for this and the remaining fluorescent tags, quantified by the straight microchannel at the mL-scale (20 µg.mL^{-1}). The results are shown in ***Figure 3.17*** and ***Table A5*** (Supplementary Material), along with the results obtained for the quantification at the mL-scale.

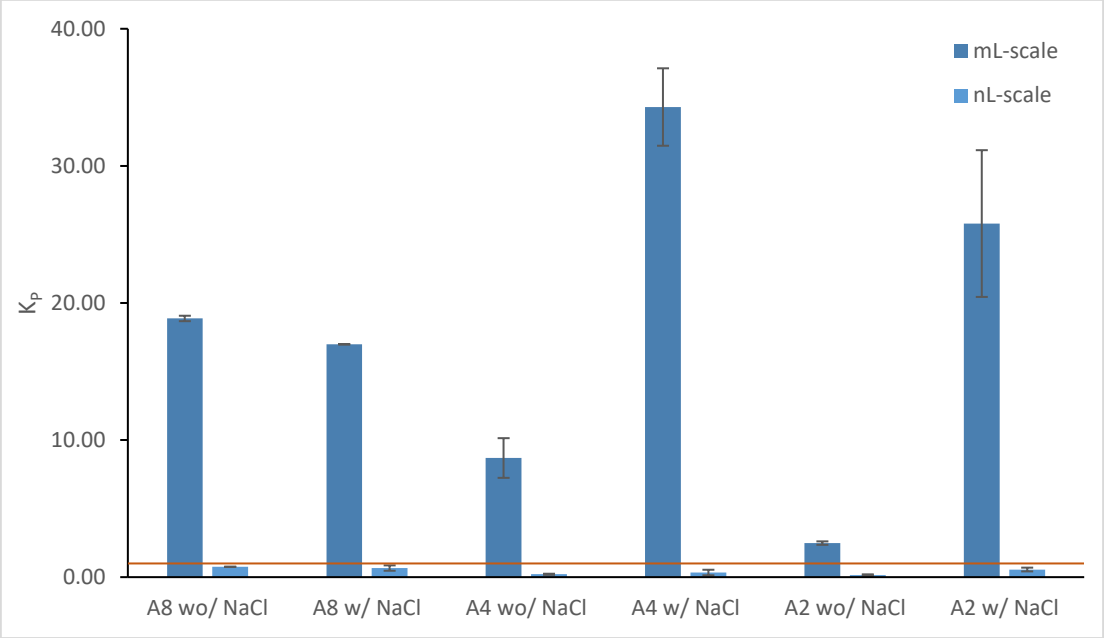

***Figure 3.17** - Graphic representation of the partition coefficient, K_P, of the IgG-Alexa Fluor® 430 NHS ester, DOL 7.6 (A8), the IgG-Alexa Fluor® 430 NHS ester, DOL 4.1 (A4) and the IgG-Alexa Fluor® 430 NHS ester, DOL 2.4 (A2), in the 12/12 PEG 3350/salt system, with and without the addition of NaCl, using fluorescence microscopy quantification methods: in a straight microchannel, mL-scale (20 µg.mL^{-1}), and in a microfluidic device, nL-scale (50 µg.mL^{-1}). The line, K_P=1, delimitates the IgG partition behaviour: when K_P<1, the partition is favoured to the salt-rich phase and when K_P>1, the partition is favoured to the PEG-rich phase. All the K_P values achieved are the average of two experiments and the error bars represent ±SD.*

By analysing ***Figure 3.17***, a major shift can be observed for the partition coefficient values obtained for the mL-scale and the nL-scale, with the biggest difference being for the conjugate with the degree of labelling of 4.1 in the system with the addition of the neutral salt NaCl: in the mL-scale, the labelled IgG partitions to the PEG-rich phase (K_P>1), 34.29±2.82, whereas, in the nL-scale, the IgG partitions to the salt-rich phase (K_P<1), 0.34±0.20. As an example, in ***Figure 3.18***, fluorescence micrographs for the labelled IgG with the dye Alexa Fluor® 430, with a degree of labelling of 2.4, dissolved in the salt-rich phase of the system 12/12 PEG 3350/salt without the addition of NaCl are presented. As can be observed, in the end of the separation microchannel, (***B***), the protein-dye conjugate remains almost completely in the salt-rich phase, with no diffusion occurring to the PEG-rich phase and resulting in a K_P value of 0.15±0.05, which fully contradicts the results obtained at the mL-scale, where the obtained K_P was of 2.48±0.13, indicating that the IgG molecule partitions to the PEG-rich phase.

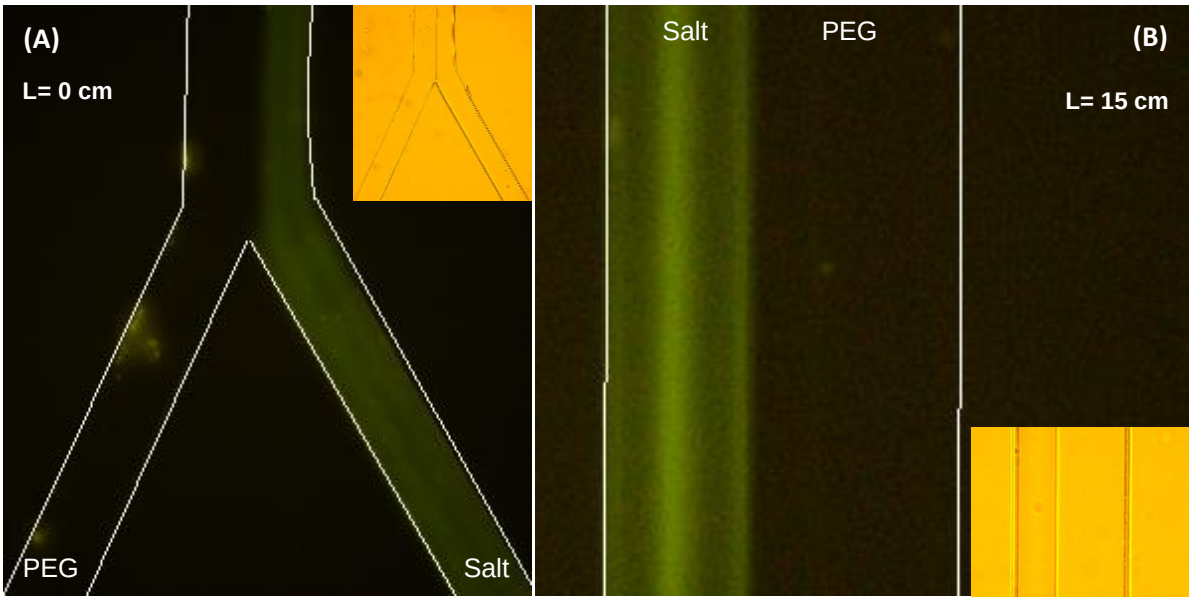

Figure 3.18 - Fluorescence micrograph obtained at the beginning of the channel, length 0 cm (A), and at the end of the microfluidic channel, length 15 cm (B), with the system 12/12 PEG 3350/salt without the addition of NaCl, with the salt-rich phase spiked with IgG labelled with Alexa Fluor® 430 NHS ester, DOL 2.4, at a concentration of 25 µg.mL^{-1} (the exposure time of 500 ms and gain of 0 dB). The corresponding bright field images are also presented as an inset.

With the addition of the NaCl to the previous system, the labelled IgG would be expected to partition to the PEG-rich phase since the addition of this neutral salt would thermodynamically favour the partitioning to this phase due to a higher ionic strength.[1] However, even in the presence of NaCl, the partition coefficient obtained in the nL-scale was 0.56±0.14, indicating that the protein did not partition to the PEG-rich phase. As can be observed in ***Figure 3.19***, the protein-dye conjugate still remains in the salt-rich phase, contradicting also the obtained results in the mL-scale, 25.79±5.35.

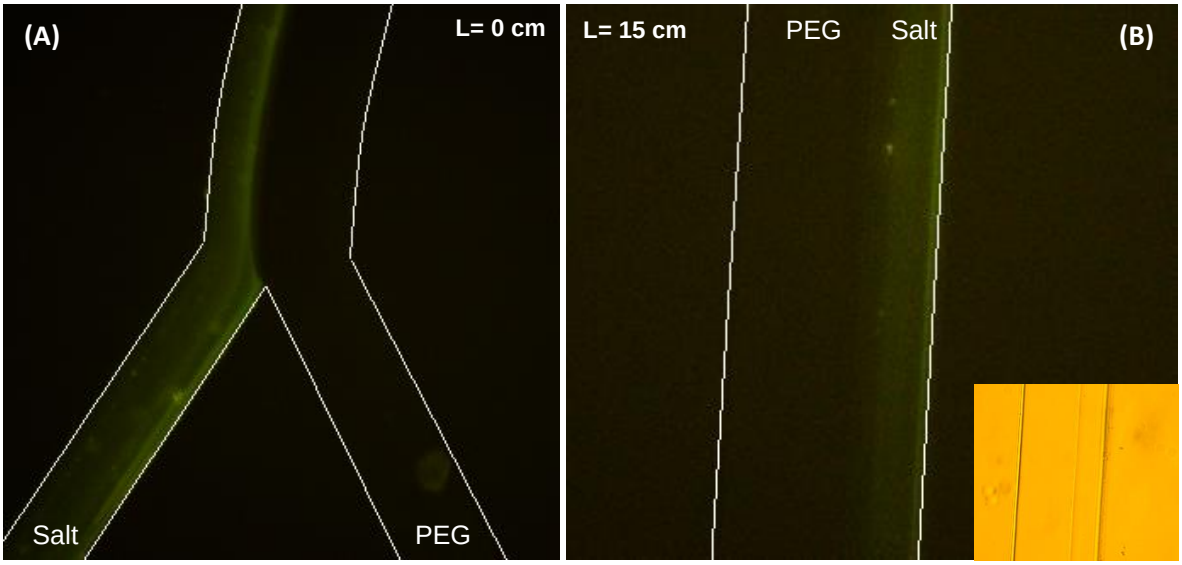

Figure 3.19 - Fluorescence micrograph acquired at the beginning of the microfluidic channel, length 0 cm (A), and at the end of the channel, length 15 cm (B), with the system 12/12 PEG 3350/salt with the addition of NaCl, with the salt-rich phase spiked with IgG labelled with Alexa Fluor® 430 NHS ester, DOL 2.4, at a concentration of 25 µg.mL^{-1} (the exposure time of 500 ms and gain of 0 dB). The corresponding bright field images are also presented as an inset.

Then, to further explore these non-intuitive results, the IgG labelled with Alexa Fluor® 430, with a degree of labelling of 2.4, was dissolved in the PEG-rich phase of the previous system, with addition

of NaCl, instead of in the salt-rich phase, and the obtained fluorescence micrographs are shown in ***Figure 3.20***.

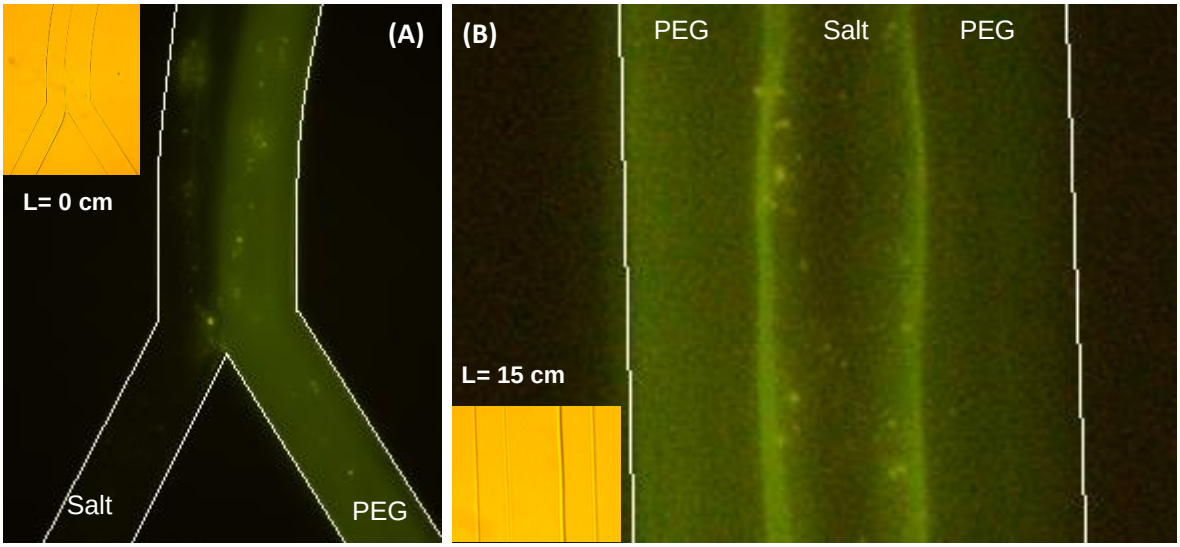

Figure 3.20 *- Fluorescence micrograph obtained at the beginning of the microfluidic channel, length 0 cm (A), and at the end of the channel, length 15 cm (B), with the system 12/12 PEG 3350/salt with the addition of NaCl, with the PEG-rich phase spiked with IgG labelled with Alexa Fluor® 430 NHS ester, DOL 2.4, at a concentration of 25 µg.mL^{-1} (the exposure time of 500 ms and gain of 0 dB). The corresponding bright field images are also presented as an inset.*

As a side note, since the polymer-rich phase has a higher affinity towards the inner PDMS walls of the microchannel compared to the salt-rich phase, the PEG-rich phase can be often be divided in two streams, each touching one of the side walls of the PDMS microchannel, as can be observed in ***Figure 3.20B***, with this phenomena not affecting the partition coefficient measured.[5] With the addition of this neutral salt and the tagged IgG being spiked in the PEG-rich phase, the labelled molecule remains in this phase, contradicting the previous results, which showed the IgG partition to the salt-rich phase. Therefore, using this fluorophore the IgG molecules remain in the phase in which they are spiked throughout the entire length of the microchannel. Additionally, at the end of the microchannel (***Figure 3.20B***), a few fluorescent aggregates can be observed, even with the optimized lower concentration aiming at preventing precipitation.

To further investigate the previous observation, two salt-rich phases from the system 12/12 PEG 3350/salt were flowed into the two inlets of the microchannel, only one of the phases being spiked with IgG labelled with the dye Alexa Fluor® 430, with a degree of labelling of 2.4, and the obtained results are shown in ***Figure 3.21***. As can be observed, the tagged IgG remains in the same salt-rich phase where it was dissolved, not diffusing into the second salt-rich phase throughout the entire length of the separation channel, confirming that this non-intuitive observation is due to diffusion limitations of the molecule.

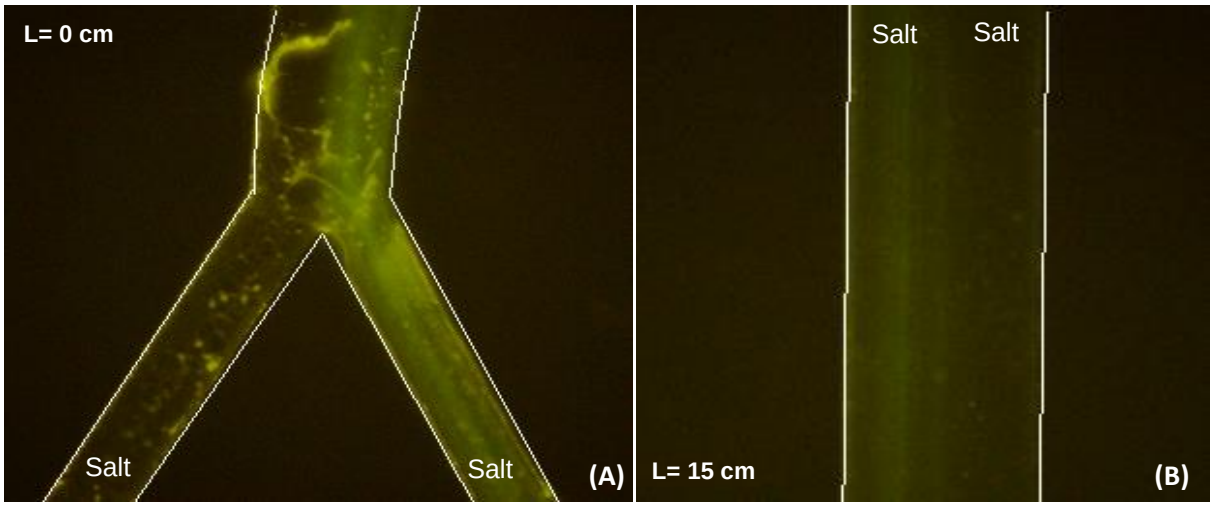

***Figure 3.21** - Fluorescence micrographs obtained throughout the microfluidic channel, with the diffusion of two phases of salt-rich phase produced from two systems 12/12 PEG 3350/salt without the addition of NaCl, where one of the phases was spiked with IgG labelled with Alexa Fluor® 430 NHS ester, DOL 2.4, at a concentration of 25 µg.mL^{-1} (the exposure time of 500 ms and gain of 0 dB): (A) at the beginning of the channel, length 0 cm; and (B) at the end of the channel, length 15 cm.*

In the mL-scale, the IgG molecules partition due to convective mixing of the solution, allowing the aggregates to effectively partition to the PEG-rich phase. However, in the nL-scale, where the salt-rich phase is spiked with the labelled IgG, due to the general absence of turbulence, there is no convective mixing of the solution and molecular transport occurs by diffusion only perpendicularly to the flow direction occur by diffusion. Additionally, to provide a stable flow-regime, flow velocities and channel dimensions must be optimized for a particular system and molecule.[49] Thus, a possible explanation for this conjugate not diffusing through the separation channel might be due to a dramatic decrease of the diffusion coefficient of this molecule with the labelling with this fluorophore due to the formation of aggregates, not having sufficient residence time (90 seconds in the PEG-rich phase and 18 seconds in the salt-rich phase) to diffuse from one phase to another in the length of the microchannel. Silva *et al*., in 2012, reported, as expected, that the lower the diffusion coefficient of a given molecule, the longer the molecule takes to diffuse and partition to the PEG-rich phase.[11] Hence, a microfluidic device with a longer separation channel could provide sufficient residence time for this conjugate, at the selected flow rates, to completely partition to the PEG-rich phase[11,49], in accordance with the results obtained at the mL-scale.

In summary, regarding the Alexa Fluor® 430 NHS ester conjugation, the labelling induces a decrease in the pI of the antibody, especially with higher degrees of labelling. These modifications in the antibody's proprieties will generate a more negative dye-protein conjugate, which tends to aggregate at neutral pH, originating a significantly different partition behaviour of the conjugate, in the mL and nL-scale, when compared to the non-labelled IgG.

3.6.3. BODIPY™ FL NHS ester

Finally, for the fluorophore BODIPY™ FL NHS ester, the optimal concentration of 50 µg.mL^{-1} of the conjugate spiked in the salt-rich phase was again used to produce adequate signal to be quantified and still be comparable to the non-labelled IgG (30 µg.mL^{-1}) and to the labelled IgG quantified by the straight microchannel at the mL-scale (20 µg.mL^{-1}). Once more, along with the results previously

obtained for the quantification in the mL-scale, using the straight microchannel, the partition coefficient achieved for each degree of labelling of the fluorophore, 2.6 and 1.4, are shown in ***Figure 3.22*** and ***Table A6*** (Supplementary Material).

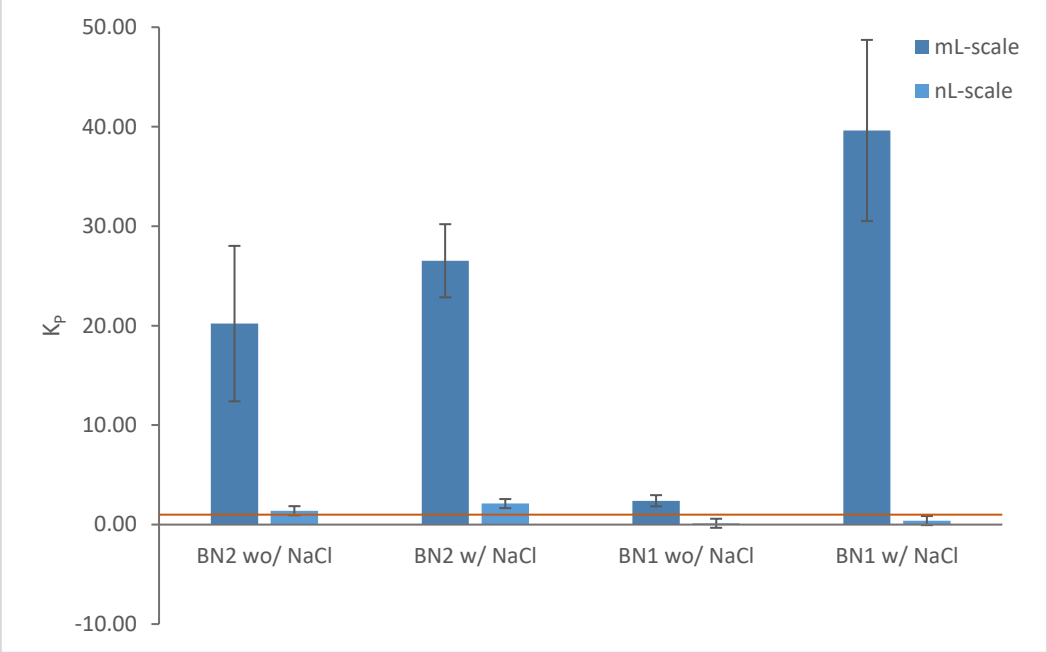

Figure 3.22 - Graphic representation of the partition coefficient, K_P, of the IgG-BODIPY ™ FL NHS Ester, DOL 2.6 (BN2), and the IgG-BODIPY ™ FL NHS Ester, DOL 1.4 (BN1), in the 12/12 PEG 3350/salt system, with and without the addition of NaCl, using fluorescence microscopy quantification methods: in a straight microchannel, mL-scale (20 µg.mL^{-1}), and in a microfluidic device, nL-scale (50 µg.mL^{-1}). The line, K_P=1, delimitates the IgG partition behaviour: when K_P<1, the partition is favoured to the salt-rich phase and when K_P>1, the partition is favoured to the PEG-rich phase. All the K_P values achieved are the average of two experiments and the error bars represent ±SD.

For the BODIPY™ FL NHS ester, a shift in the measured K_P value could be noticed comparing the mL-scale and the nL-scale (***Figure 3.22***). For example, for the degree of labelling of 1.4, with the addition of NaCl, the labelled IgG partitions to the PEG-rich phase (K_P>1) in the mL-scale, 39.62±9.11, while the IgG partitions to the salt-rich phase (K_P<1) in the nL-scale, 0.40±0.17, similarly to the results obtained for the fluorophore Alexa Fluor® 430. However, for the degree of labelling of 2.6, despite the same partition behaviour in both mL and nL scales, the partition coefficients obtained presented very different magnitudes. For example, without the addition of NaCl, in the mL-scale, the K_P value is 20.21±7.81, whereas, in the nL-scale, the K_P value is 1.40±0.25. As can be observed by ***Figure 3.23***, the fluorescent tagged IgG can indeed diffuse to the PEG-rich phase, even when dissolved in the salt-rich phase. The divergency in magnitude, as previously stated, can be due to cross-contamination existent in the quantification in the nL-scale or the different concentrations used in each scale, 20 µg.mL^{-1} for the mL-scale and 50 µg.mL^{-1} for the nL-scale, which may have a significant effect on the solubility of the protein in each phase.[34]

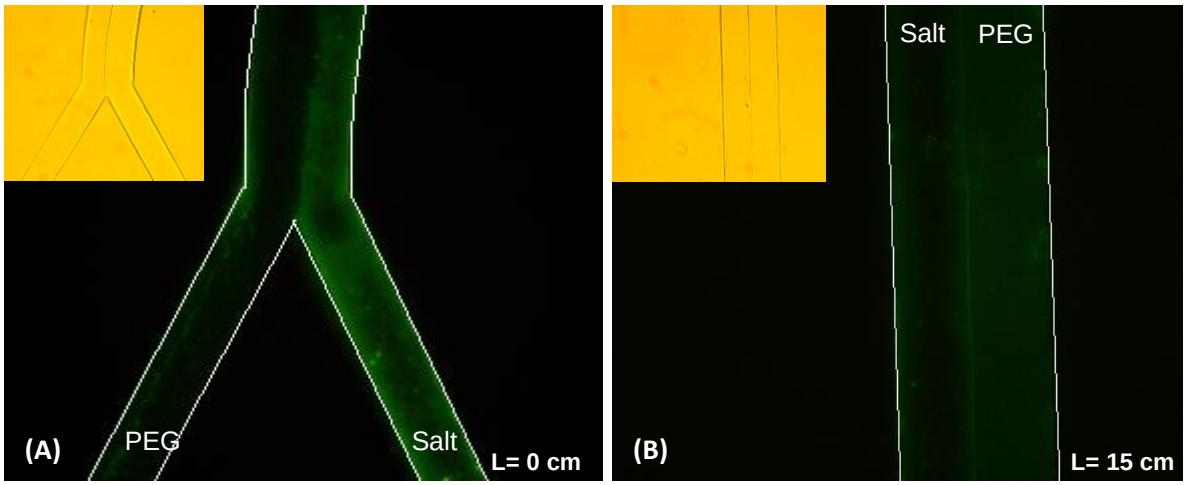

Figure 3.23 - Fluorescence micrograph obtained at the beginning of the channel, length 0 cm (A), and at the end of the microfluidic channel, length 15 cm (B), with the system 12/12 PEG 3350/salt without the addition of NaCl, with the salt-rich phase spiked with IgG labelled with BODIPY™ FL NHS ester, DOL 2.6, at a concentration of 50 µg.mL^{-1} (the exposure time of 250 ms and gain of 0 dB). The corresponding bright field images are also presented as an inset.

Regarding the BODIPY™ FL NHS ester with a degree of labelling of 1.4, as can be observed by the fluorescence images in ***Figure 3.24***, the labelled IgG does not diffuse throughout the length of the separation microchannel, remaining in the salt-rich phase. However, the protein-dye conjugate concentrates near the interphase with the PEG-rich phase, which can indicate that the diffusion in the PEG-rich phase was not yet complete.[11] As previously stated, in the mL-scale, the molecule partitions due to convective mixing of the solution, resulting in the aggregates partition to the PEG-rich phase, but, in the nL-scale, the partitions results from diffusion alone. Similarly to the previous observations using the fluorophore Alexa Fluor® 430, the labelling with will BODIPY™ FL NHS ester also promoted aggregate formation (***Figure 3.24A***), decreasing the diffusion coefficient of the conjugate and the antibody might not have time to diffuse across the two phases. Again, a microfluidic device with a longer separation channel should provide sufficient residence time to complete the extraction to the PEG-rich phase, at the optimum flow rates.[11,49]

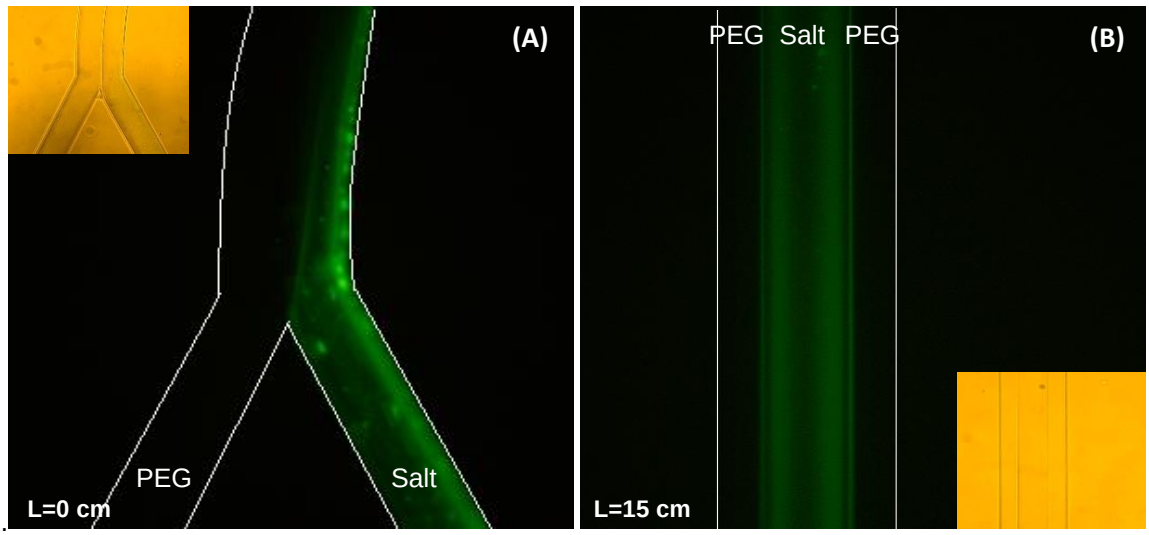

Figure 3.24 - Fluorescence micrograph obtained at the beginning of the channel, length 0 cm (A), and at the end of the microfluidic channel, length 15 cm (B), with the system 12/12 PEG 3350/salt without the addition of NaCl, with the salt-rich phase spiked with IgG labelled with BODIPY™ FL NHS ester, DOL 1.4, at a concentration of 50 µg.mL^{-1} (the exposure time of 250 ms and gain of 0 dB). The corresponding bright field images are also presented as an inset.

Contrarily to the Alexa Fluor® 430 dye, analysing the results achieved for the nL-scale, a correlation between the degree of labelling of the protein-dye conjugate and the partition coefficient was not observed. As shown in ***Figure 3.24A***, the IgG labelled with BODIPY FL™ NHS ester with a degree of labelling 1.4 tends to form more aggregates than the conjugate with a larger degree of labelling, 2.6 (***Figure 3.23A***). The pI achieved in the IEF assay show that the conjugate with the degree of labelling of 1.4 has a higher dispersion of more negative isoforms (4.55 to 8.45 for the DOL of 1.4 and 5.85 to 8.15 for the DOL of 2.6), which will cause a higher tendency of forming these aggregates. Therefore, it supports the hypotheses that the existence of aggregates in the protein-dye conjugate will difficult the diffusion of the molecule, decreasing the diffusion coefficient and not allowing sufficient time for partition from one phase to the other. Comparing both conjugates, besides the degree of labelling, the only fundamental difference was that to achieve a DOL of 2.6, PEG was added in solution during the bioconjugation step to help solubilize the dye and prevent aggregate formation. One possible explanation is that, without the addition of this molecule, the BODIPY FL™ NHS ester dye forms fluorophore aggregates which can still interact with the protein, labelling the IgG molecule. These aggregates have different photo-chemical proprieties, exhibiting a red-shifted photoluminescence at 650 nm in aqueous environments.[78,79] As the determination of the degree of labelling will excite at 505 nm, with the emission at 513 nm, the hypothetical aggregates were not taken into account in the DOL determination. Therefore, the degree of labelling may actually be significantly higher that the determined value of 1.4.

Overall, despite the similar values obtained using the conjugate with a DOL of 2.6 at the nL-scale (1.40±0.25 and 2.11±0.56, with and without the addition of NaCl) relative to the non-labelled IgG (0.73±0.01 and 2.30±1.20, with and without adding NaCl) this labelling strategy was deemed inadequate due to the significant changes in the pI of IgG and subsequent increased tendency for aggregate formation.

4. Conclusions and Outlook

In this experimental work, the amine-reactive Alexa Fluor® 430 and BODIPY™ FL NHS ester, and the thiol-reactive BODIPY™ FL maleimide were the three fluorophores evaluated to label the IgG molecules, presenting distinct global charge and reactivity, and the resulting conjugate were characterized by SDS-PAGE electrophoresis and isoelectric focusing. With the obtained dye-protein conjugates, fluorescence microscopy was used to perform aqueous two-phase extraction in microtubes (mL-scale) or microchannels (nL-scale), and the resulting partition coefficient was calculated in each case and compared to the partition coefficient of the non-labelled molecule, measured using analytical protein G chromatography. The obtained results throughout this work highlight the importance of the proper selection of the fluorophore to label antibodies to draw meaningful conclusions and to possibly extrapolate the behaviour of the protein-dye conjugate to the unlabelled molecule.

Regarding the amine-reactive fluorophores Alexa Fluor® 430 and BODIPY™ FL, the labelling will produce significant changes in the antibody properties: the labelling of the primary amines of the IgG will produce in a more negative dye-protein conjugate, decreasing the pI and overall charge. The proximity of the pI and the pH in solution resulted in the formation of aggregates at a neutral pH which will significantly affect the partition of this molecule in the mL-scale (the aggregates partition to the PEG-rich phase) and in the nL-scale (the aggregates will reduce the diffusion coefficient of the IgG molecule and the antibody might not have time to diffuse from one phase to another).

Concerning the thiol-reactive BODIPY™ FL maleimide, it was established as the more promising fluorophore since the antibody properties, the molecular weight and the pI, do not change with the labelling. The addition of TCEP was also proven to be essential to this type of labelling in the IgG molecule, generating the free thiol group necessary, prior to conjugation, to the maleimide label, without disrupting the ternary structure. As can be observed by ***Table 4.1***, the partition coefficients obtained for the IgG labelled with BODIPY™ FL maleimide using TCEP were comparable to those calculated for the non-labelled molecule, making it the most promising labelling strategy.

Table 4.1 *- The partition coefficient, K_P, for the non-labelled IgG (30 µg.mL^{-1}), quantified by protein G chromatography, and for the IgG-BODIPY™ FL maleimide using TCEP, DOL 0.5, resorting to fluorescence microscopy in a straight microchannel, mL-scale (20 µg.mL^{-1}), and in a microfluidic device, nL-scale (50 µg.mL^{-1}), in the 12/12 PEG 3350/salt system, with and without the addition of NaCl.*

	Non-labelled IgG	**IgG labelled with BODIPY™ FL maleimide using TCEP (DOL 0.5)**		
	protein G chromatography	mL-scale	nL-scale	protein G chromatography
without NaCl	0.73 ± 0.01	1.11 ± 0.36	0.75 ± 0.16	0.58 ± 0.02
with NaCl	2.30 ± 1.20	4.93 ± 0.81	1.47 ± 0.20	2.47 ± 0.70

Therefore, the selection of the proper fluorophore to label proteins, such as antibodies, is a critical step for the development of miniaturized high-throughput screening tools applied in the context of ATPE optimization, allowing to accurately extrapolate the measurements to the native non-labelled molecule. The ideal fluorophore to label the IgG molecule should not overload the protein, generating a degree of labelling preferentially lower than one, and must present sufficient water solubility to prevent the

formation aggregates. Recent progresses have been made in producing more water soluble BODIPY™ FL dyes[80–83], but, as shown in this experimental work, the addition of a low-molecular PEG in the bioconjugation step helps in solubilizing the dye, preventing aggregate formation and carry-over of free fluorophore during the diafiltration steps.

Since the molecular partitioning between both phases in ATPE is highly dependent on the surface properties of the proteins[34], such as its hydrophobicity and charge, properties which can potentially be affected by the fluorescent label, it is critical to evaluate the structural integrity of the protein. Here, SDS-PAGE and isoelectric focusing were used to characterize the conjugates, however, additional structural studies, based on nuclear magnetic resonance (NMR), X-ray diffraction, circular dichroism or Fourier-transform infrared spectroscopy (FTIR), may also be performed to provide complementary information. It should also be highlighted that this experimental work was performed by labelling Gammanorm IgG, a mixture of different subclasses of IgG and each subclass has a unique profile with different molecular weights and pIs[64], instead of monoclonal antibodies. Hence, further validation of these results applied to different monoclonal antibodies with defined pIs is required.

Although microfluidics combined with fluorescence microscopy allows the continuous monitoring and quantification of the partition of the IgG molecule in ATPE, with all its intrinsic advantages, this experimental work demonstrated that the appropriate selection of fluorophore in this context is an extremely challenging and critical task. Hence, the development of microfluidic ATPE screening devices without resorting to fluorescence microscopy would be highly advantageous, where the formation of the two immiscible phases and stabilization of the interphase could be automatically controlled by optical microscopy[50] and the collection of each phase through the three outlet[9] could be coupled to a secondary detection strategy such as on-chip analytical protein G chromatography or an immunoassay. On the other hand, to still benefit from an on-line reading of partition throughout the separation channel, the incorporation of biosensors in microfluidic devices has been recently explored[84,85], including the integration of microfluidic UV absorbance detectors[86], which could be incorporated as a dense miniaturized array along the separation column and/or aligned with the outlets of the device.

Bibliography

1. Azevedo, A., Rosa, P., Ferreira, I., Aires-Barros, M., **Optimisation of aqueous two-phase extraction of human antibodies**, *Journal of Biotechnology,* Vol. 132, pp. 209–217, 2007.

2. Azevedo, A., Rosa, P., Ferreira, F., de Vries, J., Visser, T.J., Aires-Barros M., **Downstream processing of human antibodies integrating an extraction capture step and cation exchange chromatography,** *Journal of Chromatography B*, Vol. 877, pp. 50–58, 2009.

3. Rosa, P., Azevedo, A., Summerfield, S., Mutter, M., Aires-Barros, M., Bäcker, W., **Application of aqueous two-phase systems to antibody purification: A multi-stage approach,** *Journal of Biotechnology,* Vol. 139, pp. 306–313, 2009.

4. Roque, A., Silva, C., Taipa, M., **Affinity-based methodologies and ligands for antibody purification: Advances and perspectives,** *Journal of Chromatography A*, Vol. 1160, pp. 44–55, 2007.

5. Silva, D., Azevedo, A., Fernandes, P., Chu, V., Conde, J., Aires-Barros, M., **Determination of partition coefficients of biomolecules in a microfluidic aqueous two phase system platform using fluorescence microscopy**, *Journal of Chromatography A*, Vol. 1487, pp. 242–247, 2017.

6. Sulk, B., Birkenmeier, G., Kopperschäger, G., **Application of phase partitioning and thiophilic adsorption chromatography to the purification of monoclonal antibodies from cell culture fluid**, *Journal of Immunological Methods, Vol.* 149, pp. 165–171, 1992.

7. Azevedo, A., Rosa, P., Ferreira, I., Aires-Barros, M., **Integrated process for the purification of antibodies combining aqueous two-phase extraction, hydrophobic interaction chromatography and size-exclusion chromatography,** *Journal of Chromatography A*, Vol. 1213, pp. 154–161, 2008.

8. Rosa, P., Azevedo, A., Aires-Barros, M., **Application of central composite design to the optimisation of aqueous two-phase extraction of human antibodies**, *Journal of Chromatography A*, Vol. 1141, pp. 50–60, 2007.

9. Jacinto, M. J., Soares, R., Azevedo, A., Chu, V., Tover, A., Conde, J., Aires-Barros, M., O**ptimization and miniaturization of aqueous two phase systems for the purification of recombinant human immunodeficiency virus-like particles from a CHO cell supernatant,** *Separation and Purification Technology,* Vol. 154, pp. 27–35, 2015.

10. Bras, E., Soares, R., Azevedo, A., Fernandes, P., Arévalo-Rodriguez, M., Chu, V., Conde, J.**,** Aires-Barros, M., **A multiplexed microfluidic toolbox for the rapid optimization of affinity-driven partition in aqueous two phase systems**, *Journal of Chromatography A,* Vol. 1515, pp. 252–259, 2017.

11. Silva, D., Azevedo, A., Fernandes, P., Chu, V., Conde, J., Aires-Barros, M., **Design of a**

microfluidic platform for monoclonal antibody extraction using an aqueous two-phase system, *Journal of Chromatography A,* Vol. 1249, pp. 1–7, 2012.

12. Abbas, A. K., Lichtman, A. H., Pillai, S. **Antibodies and Antigens,** *Cellular and Molecular Immunology,* Saunders, pp. 89–107, 7th Edition, 2012.

13. Vidarsson, G., Dekkers, G. Rispens, T., **IgG subclasses and allotypes: From structure to effector functions**, *Frontiers in Immunology,* Vol. 5, pp. 1–17, 2014.

14. Lipman, N., Jackson, L., Trudel, L., Weis-Garcia, F., **Monoclonal Versus Polyclonal Antibodies: Distinguishing Characteristics, Applications, and Information Resources**, *ILAR Journal,* Vol. 46, pp. 258–268, 2005.

15. Ghosh, S., Ansar, W., **Monoclonal Antibodies: A Tool in Clinical Research**, *Indian Journal of Clinical Medicine,* Vol. 9, pp. 9-21, 2013.

16. Bernett, M., Karki, S., Moore, G., Leung, I., Chen, H., Pong, E., Nguyen, D., Jacinto, J., Zalevsky, J., Muchhal, U., Desjarlaisand, J., Lazar, G., **Engineering Fully Human Monoclonal Antibodies from Murine Variable Regions**, *Journal of Molecular Biology*, Vol. 396, pp. 1474–1490, 2010.

17. Ecker, D., Jones, S., Levine, H., **The therapeutic monoclonal antibody market**, *MAbs,* Vol. 7, pp. 9–14, 2015.

18. Reichert, J., **Global antibody development trends**, *MAbs,* Vol. 1, pp. 86–87, 2009.

19. Stephenson, D., **Monoclonal Antibodies Continue to Drive Biotech Investment,** *The deal room by Firmex,* 2013. Available at: https://www.firmex.com/thedealroom/monoclonal-antibodies-continue-to-drive-biotech-investment/ (Accessed: 12th January 2018).

20. Pavlou, A., Belsey, M., **The therapeutic antibodies market to 2008**, E*uropean Journal of Pharmaceutics and Biopharmaceutics*, Vol. 59, pp. 389–396, 2005.

21. Elvin, J., Couston, R., Van Der Walle, C., **Therapeutic antibodies: Market considerations, disease targets and bioprocessing**, *International Journal of Pharmaceuticals,* Vol. 440, pp. 83–98, 2013.

22. Kelley, B., **Industrialization of mAb production technology the bioprocessing industry at a crossroads,** *Landes Bioscience,* Vol. 1, pp. 443–452, 2009.

23. Gronemeyer, P., Ditz, R., Strube, J., **Trends in Upstream and Downstream Process Development for Antibody Manufacturing**, *Bioengineering,* Vol. 1, pp. 188–212, 2014.

24. Saraswat, M., Musante, L., Ravidá, A., Shortt, B., Byrne, B., Holthofer, H., **Preparative Purification of Recombinant Proteins: Current Status and Future Trends**, *BioMed Research International,* Vol. 2013**,** 2013.

25. Rosa, P., Ferreira, I., Azevedo, A., Aires-Barros, M., **Aqueous two-phase systems: A viable**

platform in the manufacturing of biopharmaceuticals, *Journal of Chromatography A*, Vol. 1217, pp. 2296–2305, 2010.

26. Liu, H., Ma, J., Winter, C, Bayer, R., **Recovery and purification process development for monoclonal antibody production**, *MAbs,* Vol. 2**,** pp. 480–499, 2010.

27. Marichal-Gallardo, P., Álvarez, M., **State-of-the-art in downstream processing of monoclonal antibodies: Process trends in design and validation**, *Biotechnology Progress,* Vol. 28, pp. 899–916, 2012.

28. Azevedo, A., Rosa, P., Ferreira, I., Aires-Barros, M., **Chromatography-free recovery of biopharmaceuticals through aqueous two-phase processing**, *Trends in Biotechnology,* Vol. 27, pp. 240–247, 2009.

29. Peters, T., **Partition of Cell Particles and Macromolecules**, *Cell Biochemistry and Function,* Vol. 5, pp. 233–234, 1987.

30. Iqbal, M., Tao, Y., Xie, S., Zhu, Y., Chen, D., Wang, X., Huang, L., Peng, D., Sattar, A., Shabbir, M., Hussain, H., Ahmed, S., Yuan, Z., A**queous two-phase system (ATPS): an overview and advances in its applications**, *Biological Procedures Online,* Vol. 18, pp. 1–18, 2016.

31. Maestro, B., Velasco, I., Castillejo, I., Arévalo-Rodriguez, M., Cebolla, A., Sanz, J., **Affinity partitioning of proteins tagged with choline-binding modules in aqueous two-phase systems**, *Journal of Chromatography A***,** Vol. 1208, pp. 189–196, 2008.

32. Benavides, J., Rito-Palomares, M., Asenjo, J. A., **Aqueous Two-Phase Systems,** *Methods in Biotechnology*, 2011.

33. Saravanan, S., Rao, J., Nair, B., Ramasami, T., **Aqueous two-phase poly(ethylene glycol)-poly(acrylic acid) system for protein partitioning: Influence of molecular weight, pH and temperature**, *Process Biochemistry*, Vol. 43, pp. 905–911, 2008.

34. Asenjo, J., Andrews, B., **Aqueous two-phase systems for protein separation: A perspective**, *Journal of Chromatography A*, Vol. 1218, pp. 8826–8835, 2011.

35. Asenjo, J., Andrews, B., **Aqueous two-phase systems for protein separation: Phase separation and applications**, *Journal of Chromatography A*, Vol. 1238, pp. 1–10, 2012.

36. Ananthapadmanabhan, K., Goddard, E., **Aqueous Biphase Formation in Polyethylene Oxide-Inorganic Salt Systems**, *Langmuir*, Vol. **3,** pp. 25–31, 1987.

37. Willauer, H., Huddleston, J., Rogers, R., **Solute partitioning in aqueous biphasic systems composed of polyethylene glycol and salt: The partitioning of small neutral organic species**, *Industrial & Engineering Chemistry Research,* Vol. 41, pp. 1892–1904, 2002.

38. Platis, D., Labrou, N., **Development of an aqueous two-phase partitioning system for fractionating therapeutic proteins from tobacco extrac**t, *Journal of Chromatography A*, Vol.

1128, pp. 114–124, 2006.

39. Bensch, M., Selbach, B., Hubbuch, J., H**igh throughput screening techniques in downstream processing: Preparation, characterization and optimization of aqueous two-phase systems,** *Chemical Engineering Science,* Vol. 62, pp. 2011–2021, 2007.

40. Wiendahl, M., Wierling, P., Nielsen, J., Christensen, D., Krarup, J., Staby, A., Hubbuch, J., **High throughput screening for the design and optimization of chromatographic processes - Miniaturization, automation and parallelization of breakthrough and elution studies**, *Chemical Engeneering and Technology,* Vol. 31, pp. 893–903, 2008.

41. Soares, R., Novo, P., Azevedo, A., Fernandes, P., Aires-Barros, M., Chu, V., Conde, J., **On-chip sample preparation and analyte quantification using a microfluidic aqueous two-phase extraction coupled with an immunoassay**, *Lab on a Chip*, Vol. 14, pp. 4284–4294, 2014.

42. Madaboosi, N., Soares, R., Chu, V., Conde, J., **A microfluidic immunoassay platform for the detection of free prostate specific antigen: A systematic and quantitative approach**, *Analyst,* Vol. 140, pp. 4423–4433, 2015.

43. Sia, S., Whitesides, G., **Microfluidic devices fabricated in poly(dimethylsiloxane) for biological studies**, *Electrophoresis,* Vol. 24, pp. 3563–3576, 2003.

44. Zhou, J., Ellis, A., Voelcker, N., **Recent developments in PDMS surface modification for microfluidic devices,** *Electrophoresis,* Vol. 31, pp. 2–16, 2010.

45. Kim, P., Kwon, K., Park, M., Lee, S., Kim, S., **Soft Lithography for Microfluidics: a Review**, *Biochip Journal,* Vol. 2, pp. 1–11, 2008.

46. Mazutis, L., Gilbert, J., Ung, W., Weitz, D., Griffiths, A., Heyman J., **Single-cell analysis and sorting using droplet-basedmicrofluidics**, *Nature Protocols,* Vol. 8, pp. 870–891, 2014.

47. Eddings, M., Johnson, M., Gale, B., **Determining the optimal PDMS-PDMS bonding technique for microfluidic devices**, *Journal of Micromechanics and Microengineering,* Vol. 18**,** 2008,

48. Wang, G., Yang, F., Zhao, W., **There can be turbulence in microfluidics at low Reynolds number**, *Lab on a Chip*, Vol. 14, pp. 1452–1458, 2014.

49. Soares, R., Silva, D., Fernandes, P., Azevedo, A., Chu, V., Conde, J., Aires-Barros, M., **Miniaturization of aqueous two-phase extraction for biological applications: From micro-tubes to microchannels,** *Biotechnology Journal,* Vol. 11, pp. 1498–1512, 2016.

50. Silva, D., Azevedo, A., Fernandes, P., Chu, V., Conde, J., Aires-Barros, M., **Determination of aqueous two phase system binodal curves using a microfluidic device**, *Journal of Chromatography A,* Vol. 1370, pp. 115–120, 2014.

51. Nam, K., Chang, W., Hong, H., Lim, S., Kim, D., Koo, Y., **Continuous-flow fractionation of animal cells in microfluidic device using aqueous two-phase extraction**, *Biomedical Microdevices,* Vol. 7, pp. 189–195, 2005.

52. Tsukamoto, M., Taira, S., Yamamura, S., Morita, Y., Nagatani, N., Takamura, Y., Tamiya, E., **Cell separation by an aqueous two-phase system in a microfluidic device**, *Analyst, Vol.* 134, pp. 1994–1998, 2009.

53. Huh, Y., Jeong, C., Chang, H., Lee, S., Hong, W., Park, T., **Rapid separation of bacteriorhodopsin using a laminar-flow extraction system in a microfluidic device**, *Biomicrofluidics,* Vol. 4, pp. 1–10, 2010.

54. Hu, R., Feng, X., Chen, P., Fu, M., Chen, H., Guo, L., Liu, B., **Rapid, highly efficient extraction and purification of membrane proteins using a microfluidic continuous-flow based aqueous two-phase system**, *Journal of Chromatography A*, Vol. 1218, pp. 171–177, 2011.

55. Slavik, J., **Fluorescense Microscopy and Fluorescent Probes***, Springer Science+Business Media New York*, 1st Edition, 1996.

56. Valeur, B., **Molecular Fluorescence: Principles And Applications**, *Wiley-VCH Verlag GmbH*, 1st Edition, 2001.

57. Wolf, D., **Fundamentals of fluorescence and fluorescence microscopy**, *Methods in Cell Biology*, Vol. 114, pp. 69–97, 2013.

58. Lakowicz, J., **Principles of Fluorescence Spectroscopy**, *Springer, New York, USA,* 3rd Edition, 2006.

59. Thermo Fisher Scienctific, **The Molecular Probes Handbook: a Guide to Fluorescent Probes and Labeling Technologies**, 2010.

60. Hermanson, G., **Bioconjugate Techniques**, *Academic Press*, 2nd Edition, 2008.

61. Sun, M., Beam, K., Cerveny, C., Hamblett, K., Blackmore, R., Torgov, M., Handley, F., Ihle, N., Senter, P., Alley, S., **Reduction-alkylation strategies for the modification of specific monoclonal antibody bisulfides**, *Bioconjugation Chemistry,* Vol.16, pp. 1282–1290, 2005.

62. Santra, S., Yang, H., Dutta, D., Stanley, J., Holloway, P., Tan, W., Moudgil, B., Mericle, R., **TAT conjugated, FITC doped silica nanoparticles for bioimaging applications**, *Chemical Communications*, Vol. 24, pp. 2810–2811, 2004.

63. Zimmer, M., **Green fluorescent protein (GFP): Applications, structure, and related photophysical behavior**, *Chemical Reviews*, Vol. 102, pp. 759–781, 2002.

64. Pinto, I., Caneira, C., Soares, R., Madaboosi, N., Aires-Barros, M., Conde, J., Azevedo, A., Chu, V., **The application of microbeads to microfluidic systems for enhanced detection and purification of biomolecules**, *Methods,* Vol. 116, pp. 112–124, 2017.

65. Alexa Fluor® 430, *Thermo Fisher Scientific*, available at: https://www.thermofisher.com/order/catalog/product/A10169. (Accessed: 27th August 2018)

66. BDP FL maleimide, *Lumiprobe, a*vailable at: https://www.lumiprobe.com/p/bodipy-fl-maleimide. (Accessed: 27th August 2018)

67. BDP FL NHS ester, *Lumiprobe*, available at: https://www.lumiprobe.com/p/bodipy-fl-nhs-ester. (Accessed: 27th August 2018)

68. Thermo Scientific Pierce Protein Assay Technical Handbook, *Thermo Fisher Scientific,* Available at: https://tools.thermofisher.com/content/sfs/brochures/1602063-Protein-Assay-Handbook.pdf. (Accessed: 21st January 2018)

69. Andrews, B., Schmidt, A., Asenjo, J., **Correlation for the partition behavior of proteins in aqueous two-phase systems: Effect of surface hydrophobicity and charge**, *Biotechnology and Bioengineering,* Vol. 90, pp. 380–390, 2005.

70. Zaslavsky, B., **Aqueous Two-Phase Partitioning**, Marcel Dekker, Inc, 1995.

71. Vu, T., Dvorko,M., Schmidt, E., Audibert, J., Retailleau, P., Trofimov, B., Pansu, R., Clavier, G., Méallet-Renault, R., **Understanding the spectroscopic properties and aggregation process of a new emitting boron dipyrromethene (BODIPY)**, *The Journal of Physical Chemistry* C, Vol. 117, pp. 5373–5385, 2013.

72. Harris, J., **Poly(Ethylene Glycol) Chemistry: Biotechnical and Biomedical Applications**, *Springer Science+Business Media*, 1st Edition, 1992.

73. Tubio, G., Nerli, B., Picó, G., **Relationship between the protein surface hydrophobicity and its partitioning behaviour in aqueous two-phase systems of polyethyleneglycol-dextran**, *Journal of Chromatography B*, Vol. 799, pp. 293–301, 2004.

74. Cox, M., Nelson, D., **Lehninger: Principles of Biochemistry**, W.H.Freeman & CO LTD, 5th Editiion, 2005.

75. Zahler, W.,Cleland, W., **A Specific and Sensitive Assay for Disulfides**, *The Journal of Biological Chemistry*, Vol. 243, pp. 716–719, 1968.

76. Chi, E., Krishnan, S., Randolph, T., Carpenter, J., **Physical stability of proteins in aqueous solution: Mechanism and driving forces in nonnative protein aggregation**, *Pharmaceutical Research*, Vol. 20, pp. 1325- 1336, 2003.

77. Mao, L., Rogers, J., Westoby, M., Conley, L., Pieracci, J., **Downstream antibody purification using aqueous two-phase extraction**, *Biotechnology Progress*, Vol. 26, pp. 1662–1670, 2010.

78. Castillo, M., Raut, S., Price, S., Bora, I., Jameson, L., Qiu, C., Schug, K., Gryczynski, Z., Dzyuba, S., **Spectroscopic differentiation between monomeric and aggregated forms of BODIPY dyes: Effect of 1,1-dichloroethane**, *RSC Advances,* Vol. 6, pp. 68705–68708, 2016.

79. Frein, S., Camerel, F., Ziessel, R., Barbera, J., Deschenaux, R., **Highly Fluorescent liquid-crystalline dendrimers based on borondipyrromethene dyes**, *Chemistry of Materials,* Vol. 21, pp. 3950–3959, 2009.

80. Li, L., Han, J., Nguyen, B., Burgess, K., **Syntheses and spectral properties of functionalized, water-soluble BODIPY derivatives**, *Journal of Organic Chemistry*, Vol. 73, pp. 1963–1970, 2008.

81. Niu, S., Ulrich, G., Retailleau, P., Harrowfield, J., Ziessel, R., **New insights into the solubilization of Bodipy dyes**, *Tetrahedron Letters*, Vol. 50, pp. 3840–3844, 2009.

82. Niu, S., Massif, C., Ulrich, G., Ziessel, R., Renard, P., Romieu, A., **Water-solubilisation and bio-conjugation of a red-emitting BODIPY marker**, *Organic & Biomolecular Chemistry*, Vol. 9, pp. 66–69, 2011.

83. Zhu, S., Zhang, J., Vegesn, G., Luo, F., Green, S., Liu, H., **Highly water-soluble neutral BODIPY dyes with controllable fluorescence quantum yields**, *Organic Letters*. Vol. 13, pp. 438–441, 2011.

84. Soares, R., Santos, D., Chu, V., Azevedo, A., Aires-Barros, M., Conde, J., **A point-of-use microfluidic device with integrated photodetector array for immunoassay multiplexing: Detection of a panel of mycotoxins in multiple samples**, *Biosensors and Bioelectronic*, Vol. 87, pp. 823–831, 2017.

85. Pinto, I., Santos, D., Caneira, C., Soares, R., Azevedo, A., Chu, V., Conde, J., **Optical biosensing in microfluidics using nanoporous microbeads and amorphous silicon thin-film photodiodes: Quantitative analysis of molecular recognition and signal transduction**, *Journal of Micromechanics and Microengineering*, Vol. 28, 2018.

86. Zhu, L., Lee, C., DeVoe, D., **Integrated microfluidic UV absorbance detector with attomol-level sensitivity for BSA**, *Lab on a Chip*, Vol. 6, pp. 115–120, 2005.

Supplementary Material

Quantification of the non-labelled IgG

UV Absorption at 280 nm - Calibration Curve

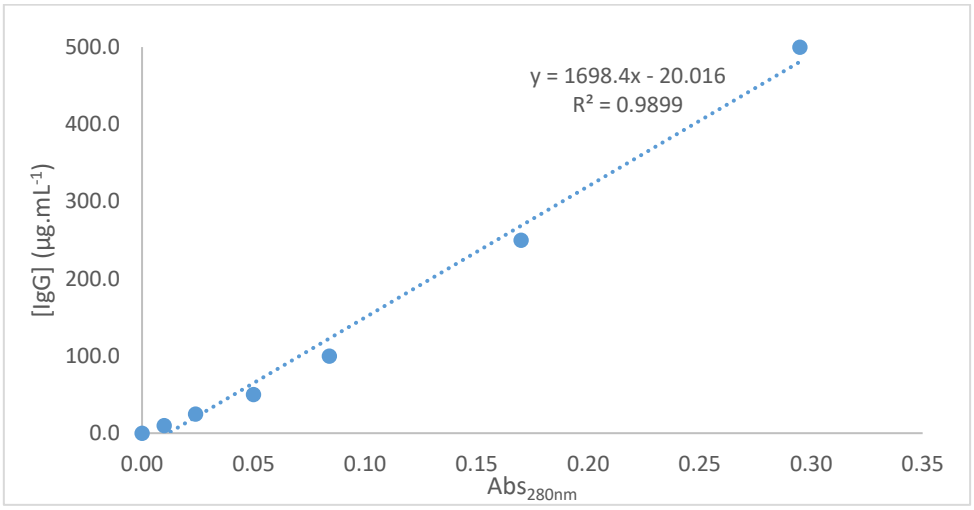

***Figure A1** - Calibration curve for IgG quantification UV absorption at 280 nm. Samples were obtained from Gammanorm® IgG stock solutions with concentrations ranging from 10 µg.mL^{-1} to 500 µg.mL^{-1}.*

Bicinchoninic Acid (BCA) - Calibration Curve

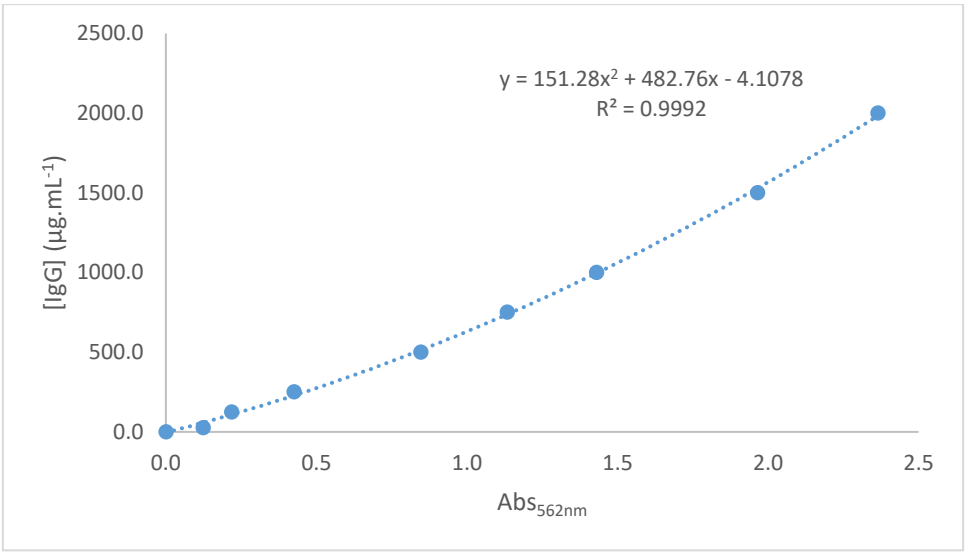

***Figure A2** - Calibration curve for IgG quantification by bicinchoninic acid (BCA) method. Samples were obtained from Gammanorm® IgG stock solutions with concentrations ranging from 25 µg.mL^{-1} to 2000 µg.mL^{-1}.*

Protein G Chromatography - Calibration Curve

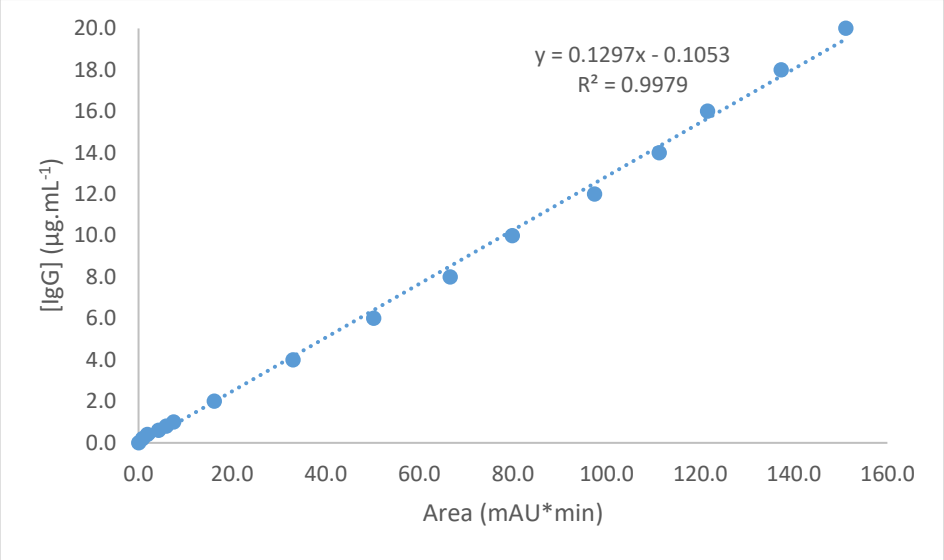

***Figure A3** - Calibration curve for IgG quantification by protein G chromatography in Äkta™ Purifier 10 system. Samples were obtained from Gammanorm® IgG stock solutions with concentrations ranging from 0.2 µg.mL^{-1} to 20 µg.mL^{-1}.*

***Table A1** - The partition coefficient, K_P, and the yield in the top phase of the system, Y_{top}, obtained for the non-labelled IgG (concentration in the system of 30 µg.mL^{-1}), quantified by protein G chromatography in Äkta™ Purifier 10 system: PEG 1500, with concentrations of polymer/salt of 15/15, 17/17 and 19/19; PEG 3350, with concentrations of polymer/salt of 12/12, 13.5/13.5 and 15/15; and PEG 8000, with concentrations of polymer/salt of 12/12, 13.5/13.5 and 15/15. All the K_P values achieved are the average of two experiments and the error represents ±SD.*

	K_P	Yield$_{Top}$ (%)
	PEG 1500	
15/15	0.58 ± 0.07	33.24 ± 2.62
17/17	3.50 ± 0.39	77.31 ± 4.63
19/19	8.25 ± 0.39	89.17 ± 0.45
	PEG 3350	
12/12	0.73 ± 0.01	38.38 ± 0.19
13.5/13.5	1.16 ± 0.09	48.35 ± 0.95
15/15	1.55 ± 0.07	57.01 ± 1.18
	PEG 8000	
12/12	0.22 ± 0.06	12.02 ± 2.92
13.5/13.5	1.01 ± 0.45	36.89 ± 10.76
15/15	2.47 ± 1.56	60.66 ± 16.87

***Table A2** - The partition coefficient, K_P, for the non-labelled IgG (concentration in the system of 30 µg.mL^{-1}), and the yield in the top phase of the system, Y_{top}, quantified by protein G chromatography in Äkta™ Purifier 10 system: PEG 3350, with concentrations of polymer/salt of 12/12, without and with the addition of 7.5% of NaCl. All the K_P values achieved are the average of two experiments and the error represents ±SD.*

	K_P	Yield$_{Top}$
without NaCl	0.73 ± 0.01	38.38 ± 0.19
with NaCl	2.30 ± 1.20	65.60 ± 16.87

Aqueous two-phase extraction using a microtube (mL-scale)

Table A3 - *The partition coefficient, K_P, of the labelled IgG in the 12/12 PEG 3350/salt system, with and without the addition of NaCl, with both phases being quantified separately by fluorescence microscopy in a straight microchannel. BT0.5: IgG-BODIPY ™ FL maleimide using TCEP, DOL 0.5; BT0.6: IgG-BODIPY ™ FL maleimide without using TCEP, DOL 0.6; A8: IgG-Alexa Fluor® 430, DOL 7.6; A4: IgG-Alexa Fluor® 430, DOL 4.1; A2: IgG-Alexa Fluor® 430, DOL 2.4; BN2: IgG-BODIPY ™ FL NHS Ester, DOL 2.6; and BN1: IgG-BODIPY ™ FL NHS Ester, DOL 1.4. The concentrations of the dye-protein conjugate were 20 µg.mL^{-1} and 15 µg.mL^{-1} for the BODIPY™ FL and the Alexa Fluor® 430, respectively. All the K_P values achieved are the average of two experiments and the error represents ±SD.*

	K_P						
	BT0.5	**BOT0.6**	**A8**	**A4**	**A2**	**BN2**	**BN1**
without NaCl	1.11 ± 0.36	7.93 ± 1.00	18.67 ± 0.20	8.69 ± 1.45	2.48 ± 0.13	20.21 ± 7.81	2.40 ± 0.56
with NaCl	4.93 ± 0.81	4.97 ± 0.62	16.98 ± 0.02	34.29 ± 2.82	25.79 ± 5.35	26.52 ± 3.68	39.62 ± 9.11

Aqueous two-phase extraction using a microfluidic device (nL-scale)

Table A4 - *The partition coefficient, K_P, of the IgG-BODIPY™ FL maleimide using TCEP, DOL 0.5 (BT0.5) and the IgG-BODIPY™ FL maleimide without using TCEP, DOL 0.6 (BT0.6), in the 12/12 PEG 3350/salt system, with and without the addition of NaCl, using different quantification methods: by fluorescence microscopy in a straight microchannel, mL-scale (20 µg.mL^{-1}), and in a microfluidic device, nL-scale (50 µg.mL^{-1}), and protein G chromatography in Äkta™ Purifier 10 system (30 µg.mL^{-1}). All the K_P values achieved are the average of two experiments and the error represents ±SD.*

	K_P		
	with TCEP (DOL 0.5)		
	mL-scale	nL-scale	Äkta 10 Purifier
without NaCl	1.11 ± 0.36	0.75 ± 0.16	0.58 ± 0.02
with NaCl	4.93 ± 0.81	1.47 ± 0.20	2.47 ± 0.70
	without TCEP (DOL 0.6)		
	mL-scale	nL-scale	Äkta 10 Purifier
without NaCl	7.93 ± 1.00	3.04 ± 0.82	0.82 ± 0.11
with NaCl	4.97 ± 0.62	1.95 ± 0.27	1.71 ± 0.44

Table A5 - *The partition coefficient, K_P, of the IgG-Alexa Fluor® 430, DOL 7.6 (A8), the IgG-Alexa Fluor® 430, DOL 4.1 (A4) and the IgG-Alexa Fluor® 430, DOL 2.4 (A2), in the 12/12 PEG 3350/salt system, with and without the addition of NaCl, using fluorescence microscopy quantification methods: in a straight microchannel, mL-scale (20 µg.mL^{-1}), and in a microfluidic device, nL-scale (50 µg.mL^{-1}). All the K_P values achieved are the average of two experiments and the error represents ±SD.*

	K_P					
	DOL 7.6		**DOL 4.1**		**DOL 2.4**	
	mL-scale	nL-scale	mL-scale	nL-scale	mL-scale	nL-scale
without NaCl	18.67 ± 0.20	0.76 ± 0.00	8.69 ± 1.45	0.21 ± 0.04	2.48 ± 0.13	0.15 ± 0.05
with NaCl	16.98 ± 0.02	0.66 ± 0.20	34.29 ± 2.82	0.34 ± 0.20	25.79 ± 5.35	0.56 ± 0.14

Table A6 - *The partition coefficient, K_P, of the IgG-BODIPY ™ FL NHS Ester, DOL 2.6 (BN2), and the IgG-BODIPY ™ FL NHS Ester, DOL 1.4 (BN1), in the 12/12 PEG 3350/salt system, with and without the addition of NaCl, using fluorescence microscopy quantification methods: in a straight microchannel, mL-scale (20 µg.mL^{-1}), and in a microfluidic device, nL-scale (50 µg.mL^{-1}) . All the K_P values achieved are the average of two experiments and the error represents ±SD.*

	K_P			
	DOL 2.6		**DOL 1.4**	
	mL-scale	nL-scale	mL-scale	nL-scale
without NaCl	20.21 ± 7.81	1.40 ± 0.25	2.40 ± 0.56	0.13 ± 0.02
with NaCl	26.52 ± 3.68	2.11 ± 0.56	39.62 ± 9.11	0.40 ± 0.17